UNESP - Universidade Estadual Paulista

"Júlio de Mesquita Filho"

Faculdade de Odontologia de Araraquara

RAFAEL SCAF DE MOLON

PATOFISIOLOGIA DE OSTEONECROSE INDUZIDA POR BISFOSFONATOS E INIBIDORES DE RANK-L

Araraquara

2016

UNESP - Universidade Estadual Paulista

"Júlio de Mesquita Filho"

Faculdade de Odontologia de Araraquara

RAFAEL SCAF DE MOLON

PATOFISIOLOGIA DE OSTEONECROSE INDUZIDA POR BISFOSFONATOS E INIBIDORES DE RANK-L

Tese apresentada ao Programa de Pós-Graduação em Odontologia – Área de Periodontia da Faculdade de Odontologia de Araraquara da Universidade Estadual Paulista para titulo de Doutor em Odontologia

Orientador: Prof. Dr. Joni Augusto Cirelli

Araraquara

2016

de Molon, Rafael Scaf
Patofisiologia de osteonecrose induzida por bisfosfonatos e inibidores de RANK-L / Rafael Scaf de Molon .-- Araraquara: [s.n.], 2016.
123 f. ; 30 cm.

Tese (Doutorado) – Universidade Estadual Paulista, Faculdade de Odontologia
Orientador: Prof. Dr. Joni Augusto Cirelli

1. Perda óssea alveolar 2. Camundongos 3. Osteoclasto 4. Doenças periodontais 5. Artrite reumatoide I. Título

Ficha catalográfica elaborada pela Bibliotecária Marley C. Chiusoli Montagnoli, CRB-8/5646
Serviço Técnico de Biblioteca e Documentação da Faculdade de Odontologia de Araraquara / UNESP

RAFAEL SCAF DE MOLON

PATOFISIOLOGIA DE OSTEONECROSE INDUZIDA POR BISFOSFONATOS E INIBIDORES DE RANK-L

Tese para obtenção do grau de doutor

Comissão julgadora

Presidente e Orientador: Prof. Dr. Joni Augusto Cirelli

2° Examinador: Prof. Dr. Juliano Milanezi de Almeida

3° Examinador: Profa. Dra. Daniela Bazan Palioto

4° Examinador: Prof. Dr. Pedro Paulo Chaves de Souza

5° Examinador: Prof. Dr. Francisco Humberto Nociti Junior

Araraquara, 24 de Março de 2016.

DADOS CURRICULARES

RAFAEL SCAF DE MOLON

NASCIMENTO	06.03.1982 - São Paulo, São Paulo
FILIAÇÃO	Antonio de Molon Filho e Sandra Scaf de Molon
2000 / 2004	Graduação em Odontologia - Faculdade de Odontologia da Universidade do Sagrado Coração, USC, Bauru, SP.
2005 / 2006	Estágio de Atualização na Disciplina de Cirurgia e Traumatologia Buco-Maxilo-Facial da Faculdade de Odontologia de Araraquara - UNESP
2006 / 2008	Especialização em Implantodontia - Sociedade de Promoção Social do Fissurado Lábio Palatal - PROFIS, Bauru, SP
2009 / 2011	Especialização em Periodontia - Faculdade de Odontologia de Araraquara - UNESP
2010 / 2012	Curso de Pós-Graduação em Odontologia, Área de concentração em Periodontia, nível Mestrado - Faculdade de Odontologia de Araraquara - UNESP
2013 / 2015	Doutorado Sanduíche - University of California at Los Angeles - UCLA School of Dentistry, Los Angeles, CA, USA.

2012 / 2016	Curso de Pós-Graduação em Odontologia, Área de concentração em Periodontia, nível Doutorado - Faculdade de Odontologia de Araraquara - UNESP

Dedicatória

Dedico este trabalho...

A **Deus**, por estar presente em todos os momentos da minha vida, por sempre conduzir meus passos em busca do melhor caminho, pela força em todos os momentos difíceis e também pelos momentos de alegria e por ter sempre colocado na minha vida, pessoas maravilhosas que sempre me ajudaram a seguir em frente em busca de novas conquistas.

Aos meus pais Antonio e Sandra, pelo exemplo durante minha criação, pelo incentivo e apoio em todas as minhas escolhas, por todo amor, confiança e dedicação, por estarem sempre ao meu lado, permitindo que eu realize todos os meus sonhos e acima de tudo, pelo exemplo positivo que vocês foram e continuam sendo em minha vida.

Aos meus irmãos Gustavo, Melissa e Marina, pelo incentivo, pelo apoio, carinho, compreensão e amizade.

A minha esposa, Erica

Por estar sempre ao meu lado, compartilhando todos os momentos, pelo incentivo a pesquisa e a pós-graduação e por todo o conhecimento e ensinamentos passados desde o inicio da minha caminhada na pós-graduação. Você é um exemplo de ser humano e de profissional. Obrigado por todos esses anos juntos, por todo amor, pelo imenso respeito, pela lealdade e por todo o incentivo. Agradeço a Deus todos os dias por ter tido você em minha vida; Um grande amor caminhando junto torna a busca pelo sucesso mais real e encorajador. Você e todos os nossos sonhos são minha maior motivação.

Agradecimentos Especiais

Ao meu orientador Prof. Dr. Joni Augusto Cirelli

Muito obrigado. Obrigado pelos ensinamentos, exemplo de conduta profissional, pela confiança. Obrigado por acreditar e confiar no meu trabalho, obrigado por me permitir crescer. O seu apoio, ensinamento, e dedicação foi muito importante para minha formação acadêmica e profissional. Minha admiração, respeito e gratidão.

Ao Prof. Dr. Sotirios Tetradis

Thank you Dr. Tetradis for all the great opportunities, knowledgement, and for the great life I had in LA. Thank you for receiving me so nicely in your lab. Thank you for all the support and efforts in all the projects we worked on. I am very grateful for the respect, trustful, and for all the happy moments during the 18 months I spent in your lab. I also would like to thank all member from your laboratory especially Olga Bezouglaia, and Prof. Dr. Tara Aghaloo. I am sure we will continue our collaboration.

A Profa. Dra. Gulnara Scaf

Pelas primeiras orientações no desenvolvimento de trabalhos científicos, pela amizade, convívio, pelo apoio, confiança, e pelo exemplo de honestidade e de conduta profissional.

Aos grandes amigos da pós-graduação

Aos amigos Jõao Paulo Steffens, Fausto Frizzera, Jonatas Esteves, Mario Verzola, Rubens Moreno, Guilherme Oliveira, Luiz Guilherme Freitas, Joao Antônio Souza, Pedro Souza e

Vinicius Ibiapina acima de tudo pela amizade sincera conquistada, e por todos os momentos de alegria, companheirismo e convivência diária durante esses seis últimos anos. Tenho certeza que mesmo após o fim dos nossos cursos, nossa amizade permanecerá.

Aos queridos amigos de Araraquara

João Paulo, Pablo, Fausto, Fernanda Rocha, Giovana, Marcell, Sabrina, Andressa, Mario, Luana, Lívia, Luizinho, Pedrão, Gui, Piauí, João Antônio. Espero que esta amizade permaneça ao longo de nossas vidas.

Agradecimentos

À Faculdade de Odontologia de Araraquara, Universidade Estadual Paulista "Júlio de Mesquita Filho" – UNESP

Na pessoa de seu Diretor Profa. Dra. Andreia Affonso Barretto Montandon e a Vice-Diretora, Profa. Dra. Elaine Maria Sgavioli Massucato.

À Coordenação do Pós-Graduação em Odontologia, Faculdade de Odontologia de Araraquara – UNESP, representada pelo coordenador Prof. Dr. Carlos Rossa Jr e pelo Vice-coordenador Prof. Dr. Joni Augusto Cirelli.

Pela enorme admiração, pela competência, dedicação, responsabilidade e exemplo de conduta e profissionalismo.

Aos docentes do curso de Pós-Graduação em Odontologia, Periodontia da Faculdade de Odontologia de Araraquara – UNESP

Prof. Dr. Elcio Marcantonio Junior, Prof. Dr. José Eduardo César Sampaio, Profa. Dra. Rosemary Adriana Chiérici Marcantonio, Prof. Dr. Joni Augusto Cirelli, Prof. Dr. Carlos Rossa Junior, Profa. Dra. Silvana Regina Perez Orrico, Profa. Dr. Daniela Zandim pela formação, orientação e exemplo de dedicação e conduta profissional.

À Fundação de Amparo a Pesquisa do Estado de São Paulo, FAPESP

Pelo apoio financeiro concedido durante o doutorado, indispensável para a realização deste trabalho, por permitir e subsidiar a minha vida em Araraquara (Processo # 2012/09968-5).

À Coordenação de Aperfeiçoamento de Pessoal do Nível Superior, CAPES

Pelo apoio financeiro concedido durante o doutorado Sanduiche, indispensável para a realização deste trabalho, por permitir e subsidiar a minha vida em Los Angeles, US (Processo #11575-13-1).

A todos os funcionários da Faculdade de Odontologia de Araraquara – UNESP

Especialmente a Claudinha e ao Leandro, por toda a ajuda e ensinamentos durante o processamento histológicos, Exact e na preparação de soluções para o laboratório. Regina Lúcia, Cláudia, D. Maria do Rosário, Maria José e Esther, pela amizade, carinho e respeito que sempre me dispensaram. Aos funcionários da Seção de Pós-Graduação pela competência, paciência e pela colaboração dedicada. Aos funcionários da biblioteca: Marley, Adriano, Ceres, Eliana e Sílvia pela colaboração.

A todas as pessoas que participaram direta ou indiretamente na realização desse trabalho, e que não estão citadas nominalmente, meus sinceros agradecimentos.

“*A nossa ciência, comparada com o mundo que descreve, é pequena e infantil. No entanto, é a coisa mais preciosa que temos*”

Albert Einstein

de Molon RS. Patofisiologia de osteonecrose induzida por bisfosfonatos e inibidores de RANK-L [Tese de Doutorado]. Araraquara: Faculdade de Odontologia da UNESP; 2016.

RESUMO

A patogênese de osteonecrose dos maxilares (ONJ) e os fatores de risco ainda não estão totalmente elucidados e continuam sendo foco de contínuos estudos visando estabelecer um correto diagnóstico, prevenção e tratamento. Assim, os objetivos do presente estudo foram: (1) desenvolver em camundongos, um modelo experimental de ONJ induzido por bisfosfonatos (BPs) e inibidores de RANK-L associado a doença periodontal espontânea; (2) investigar neste modelo se a descontinuação desses medicamentos alteraria as características clinicas e radiográficas de osteonecrose e, (3) avaliar a influência da artrite reumatoide (AR) no agravamento de ONJ experimental. As análises em todos os estudos foram estabelecidas por meio de avaliações radiográficas, por microtomógrafo, e histológicas. No primeiro estudo, foi estabelecido um novo modelo experimental animal utilizando-se diferentes medicamentos anti-reabsortivos, resultando em características clinicas semelhantes ao que ocorre em humanos, ou seja, extensas áreas necróticas e com exposição óssea a cavidade oral. Os resultados do estudo 2 demonstraram que a descontinuação de OPG-Fc, um inibidor de RANK-L, mas não de BPs reverteu todas as características clinicas e radiográficas de ONJ. Além disso, os resultados do estudo 3 sugerem que a AR associada ao tratamento com altas doses de BPs exacerba a incidência e a severidade de ONJ em camundongos. Com base nos achados do presente estudo, conclui-se que ONJ induzida por BPs e por inibidores de RANK-L como OPG-Fc e RANK-Fc apresentam grande similaridade nas características radiográficas e histológicas, entre si e com a doença em humanos, mas somente a descontinuação do tratamento com OPG-Fc leva a uma reversão completa das alterações clinicas da doença. Os dados suportam a relevância da AR como um fator de risco para o desenvolvimento de ONJ.

Palavras-chave: Perda óssea alveolar. Camundongos. Osteoclasto. Doenças periodontais. Artrite reumatoide.

de Molon RS. Pathophysiology of osteonecrosis of the jaws induced by bisphosphonates and RANK-L inhibitors [Tese de Doutorado]. Araraquara: Faculdade de Odontologia da UNESP; 2016.

ABSTRACT

The pathogenesis of the osteonecrosis of the jaw (ONJ) and its risk factors still remain poorly understudied and continue to be the focus on ongoing studies to establish a proper diagnosis, prevention and treatment. Thus, the aims of this study were: (1) to develop in mice, an experimental model of osteonecrosis induced by bisphosphonates (BPs) and RANK-L inhibitors associated with spontaneously periodontal disease. Then, (2) using the same experimental model in mice, to investigate if the discontinuation of these drugs alters the clinical and radiographic features of ONJ. In addition, (3) the influence of systemic diseases such as rheumatoid arthritis (RA), and ONJ was assessed as a possible risk factor for worsening ONJ characteristics. The analyses in all studies were established through radiographic, by means of micro-computed tomography, and histological assessments. In the first study, a new experimental animal model using different antiresorptive drugs was established with clinical features similar to what occurs in humans, with extensive necrotic areas and exposed bone o the oral cavity. The results of the study 2 showed that discontinuing OPG-Fc, a RANK-L inhibitor, but not BPs reversed all the clinical and radiographic features of ONJ. Furthermore, the results of study 3 suggest that treatment with high doses of BPs associated with the presence of RA exacerbated the incidence and severity of ONJ in mice. These data evidenced that BPs and RANK-L inhibitors possess great similarity in the radiographic and histologic findings, including the incidence of osteonecrosis and bone exposure, but only the OPG-Fc discontinuation completely reverses ONJ features. The data further support the relevance of RA as a risk factor for ONJ development.

Keywords: Alveolar bone loss. Mice. Osteoclasts. Periodontal disease. Rheumatoid arthritis.

SUMÁRIO

1 INTRODUÇÃO.....17

2 PROPOSIÇÃO.....26

3 PUBLICAÇÕES.....27

3. 1 Publicação 1.....27

3.2 Publicação 2.....36

3.3 Publicação 3.....58

4 CONSIDERAÇÕES FINAIS.....99

5 CONCLUSÃO.....104

REFERÊNCIAS.....105

ANEXO.....116

1 INTRODUÇÃO

O desenvolvimento e ativação de osteoclastos é um processo essencial na homeostase metabólica mineral e óssea durante o crescimento e renovação do esqueleto. Estes processos envolvem a reabsorção de osso mineralizado por osteoclastos[92], (células multinucleadas derivadas de precursores da linhagem de monócitos/macrófagos, e são responsáveis pela degradação da matriz óssea mineralizada), seguida pela subsequente formação e mineralização de nova matriz óssea pela ação dos osteoblastos[24,65]. Em várias patologias, tais como osteoporose, metástases tumorais osteolíticas, artrite reumatoide e doença periodontal, a quantidade de osso reabsorvido pelos osteoclastos excede aquela substituída durante a formação óssea, levando a uma perda de massa óssea, aumento da fragilidade óssea e risco de fratura[89].

O aumento da expressão e produção de RANKL (ligante do receptor de ativação do fator nuclear κB), observado por exemplo, com a privação de estrógeno ou durante o curso da doença periodontal e osteoporose, é um mecanismo central da ativação e diferenciação de osteoclastos e aumento da reabsorção óssea[39,105]. Neste contexto, duas citocinas surgem como protagonistas essenciais e suficientes para induzir a diferenciação de osteoclastos: o fator estimulante de colônias de macrófagos (M-CSF) e RANKL[40,58,114]. M-CSF liga-se ao c-Fms, um receptor único de domínio transmembrana da família da tirosina quinase, e RANKL se liga ao RANK, um receptor único transmembrana da família de receptores do fator de necrose tumoral (TNF). O mecanismo de ação envolve a ativação da proliferação e sobrevivência de células da linhagem de monócitos-macrófagos e a expressão de RANK pelo M-CSF, permitindo a ação do RANKL que, em conjunto com M-CSF, constitui uma exigência absoluta para a progressão de precursores iniciais ao longo da linhagem de osteoclasto[14,23,70]. A diferenciação a partir de precursores de osteoclastos para osteoclastos multinucleados é então induzida por RANKL, novamente por meio da expressão de M-CSF-dependente de RANK na superfície celular destes precursores precoces. Tanto M-CSF como RANKL são secretados pelas células do estroma da medula óssea e osteoblastos, bem como por células T e B. A maioria das células que produzem RANKL também produz um receptor, denominado osteoprotegerina (OPG) que atua como antagonista da sinalização de RANKL e osteoclastogênese[55]. Em última análise, é a relação entre RANKL e OPG que determina o nível de ativação de RANK e, desse modo, o grau em que é ativado a osteoclastogênese. Quase todos os tratamentos farmacológicos atuais envolvendo doenças metabólicas ósseas,

como a osteoporose, utilizam drogas que inibem a reabsorção óssea. Dentre estas drogas, estão incluídas: bisfosfonatos (BPs), raloxifeno e calcitonina.

Uma nova e recente abordagem visa atuar no sistema RANK/RANKL de uma maneira específica. O papel indispensável da via RANK/RANKL na remodelação óssea foi demonstrada por doenças monogênicas em humanos, em que a ausência funcional de RANK ou RANKL resultaram em osteopetrose[45,99]. Estudos clínicos demonstram que a inibição de RANKL foi alcançada por meio de diferentes dosagens de Fc-OPG (0.3, 1 e 3 mg/kg) em mulheres na menopausa levando a uma rápida e sustentada inibição da reabsorção óssea[18,31]. Recentes investigações têm avaliado amplamente uma nova droga, denominada denosumab (DMAb). Este anticorpo monoclonal humano, se liga e inibe RANKL impedindo o processo de reabsorção óssea. Medicamentos anti-reabsortivos tais como BPs, e o inibidor de RANKL DMAb, impedem a reabsorção óssea osteoclástica e são utilizados na clínica para gerenciar doenças ósseas, como malignidade óssea primária ou metastática e osteoporose. Estes medicamentos, estudados em pacientes com câncer e em mulheres na pós-menopausa, agem reduzindo complicações ósseas, diminuindo a carga tumoral, reduzindo a dor óssea, e diminuindo a incidência de fraturas osteoporóticas, contribuindo, desta forma, para melhorar a qualidade de vida dos pacientes[69,83,104,106].

A eficácia clínica dos BPs está baseada em duas propriedades chave: (1) na habilidade de se ligar fortemente ao osso mineralizado e (2) no efeito inibitório sobre os osteoclastos maduros[90]. A forte ligação dos BPs ao osso confere aos bisfosfonatos a propriedade única de captação seletiva pelo órgão-alvo a que se destina. Os BPs ligam-se seletivamente ao osso mineral, e assim inibem osteoclastos maduros nos sítios de reabsorção óssea. Ao mesmo tempo em que os BPs admitem uma estrutura química similar à molécula inorgânica pirofosfato, diferem-se deste por possuírem uma ligação fósforo-carbono-fósforo (P-C-P) ao invés de uma ligação fósforo-oxigênio-fósforo (P-O-P). Esta ligação P-C-P é altamente resistente à hidrólise, tornado os BPs fortemente resistentes a degradação biológica. BPs contendo nitrogênio, tais como: o alendronato, ibandronato, minodronato, pamidronato, risedronato, neridronato e zoledronato, apresentam uma cadeia lateral que contém um átomo de nitrogênio. Uma vez absorvido pelos osteoclastos, estes compostos são capazes de inibir a reabsorção óssea por meio de efeitos intracelulares. BPs contendo nitrogênio atuam principalmente através da inibição da via farnesil-pirofosfato sintase (FPP) - uma enzima da via do mevalonato - impedindo, desta forma, a modificação pós-translacional (prenilação) das proteínas de ligação (guanosina trifosfato - GTP), essenciais para função e sobrevivência dos osteoclastos[90]. Como resultado, BPs inibem o funcionamento dos osteoclastos ao danificar a

diferenciação, perturbar o citoesqueleto, diminuir o transporte intracelular, e induzir apoptose (Figura 1)[53,103].

Figura 1 - *Via de sinalização do mevalonato demonstrando o mecanismo de ação dos bisfosfonatos.*

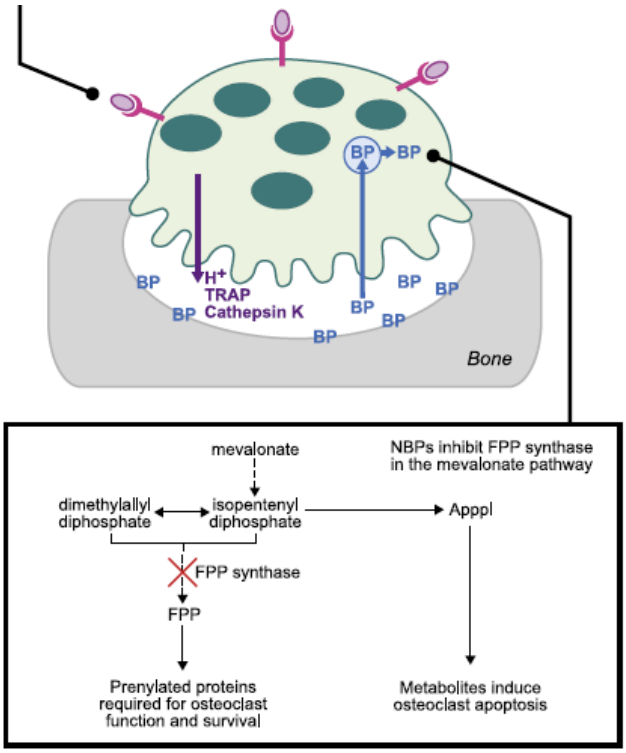

Autor: Baron et al.[16]

Fonte: *Bone* 2011; 48(4): 677-92

O mecanismo de ação do DMAb difere dos BPs. DMAb impede a ligação do RANKL ao receptor RANK, inibindo, assim, o desenvolvimento, a ativação e a sobrevivência de osteoclastos. Os efeitos da inibição de RANK-L foram inicialmente analisados em estudos em animais e em humanos com proteínas fusionadas Fc (Figura 2)[19,72,93,95,108]. Fc-OPG (derivado da *Escherichia coli*), OPG-Fc (expressados nas células mamárias do hospedeiro) e RANK-Fc foram fusionados à porção Fc da imunoglobulina humana G1 (IgG_1) e os respectivos efeitos foram avaliados[19,72]. Fc-OPG foi administrado pela primeira vez em humanos em 1998[18]. Neste estudo clínico de primeira fase, os autores constataram um rápido declínio dos marcadores de remodelação óssea, com um efeito durador de até 6 semanas. Contudo, somente em 2004, os efeitos farmacológicos de Fc-OPG derivados da *E. coli* foram compreendidos[111], revelando mutações genéticas em RANK e OPG associadas com desordens

esqueléticas humanas caracterizadas por excessiva atividade osteoclástica. Por este motivo, a continuidade no desenvolvimento do Fc-OPG foi interrompida. Como uma alternativa ao uso do Fc-OPG, OPG-Fc passou a ser produzido a partir de células mamárias de hamsters. As características observadas em relação ao Fc-OPG foram efeito prolongado (de até 10 vezes) e potência de até três vezes comparado com os demais construtos[57]. Em relação a molécula RANK-Fc, esta foi desenvolvida a partir da fusão com o domínio extracelular de RANK à porção Fc da IgG_1[100]. Contudo, estudos prévios identificaram risco significativo de hipercalcemia, pela ativação de auto-anticorpos, em primatas, contra o receptor RANK por meio de repetidas doses desta molécula. Evidências de uma resposta imune ao utilizar RANK endógeno em pacientes (observações não publicadas - Amgen), levou a descontinuação da produção de RANK-Fc. Assim, a decisão de interromper os estudos com todos os construtos foi estabelecida em favor do desenvolvimento de um anticorpo, tendo como molécula alvo o RANKL, ao invés de receptores, como nos construtos.

Figura 2 - *Evolução dos inibidores recombinantes de RANKL.*

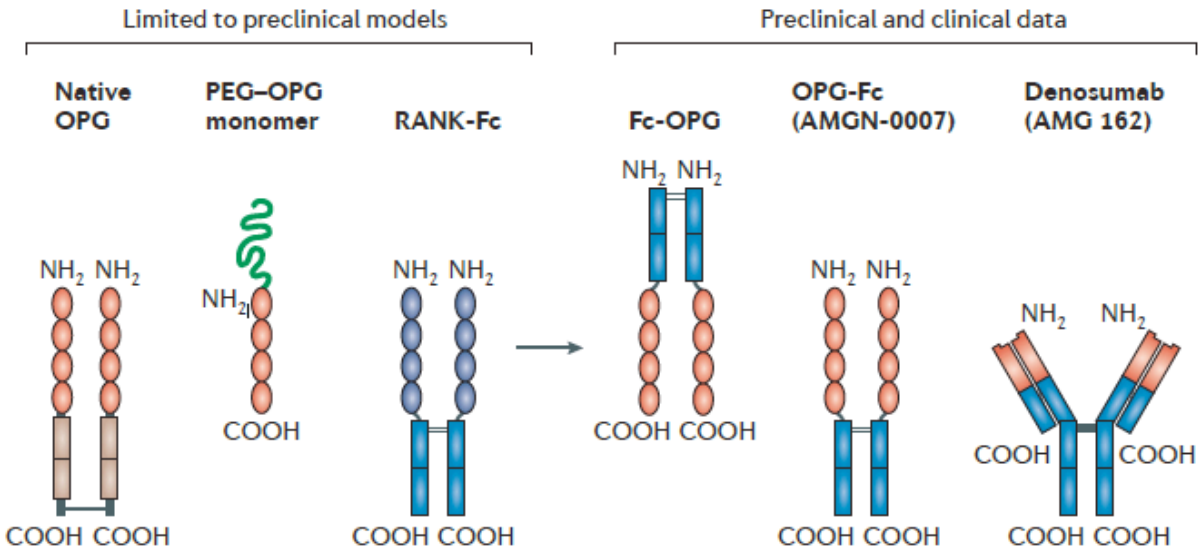

Autor: Lacey et al.[57]

Fonte: *Nature Reviews - Drug Discovery* 2012; 11(5): 401-19

DMAb apresenta varias vantagens com relação aos construtos OPG-Fc, Fc-OPG e RANK-Fc[68]. Dentre estas, (1) DMAb não se liga ao TRAIL (ligante indutor de apoptose relacionado ao TNF) ou a outros membros da superfamília do TNF, tais como CD40, TNF-α e TNF-β; (2) a meia vida é prolongada comparada com os construtos, especialmente pela massa

molecular; (3) apesar de ambos DMAb e OPG-Fc admitirem o mesmo alvo, o DMAb é mais específico reconhecendo apenas RANKL humano, em contraste com OPG-Fc, que também se liga ao RANKL de ratos e camundongos, bem como TRAIL[41,56]. Por conseguinte, o mecanismo de ação do DMAb difere-se dos BPs (Figura 3), os quais se ligam ao osso mineral e inibem a função dos osteoclastos, principalmente, por serem absorvidos por osteoclastos em locais de reabsorção óssea. A principal diferença na forma de ação entre DMAb e BPs em osteoclastos é que o segundo age somente no interior das células, enquanto que o DMAb atua no meio extracelular[16].

Figura 3 - *Ilustração dos mecanismos de inibição de osteoclastos mediada por BPs e DMAb.*

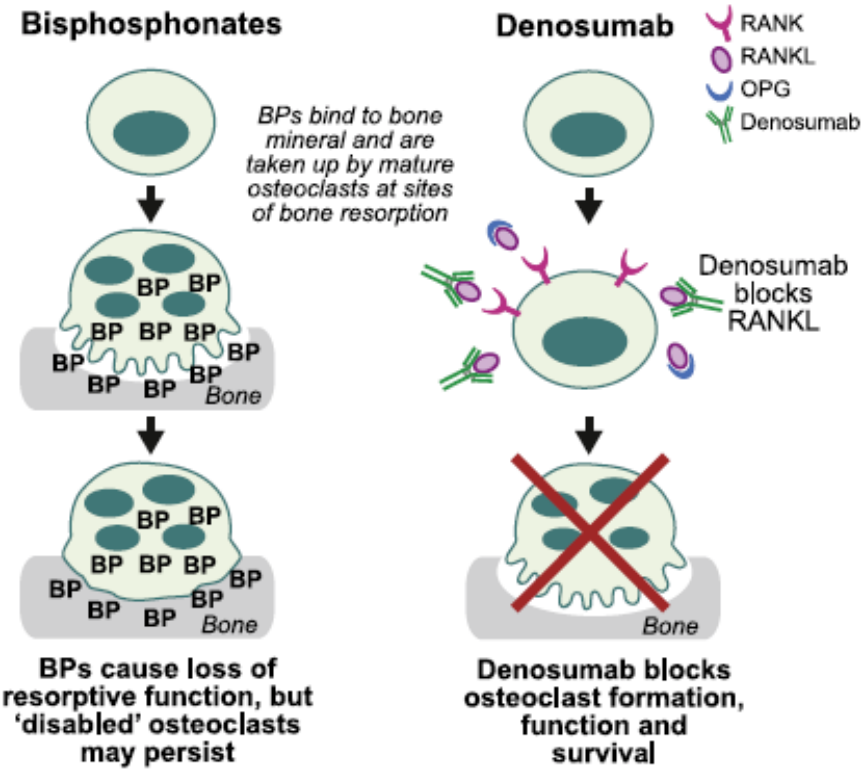

Autor: Baron et al.[16]

Fonte: *Bone* 2011; 48(4): 677-92.

O tratamento a longo prazo com BPs tem sido associado com um aumento do número de osteoclastos, incluindo osteoclastos gigantes, hiper-nucleados, não aderidos à superfície óssea, e que passam por apoptose[110]. A inibição da atividade dos osteoclastos por meio dos BPs poderia desencadear um ciclo de feedback que resultaria em um aumento de RANKL no osso. A superprodução de RANKL poderia, por sua vez, estimular os precursores de

osteoclastos a fundirem-se em osteoclastos multinucleados. Esta hipótese é apoiada pela evidência de um aumento no número de osteoclastos sobre as superfícies ósseas em camundongos huRANKL ovariectomizados tratados com alendronato, ao passo que fora constatado um desaparecimento quase completo de osteoclastos neste modelo na presença de DMAb[79]. Resultados preliminares comparando os efeitos do tratamento de artrite com inibidores de RANKL e BPs, indicaram que o OPG reduziu significativamente a presença de RANKL no osso, enquanto que o ácido zoledrônico causou um aumento de duas vezes na expressão deste ligante[101].

Apesar de o mecanismo de ação farmacológico ser distintamente diferente, BPs e DMAb estão associados com osteonecrose dos maxilares (ONJ), um infrequente, mas grave efeito adverso, particularmente quando administrado em doses elevadas[11]. ONJ é definido como osso exposto ou osso que pode ser sondado através de uma fístula intra-oral ou extra-oral na região maxilofacial, que persiste por mais de 8 semanas em pacientes em tratamento atual ou anterior com medicamentos anti-reabsortivos e sem histórico de terapia de radiação nos maxilares ou com doença metastática na maxila e mandíbula[50,52,87]. Com o aumento no número de casos de ONJ em pacientes que fazem uso de DMAb, a Sociedade Americana de Cirurgiões Oral e Maxilofacial (AAOMS) recomendou o uso do termo osteonecrose dos maxilares relacionada a medicamentos (MRONJ)[87]. Nesse contexto, pacientes expostos a administração intravenosa de BPs para tratamento de doenças malignas, a incidência de ONJ varia entre 0 a 12.222 para cada 100.000 pacientes / ano[12,15,17,22] e a incidência de ONJ em pacientes tratados com DMAb varia de 0 a 2.316 para cada 100.000 pacientes / ano[43,62,96,98,102]. Por outro lado, a incidência de ONJ em pacientes que fazem uso de BPs por via oral, especialmente para tratamento de osteoporose, varia entre 1.04 a 69 para cada 100.000 pacientes / ano[32,51,81] e para os pacientes que fazem uso de DMAb varia de 0 a 30.2 para cada 100.000 pacientes / ano[13,30,73,76]. Embora a incidência de ONJ seja pequena, o desenvolvimento da doença resulta em serias complicações para estes pacientes.

O atual sistema de classificação de ONJ envolve os estágios 0-3 e baseia-se na apresentação clínica do paciente. Apesar de um paciente em estágio 0 não apresentar osso exposto, o que o torna de difícil diagnóstico, os estágios 1 a 3 são definidos em parte pelo osso exposto à cavidade oral. Pacientes em estágio 1 são assintomáticos e não mostram sinais de infecção; por outro lado, pacientes em fase 2 apresentam infecção frequentemente associada com dor, eritema e drenagem purulenta. Em um estado mais avançado, a fase 3 envolve a presença de osso necrosado estendendo-se além do alvéolo dentário, com possível chance de fratura patológica da mandíbula, fístula extraoral, e comunicação nasal[85]. Na

grande maioria dos casos, ONJ ocorre após extração dentária e ao redor de dentes com doença periodontal ou periapical[67,86]. Assim, o histórico do paciente e o exame clínico são as ferramentas de diagnóstico mais sensíveis para esta condição. Áreas de osso necrosado podem permanecer assintomáticas por semanas, meses ou anos podendo resultar em dor ou osso exposto na maxila ou mandíbula[85]. Estas lesões tornam-se sintomáticas com a inflamação dos tecidos circundantes e/ou quando houver evidência clínica de exposição óssea. Os sinais e sintomas que antecedem o desenvolvimento da osteonecrose clinicamente detectável incluem dor, mobilidade do dente, inchaço da mucosa, eritema, e ulceração. Estes podem ocorrer espontaneamente ou mais comumente no local da cirurgia dento-alveolar[84].

Embora os primeiros casos de ONJ tenham sidos descritos há mais de 10 anos, tanto a etiologia quanto a patogênese ainda permanecem desconhecidas. Alguns fatores como inibição de osteoclastos e supressão da remodelação óssea, inflamação e infecção, inibição de angiogênese, função alterada das células imunes do hospedeiro, e baixo turnover ósseo são algumas das hipóteses propostas que fundamentam o desenvolvimento e progressão de ONJ[9-11,49]. Fatores que aumentam a incidência e o risco de ONJ incluem: (1) dose e duração do tratamento com medicamentos inibidores de reabsorção óssea; (2) cirurgias dento-alveolares e doenças bucais; (3) doenças sistêmicas e (4) infecção bacteriana[9-11,78]. Esses fatores de risco podem levar a complicações durante a evolução da doença.

Dentre as hipóteses existentes para elucidar a patogênese de ONJ, inflamação e infecção desempenham um papel importante (Figura 4). Estudos recentes apontam para alguns fatores adicionais, além do uso de BPs ou DMAb, que contribuem para o desenvolvimento de necrose, tais como: extrações dentárias, doença periodontal, e doença periapical[22,67,87]. Modelos de estudo de inflamação e infecção tem sido desenvolvidos em animais na tentativa de reproduzir os achados clínicos de ONJ em pacientes com patologias dentais. Os resultados tem mostrado que a presença de infecção e inflamação são suficientes para o desenvolvimento de necrose óssea[3,5,6,27,48,115]. Além disso, o papel da infecção bacteriana na patogênese de ONJ é destacada pela redução da incidência de osteonecrose em pacientes com câncer após a melhoria na higiene dental[20,71,81]. Supressão da imunidade inata ou adquirida causada por corticosteroides ou por quimioterapia também induziu o surgimento de ONJ após a administração de BPs[87]. Este achado fora suportado por um estudo recente[21], em que os autores confirmaram a inflamação estéril nos tecidos moles em torno do maxilar como não suficiente para induzir ONJ. Em um modelo experimental em ratos, o tratamento com antibióticos e fechamento do retalho mucoperiosteal no dia da extração dentária impediu o desenvolvimento de osteonecrose[1,63]. Não obstante, pode-se concluir que o estado

imunocomprometido do paciente em função de doenças, tais como diabetes e artrite reumatoide, e uso de medicamentos, como esteroides e quimioterápicos, podem aumentar a prevalência e a severidade de ONJ quando combinados com infecção / inflamação oral ou trauma e na presença de drogas que inibem a reabsorção óssea[26,28,29,115].

Figura 4 - *Ilustração dos mecanismos propostos para o desenvolvimento de ONJ.*

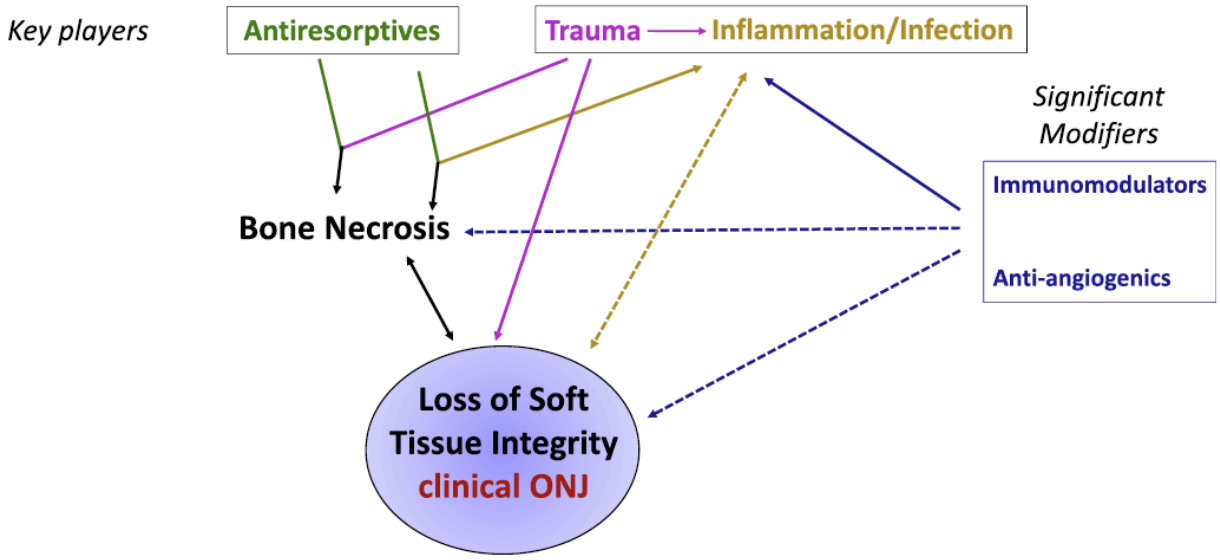

Autor: Aghaloo et al.[2]

Fonte: *Oral Maxillofacial Surg Clin N Am* 2015; 27(4): 489-96.

Assim, o progresso significativo no conhecimento da patogênese de ONJ é dependente do desenvolvimento de modelos animais que reproduzam fielmente as manifestações clínicas da doença[6]. Perguntas mais básicas sobre a fisiopatologia, tais como causa / efeito dos BPs e DMAb, o papel das doses / durações do tratamento, e quais os outros co-fatores que contribuem para o surgimento e/ou severidade da doença, poderiam ser rapidamente respondidas em uma situação pré-clínica, e possivelmente reduziriam os vieses em pesquisas subsequentes em humanos[8]. Progressos no desenvolvimento de modelos animais de MRONJ começaram lentamente, e em muitos casos, houve poucos avanços na compreensão da doença. Atualmente, modelos experimentais recapitulando as características de ONJ em roedores e em animais de grande porte, tratados com BPs ou DMAb, tem ampliado o conhecimento sobre a patogênese de ONJ[3,5,27,77,107,115]. Contudo, modelos animais de osteonecrose induzidos por BPs e inibidores de RANKL associando diferentes modelos de indução de doença periodontal

e periapical, permitem o melhor entendimento da patofisiologia da doença, com a vantagem de reduzir os vieses dos estudos clínicos e por fim, auxiliar na promoção de uma melhor atenção médica e periodontal aos pacientes com ONJ. Na literatura científica, estudos focando no desenvolvimento de modelos animais e possíveis investigações mostrando a relação da terapia medicamentosa com possível resolução das características clinicas de necrose, bem como a indução concomitante de ONJ, doença periodontal e doença sistêmica (artrite reumatoide) ainda são escassos. Em uma tentativa de esclarecer alguns dos questionamentos citados ao longo do texto com relação a patogênese de ONJ, nós dividimos este estudo em 3 capítulos nos quais os objetivos específicos de cada um serão explicados a seguir.

2 PROPOSIÇÃO

O presente estudo teve como objetivo desenvolver um modelo experimental de ONJ em camundongos e avaliar a influência de fatores de risco na incidência e severidade da doença. Para isto o estudo foi subdividido em 3 capítulos com objetivos específicos descritos a seguir:

Proposição específica publicação 1

Considerando que a patofisiologia de ONJ ainda não está totalmente estabelecida, o uso de modelos experimentais em animais, com particularidades que se assemelham com as características das condições humanas, se tornam ferramentas indispensáveis para fornecer estratégias de tratamento e prevenção. Assim, o objetivo do primeiro estudo foi desenvolver um novo modelo experimental de ONJ em camundongos, induzidos por diferentes inibidores de reabsorção óssea, associado com doença periodontal espontânea.

Proposição específica publicação 2

Considerando que as recomendações para reduzir o risco de incidência de ONJ ainda continuam altamente controversas e indefinidas, o objetivo do segundo estudo foi investigar se a descontinuação de diferentes inibidores de reabsorção óssea (*receptor activator of NF-kBligand (RANKL) inhibitor OPG-Fc, e Zoledronic Acid*) promoveria alteração nas características clinicas e radiográficas, e na diminuição da incidência de ONJ em camundongos

Proposição específica publicação 3

Considerando que existem fatores de risco que aumentariam as chances do desenvolvimento de ONJ, incluindo dose e duração dos medicamentos, doenças sistêmicas, infecção bacteriana, entre outras, o objetivo do terceiro estudo foi avaliar interações entre artrite reumatoide e ONJ em camundongos utilizando-se diferentes modelos de indução de ONJ na maxila e mandíbula por meio de análises tomográfica e histológica.

Bone 68 (2014) 11–19

Contents lists available at ScienceDirect

Bone

journal homepage: www.elsevier.com/locate/bone

Original Full Length Article

Spontaneous osteonecrosis of the jaws in the maxilla of mice on antiresorptive treatment: A novel ONJ mouse model

Rafael Scaf de Molon [a,b,1], Simon Cheong [c,1], Olga Bezouglaia [a], Sarah M. Dry [d], Flavia Pirih [e], Joni Augusto Cirelli [b], Tara L. Aghaloo [a,*], Sotirios Tetradis [a,f,**]

[a] Division of Diagnostic and Surgical Sciences, UCLA School of Dentistry, Los Angeles, CA 90095, USA
[b] Department of Diagnosis and Surgery, School of Dentistry at Araraquara, São Paulo State University, Araraquara 14801–903, Brazil
[c] Ostrow School of Dentistry, University of Southern California, Los Angeles, CA, USA
[d] Department of Pathology and Laboratory Medicine, David Geffen School of Medicine at UCLA, Los Angeles, CA 90095, USA
[e] Division of Associated Specialties, UCLA School of Dentistry, Los Angeles, CA 90095, USA
[f] Molecular Biology Institute, UCLA, Los Angeles, CA 90095, USA

ARTICLE INFO

Article history:
Received 26 April 2014
Revised 2 July 2014
Accepted 20 July 2014
Available online 2 August 2014

Edited by: Robert Recker

Keywords:
Osteonecrosis of the jaw
ONJ
Antiresorptives
Bisphosphonates
Alveolar bone
Osteoclasts

ABSTRACT

Although osteonecrosis of the jaws (ONJ), a serious complication of antiresorptive medications, was reported a decade ago, the exact mechanisms of disease pathophysiology remain elusive. ONJ-like lesions can be induced in animals after antiresorptive treatment and experimental interventions such as tooth extraction or periapical or periodontal disease. However, experimental induction and manipulation of disease progression does not always reflect clinical reality. Interestingly, naturally occurring maxillofacial abscesses, inducing aggressive inflammation of the peri-radicular mucosa with significant osteolysis and alveolar bone expansion, have been reported in mice. Here, we aimed to explore whether osteonecrotic lesions would develop in areas of maxillary peri-radicular infections, in mice on antiresorptive medications with distinct pharmacologic action, thus establishing a novel ONJ animal model. Mice were treated with RANK-Fc or OPG-Fc that bind to RANKL or with the potent bisphosphonate zoledronic acid (ZA). Maxillae were assessed radiographically and histologically. μCT imaging of vehicle mice revealed several maxillae with altered alveolar bone morphology, significant ridge expansion and large lytic areas. However, in RANK-Fc, OPG-Fc and ZA treated animals the extent of bone loss was significantly less, but exuberant bone deposition was noted at the ridge periphery. BV and BV/TV were increased in the diseased site of antiresorptive vs. veh animals. Histologically, extensive inflammation, bone resorption and marginal gingival epithelium migration were seen in the diseased site of vehicle animals. Rank-Fc, OPG-Fc and ZA reduced alveolar bone loss, increased periosteal bone formation, and induced areas of osteonecrosis, and bone exposure that in many animals covered significant part of the alveolar bone. Collectively, our data demonstrate ONJ-like lesions at sites of maxillary peri-radicular infection, indistinguishable in mice treated with RAKL inhibitors vs. zoledronate. This novel mouse model of spontaneous ONJ supports a central role of osteoclast inhibition and infection/inflammation in ONJ pathogenesis and validates and complements existing animal models employing experimental interventions.

© 2014 Elsevier Inc. All rights reserved.

Introduction

Osteonecrosis of the jaws (ONJ) is a serious side effect of antiresorptive medications such as bisphosphonates (BPs) and denosumab that ranges in severity from painless, small areas of exposed bone to significant bone exposure associated with severe pain, sequestration, infection, fistula or jaw fracture [1–3]. Although many clinical and animal studies attempt to characterize features of ONJ, the pathogenetic mechanisms of the disease remain elusive [4–6].

Osteoclastic inhibition appears central in the disease process since agents that target osteoclast function, but with distinct pharmacologic properties result in the same clinical outcome [1,4–7]. Bisphosphonates and particularly nitrogen-containing ones, such as zoledronic acid (ZA), pamidronate, and alendronate, inhibit farnesyl diphosphate synthase in the cholesterol biosynthesis pathway, which prevents prenylation of small guanosine triphosphatase (GTPase) signaling proteins [8,9]. As a result, BPs inhibit functioning osteoclasts by impairing differentiation,

* Correspondence to: T.L. Aghaloo, Diagnostic and Surgical Sciences, UCLA School of Dentistry, 10833 Le Conte Ave. CHS Rm. 53–009, Los Angeles, CA 90095–1668, USA. Fax: +1 310 825 7232.
** Correspondence to: S. Tetradis, Diagnostic and Surgical Sciences, UCLA School of Dentistry, 10833 Le Conte Ave. CHS Rm. 53–068, Los Angeles, CA 90095–1668, USA. Fax: +1 310 825 7232.
E-mail addresses: taghaloo@dentistry.ucla.edu (T.L. Aghaloo), stetradis@dentistry.ucla.edu (S. Tetradis).
[1] These authors contributed equally to this work.

http://dx.doi.org/10.1016/j.bone.2014.07.027
8756-3282/© 2014 Elsevier Inc. All rights reserved.

disrupting the cytoskeleton, decreasing intracellular transport, and inducing apoptosis [9,10]. In contrast, denosumab binds directly to the receptor activator of nuclear factor kappa-B (RANK) ligand (RANKL) to prevent its interaction with RANK on osteoclasts. This binding inhibits osteoclast formation, differentiation, and function [11]. Although acting through diverse mechanisms, both BPs and denosumab show similar prevalence of ONJ in patients with multiple myeloma, breast, and prostate cancer [12–14].

ONJ occurs mostly after tooth extraction or around teeth with dental disease [15,16]. Teeth in adult patients are extracted mainly as a result of unrestorable caries or periodontal disease [17,18]. Thus, infection/inflammation due to dental disease appears to be present in most ONJ cases. Paralleling these clinical observations, animal findings demonstrate ONJ-like lesions after experimental interventions such as tooth extraction or periapical or periodontal disease [19–30]. These interventions are employed to simulate clinical scenarios that precipitate disease pathogenesis in a controlled and reproducible manner.

Interestingly, naturally occurring maxillofacial abscesses have been described in mice [31]. Hair impaction from grooming enters the oral cavity, and inserts into the gingival sulcus where bacterial colonization occurs [31–33]. This natural process leads to the development of reproducible bone disease in C57BL/6 mice, which serves as an interesting contrast to the experimentally induced dental disease studies in mice and rats [19,20,23].

Here capitalizing on the natural occurrence of alveolar lesions, we aimed to explore the radiographic and histologic changes in the maxillae of mice treated with agents possessing distinct pharmacologic inhibition of osteoclastic activity. Our data suggest that in this novel ONJ animal model, naturally occurring peri-radicular infection and antiresorptive treatment are sufficient to induce osteonecrotic lesions in the mouse maxilla.

Materials and Methods *

Animal Care

Animals were kept and treated according to guidelines of the UCLA Chancellor's Animal Research Committee. Throughout the experimental period, mice were housed in plastic cages, fed a standard laboratory diet, and given water ad libitum. Seventy-six 4-month old C57BL/6J male mice (Jackson Laboratories, Bar Harbor, ME, USA) received intraperitoneal (IP) injections of veh (endotoxin free saline) or 200 μg/kg zoledronic acid (ZA, Z-5744 LKT Laboratories, St. Paul, MN) three times per week or 10 mg/kg mouse RANK-Fc (composed of the extracellular domain of RANK fused to the Fc portion of IgG [34], kindly provided by Amgen, Inc., Thousand Oaks, CA) three times per week, or 10 mg/kg rat OPG-Fc (composed of the RANKL-binding domains of osteoprotegerin linked to the Fc portion of IgG [34,35], kindly provided by Amgen, Inc., Thousand Oaks, CA) once per week for a total of 12 weeks. The time and dose of these antiresorptives have been previously shown to induce ONJ-like lesions in mice with periapical disease [19,23]. There were 17 veh, 19 ZA, 20 OPG-Fc and 20 RANK-Fc treated animals. At the end of the experiment, animals were sacrificed via isoflurane overdose, and maxillae were dissected, placed in 4% paraformaldehyde for 48 hours and stored in 70% ethanol.

μCT Scanning

Dissected maxillae were imaged by μCT scanning (μCT SkyScan 1172; SkyScan, Kontich, Belgium) utilizing 57 kVp, 184 μA, 0.5 mm aluminum filtration and 10 μm resolution. For linear measurements, volumetric image data were converted to DICOM format and imported in the Dolphin Imaging software (Chatsworth, CA) to generate 3D and multiplanar reconstructed images. The periodontal ligament (PDL) space width was measured at the furcation area of the first molar. The cemento-enamel junction (CEJ) to the alveolar crest (AC) distance was measured at the distal surface of the first molar. Both measurements were performed on a sagittal slice through the middle of the furcation area along the mesio-distal axis of the teeth, as previously described [19]. To assess alveolar bone thickness, axial slices were oriented parallel to the occlusal plane and the bone width was measured at the buccal side of the alveolar ridge at the level of the apical third of the roots.

To measure alveolar bone volume (BV) and tissue volume (TV), a region of interest (ROI) was delineated from the mesial root of the first molar to the distal root of the third molar, and from the alveolar crest to the root apices, comprising the entire alveolar bone. The teeth roots were not included in the ROI. BV and TV were measured utilizing the CtAn software (CT Analyzer 1.10.1.0 - Skyscan, Kontich, Belgium).

Histology and TRAP staining

Maxillae were decalcified in 14.5% ethylenediaminetetraacetic acid (EDTA) solution for 3 weeks. Samples were paraffin embedded and 5 μm-thick cross sections were made perpendicular to the long axis of the alveolar ridge at the area of maximum radiographic changes, as assessed by μCT analysis. If no radiographic evidence of disease was present in either of the sides of the alveolar bone, then sections were made along the distal root of the first molar. Hematoxylin and eosin (H&E) stained slides were digitally scanned utilizing the Aperio AT automated slide scanner and the Aperio ImageScope software (Aperio Technologies, Inc., Vista, CA, USA). The area of the alveolar bone, from the alveolar crest to the superior border of the alveolar bone and the floor of the nasal cavity, was defined as the region of interest (ROI). All subsequent measurements were made in this area.

Histologic measurements were made as previously described [19]. The distance between the most apical point of the junctional epithelium to the most coronal point of the alveolar crest (JE-AC) was measured on the palatal side of the maxilla. Periosteal bone thickness was assessed by measuring the three greatest areas of palatal or buccal periosteal thickness that were then averaged. The total number of osteocytic lacunae, the number of empty lacunae, the surface of total bone area and the surface of osteonecrotic area(s) were quantified. An area of osteonecrosis was defined as a loss of more than five contiguous osteocytes with confluent areas of empty lacunae. All histology and digital imaging was performed at the Translational Pathology Core Laboratory (TPCL) at UCLA.

For enumeration of osteoclasts, tartrate-resistant acid phosphatase (TRAP) staining was performed from all the groups utilizing the leukocyte acid phosphatase kit (387A-IKT Sigma Aldrich, St. Louis, MO, USA). Positive cells were identified as multinucleated (≥3) TRAP-positive cells in contact with or very close proximity to the bone surface, in the ROI.

Statistics

Raw data were analyzed using the GraphPad Prism Software (GraphPad Software, Inc., La Jolla, CA). Descriptive statistics were used to calculate the mean and the standard error of the mean (SEM). Data among groups were analyzed using one-way analysis of variance (ANOVA) followed by the post-hoc Tukey's test for multiple comparisons. Data between groups (healthy vs. diseased) were compared using the Student's t test. Categorical data (Table 1) were analyzed using the Fisher's exact test.

Results

μCT imaging of the maxillae revealed many animals with normal alveolar bone architecture, reflected by a uniform periodontal ligament (PDL) space (Fig. 1, thin arrow) and a continuous thin lamina dura around the roots of the teeth in all treatment groups. However, several veh treated mice presented altered alveolar bone morphology. Large lytic areas were noted around the roots and the furcational area of the

* Ver anexo A

Table 1
Radiographic and histologic findings in veh and antiresorptive treatment groups.

Group	Total hemimaxillae	Healthy (%)	Diseased (%)	Bone expansion (%)	Osteonecrosis (%)	Bone exposure (%)
Veh	33	20 (60.6)*	13 (39.4)*	13 (39.4)* (100)#	0** (0)* (0)#	0** (0)* (0)# (0)+
RANK-Fc	40	19 (47.5)*	21 (52.5)*	21 (52.5)* (100)#	10 (25)* (47)#	7 (17.5)* (33.3)# (70)+
OPG-Fc	40	19 (47.5)*	21 (52.5)*	21 (52.5)* (100)#	15 (37.5)* (71)#	11 (27.5)* (52)# (73)+
ZA	38	16 (42)*	22 (58)*	22 (58)* (100)#	10 (26.3)* (45)#	8 (21)* (36.4)# (80)+

** Statistically significantly different compared to the RANK-Fc, OPG-Fc or ZA groups, $p < 0.05$.
* % of total hemimaxillae.
# % of diseased hemimaxillae.
+ % of hemimaxillae with osteonecrosis.

maxillary molars that in select animals extended almost to the root apex and surrounded the entire root (Fig. 1, arrow). Additionally, significant superior, buccal and palatal expansion of the alveolar ridge was observed (Fig. 1, arrowheads). Several RANK-Fc, OPG-Fc and ZA treated animals showed similar lytic lesions to the veh group, although the extent of bone loss was significantly less (Fig. 1, arrows). Substantial periosteal bone apposition was noted at the periphery of the alveolar ridge that resulted in marked bone expansion (Fig. 1, arrowheads). The radiographic appearance of the alveolar bone was indistinguishable among the RANK-Fc, OPG-Fc or ZA groups.

To quantify the amount of bone loss in the diseased sites, the distance from the cemento-enamel junction (CEJ) to the alveolar crest (AC) at the distal surface of the 1st molar was measured. An increased CEJ-AC distance denotes increased bone loss. Diseased vs. healthy sites demonstrated statistically significantly increased CEJ-AC distance for all treatment groups (Fig. 2A). Importantly, statistically significantly larger CEJ-AC distance was seen in the diseased site of veh group compared to the same site in the RANK-Fc, OPG-Fc and ZA groups (Fig. 2A). No difference among the three antiresorptive treated groups was detected.

To evaluate effects on PDL space, the PDL space width was assessed at the furcation of the first maxillary molars [19,20,23]. No differences were seen among the healthy sites in any of the treatment groups. For all groups, a statistically significant widening of the PDL space was observed in the diseased vs. healthy sites (Fig. 2B). Diseased sites in veh treated animals showed a significantly higher increase in PDL space width compared to the antiresorptive treatment groups (Fig. 2B).

To quantify the alveolar bone expansion, the buccal bone thickness at the level of the apical third of the roots was measured (Fig. 2C). A significant expansion of the alveolar bone was seen at the diseased vs. healthy site in all groups. However, a statistically significantly greater increase was present in the RANK-Fc, OPG-Fc and ZA vs. veh groups, while no difference was detected among antiresorptive treated animals (Fig. 2C).

To evaluate the overall effects of the maxillary infection and antiresorptive treatment in the bone architecture, BV, TV and BV/TV of

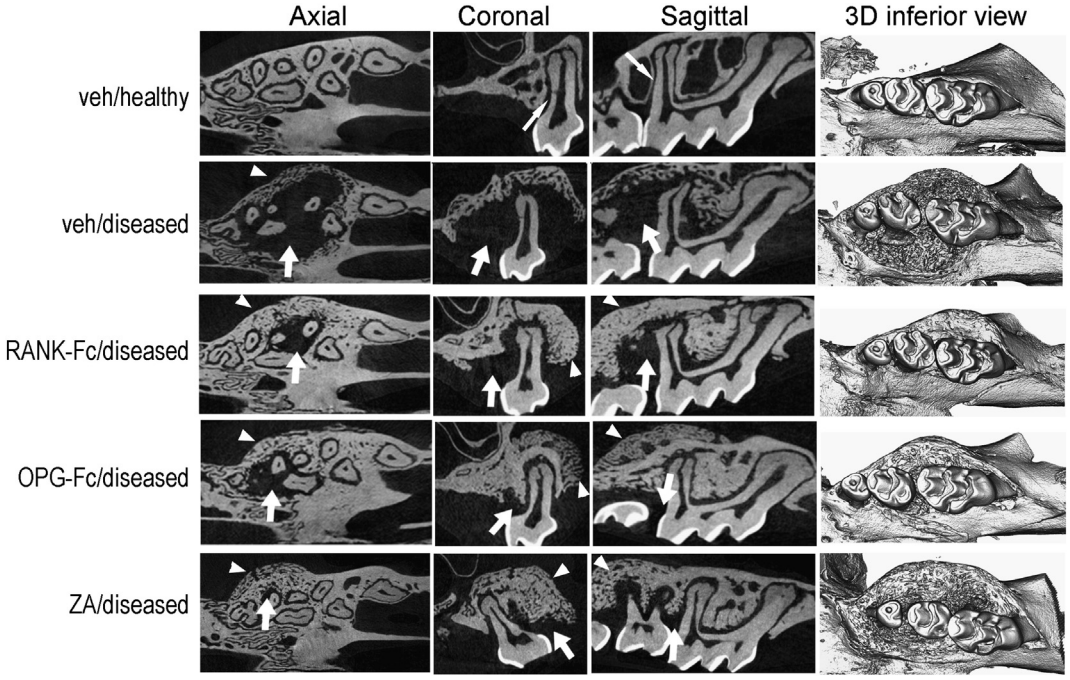

Fig. 1. Radiographic changes of the maxillary alveolar ridge. Representative axial, coronal and sagittal μCT slices and three-dimensional views of the maxillary molars of healthy (veh) or diseased site from veh, RANK-Fc, OPG-Fc and ZA treated animals are shown. Thin arrows point to the lamina dura around the roots of the veh/healthy animals. Thick arrows point to areas of osteolysis and arrowheads to areas or bone expansion in the diseased site of veh, RANK-Fc, OPG-Fc and ZA treated mice.

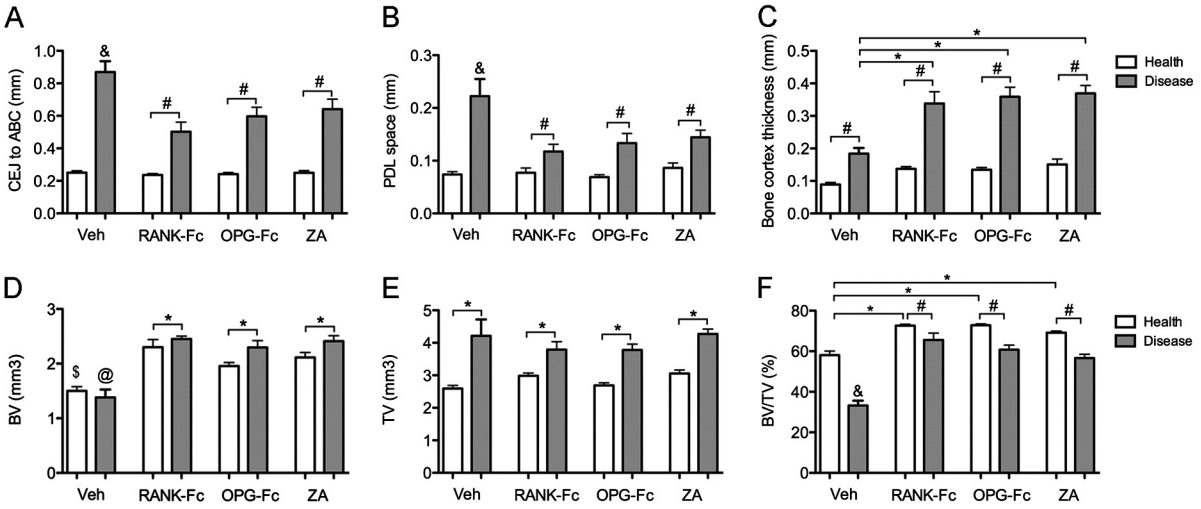

Fig. 2. Quantification of radiographic findings in the healthy and diseased sites of veh, RANK-Fc, OPG-Fc and ZA treated mice. To quantify amount of bone loss, the distance from the CEJ to the alveolar bone crest (ABC) was measured at the distal surface of the 1st molar (A) and the width of the PDL space was measured at the furcation area of the 1st molar (B). To assess alveolar bone expansion, the thickness of the buccal bone was measured, at the level of the apical third of the roots (C). To quantify the changes in the bone architecture, BV (D), TV (E) and BV/TV (F) were measured at the area of the alveolar ridge. &, statistically significantly different from healthy veh, diseased RANK-Fc, diseased OPG-Fc or diseased ZA, $p < 0.001$. *, statistically significantly different from indicated groups, $p < 0.05$. #, statistically significantly different from indicated groups, $p < 0.01$. $, statistically different from healthy RANK-Fc, healthy OPG-Fc or healthy ZA, $p < 0.01$. @, statistically significantly different from diseased RANK-Fc, diseased OPG-Fc or diseased ZA, $p < 0.01$.

the alveolar ridge were measured (Fig. 2D–F). No difference was seen between the healthy vs. diseased sites in veh animals. Healthy alveolar bone in RANK-Fc, OPG-Fc and ZA showed a similar increase in BV vs. the veh group. Diseased sites in the antiresorptive treated mice showed an even further increase in BV, compared to the healthy site of the same animals or the healthy or diseased site of the veh group (Fig. 2D). TV was similarly increased in the diseased site of all groups (Fig. 2E), reflecting the observed alveolar bone expansion. BV/TV was significantly decreased in the diseased site of veh group compared to the healthy site of the same animals, but also compared to the healthy or diseased site of all antiresorptive treatment groups (Fig. 2F). As expected, antiresorptive vs. veh animals showed increased BV/TV in the healthy sites (Fig. 2F). Finally, a small but statistically significant decrease in BV/TV was noted for the diseased vs. healthy site in each of the RANK-Fc, OPG-Fc and ZA groups (Fig. 2F).

After μCT assessment, histologic evaluation of the maxillae was performed (Fig. 3). Healthy sites in all groups showed normal alveolar bone and marginal epithelium (Fig. 3A–D, turquoise and red arrows).

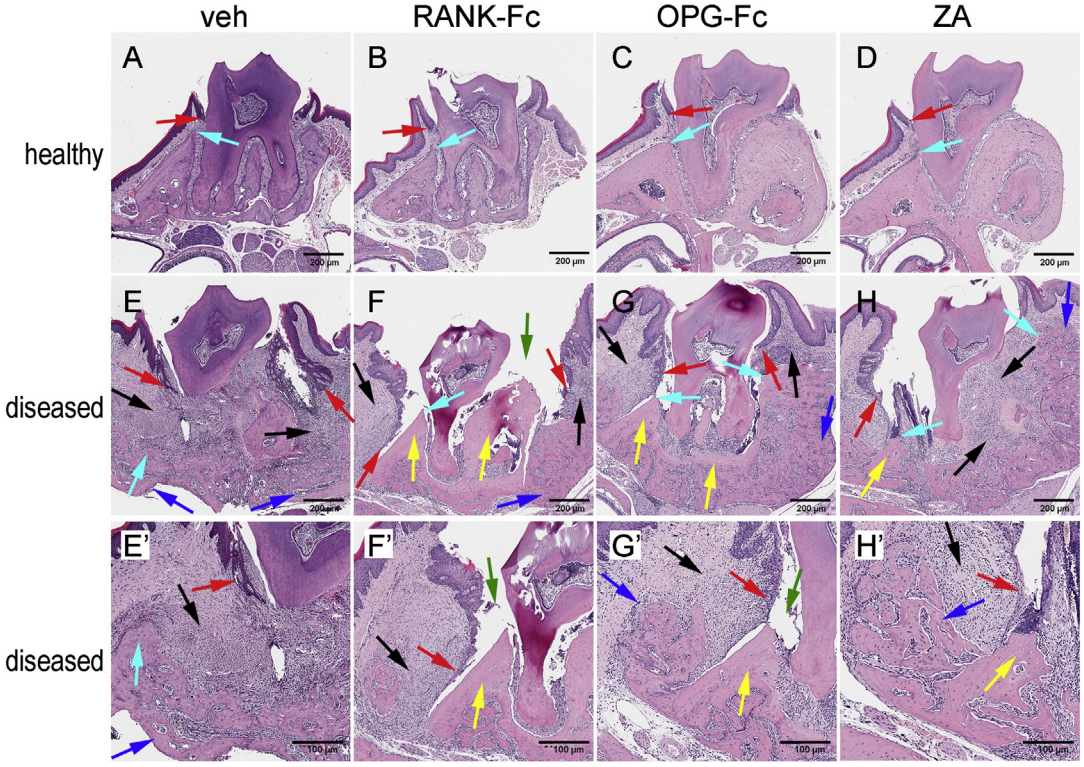

Fig. 3. Histologic examination of the periodontal and alveolar bone area. Healthy site of (A) veh, (B) RANK-Fc, (C) OPG-Fc, and (D) ZA treated animals. Diseases site of (E and E′) veh, (F and F′) RANK-Fc, (G and G′) OPG-Fc and (H and H′) ZA treated animals. Red arrows point to marginal gingival epithelium, turquoise arrows to alveolar crest, black arrows to areas of inflammation, blue arrows to periosteal bone deposition, yellow arrows to osteonecrotic areas, and green arrows to areas of bone exposure.

In vehicle treated animals, an abundant inflammatory infiltrate (Fig. 3E and E′, black arrows) composed of acute (neutrophils) and chronic (lymphocytes) inflammatory cells was noted. Inflammation was present in both the epithelium and underlying mucosa. Migration of the marginal epithelium (Fig. 3E and E′, red arrows) was paralleled by marked bone loss (Fig. 3E and E′, turquoise arrows) such that the marginal epithelium distance appeared increased. No histologic evidence of osteonecrosis was seen in any of the samples. However, new bone formation at the alveolar bone perimeter (Fig. 3E and E′, blue arrows) was present.

Comparable histologic features were present at the diseased site among animals treated with all three antiresorptive treatments—RANK-Fc (Fig. 3F and F′), OPG-Fc (Fig. 3G and G′) and ZA (Fig. 3H and H′). Similar to the veh treated animals, abundant mixed (acute and chronic) inflammatory infiltrate was noted in both the epithelium and soft tissue (Fig. 3F, F′, G, G′, H, and H′, black arrows). Bone loss was present compared to healthy sites, but appeared less compared to the diseased site of the veh treated mice (Fig. 3F, F′, G, G′, H, and H′, turquoise arrows). However, marked marginal epithelium migration was noted (Fig. 3F, F′, G, G′, H, and H′, red arrows), such that the epithelium to alveolar crest distance was reduced. Areas of osteonecrosis, with empty osteocytic lacunae, were present in many specimens from the diseased site of all antiresorptive treated animals (Fig. 3F, F′, G, G′, H, and H′, yellow arrows). In several specimens, the necrotic bone was not covered by oral mucosa, but was exposed to the oral cavity (Fig. 3F, F′, and G′, green arrows).

Three main patterns of histologic appearance were noted in the diseased site of antiresorptive treated animals (Fig. 4) that were indistinguishable among the antiresorptive treatment groups (RANK-Fc (Fig. 4A–C), OPG-Fc (Fig. 4D–F) or ZA (Fig. 4G–I). First, abundant inflammation and periosteal bone formation were present (Fig. 4A, D, and G, black and blue arrows). However, no areas of osteonecrosis were detected. Second, in addition to the inflammatory bone changes, specimens showed areas of osteonecrosis with empty osteocytic lacunae (Fig. 4B, E, and H, black, blue and yellow arrows). Epithelial migration towards the osteonecrotic areas was noted; however, no bone exposure was observed (Fig. 4B). The third pattern, in addition to inflammation and osteonecrosis, presented with bone exposure (Fig. 4C, F, and I, black, yellow and green arrows). Significant epithelial migration along the surface of the necrotic bone to the level of vital bone resulted in significant exposure of the osteonecrotic areas to the oral cavity (Fig. 4C, F, and I, red arrows) that included the palatal alveolar ridge and extended nearly to the midline.

Table 1 summarizes the radiographic and histologic observations of these studies. The incidence of peri-radicular disease in the various treatment groups ranged from 39.4 to 58% with no statistical significant differences detected among the various groups. The diseased site of all animals showed alveolar bone expansion, irrelevant of the treatment. Osteonecrosis and bone exposure were only observed in animals on antiresorptives. Interestingly, only 45–71% of the diseased hemimaxillae showed areas of osteonecrosis. However, from the sites with osteonecrosis, 70–80% presented with bone exposure. No difference on the incidence of osteonecrosis or bone exposure was detected among RANK-Fc, OPG-Fc or ZA treated groups.

We then quantified histologic findings and performed comparisons among treatment groups. A significant increase of the JE-AC distance was noted for the diseased site of the veh treated group, probably reflecting the significant periradicular bone loss (Fig. 5A). In contrast,

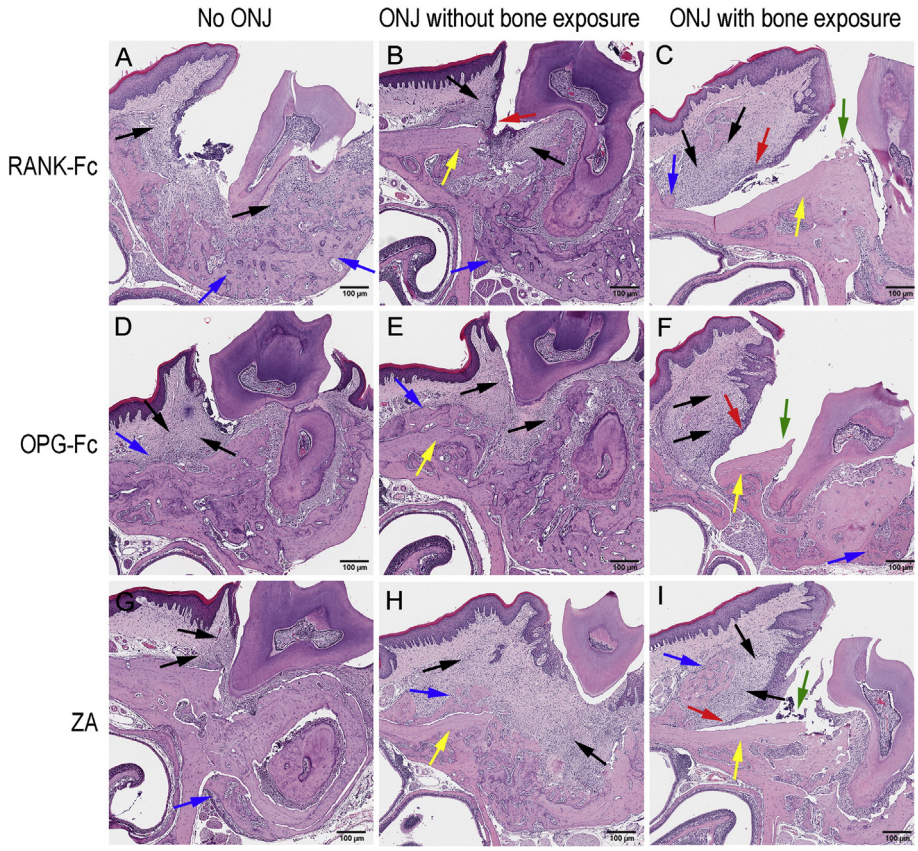

Fig. 4. Three histologic presentations of the diseased site in mice treated with antiresorptives. (A–C) RANK-Fc treated animals. (D–F) OPG-Fc treated animals. (G–I) ZA treated animals. No osteonecrosis (A, D, and G), presence of osteonecrosis (B, E, and H), and presence osteonecrosis (C, F, and I) with bone exposure were noted. Red arrows point to marginal gingival epithelium, black arrows to areas of inflammation, blue arrows to periosteal bone deposition, yellow arrows to osteonecrotic areas, and green arrows to areas of bone exposure.

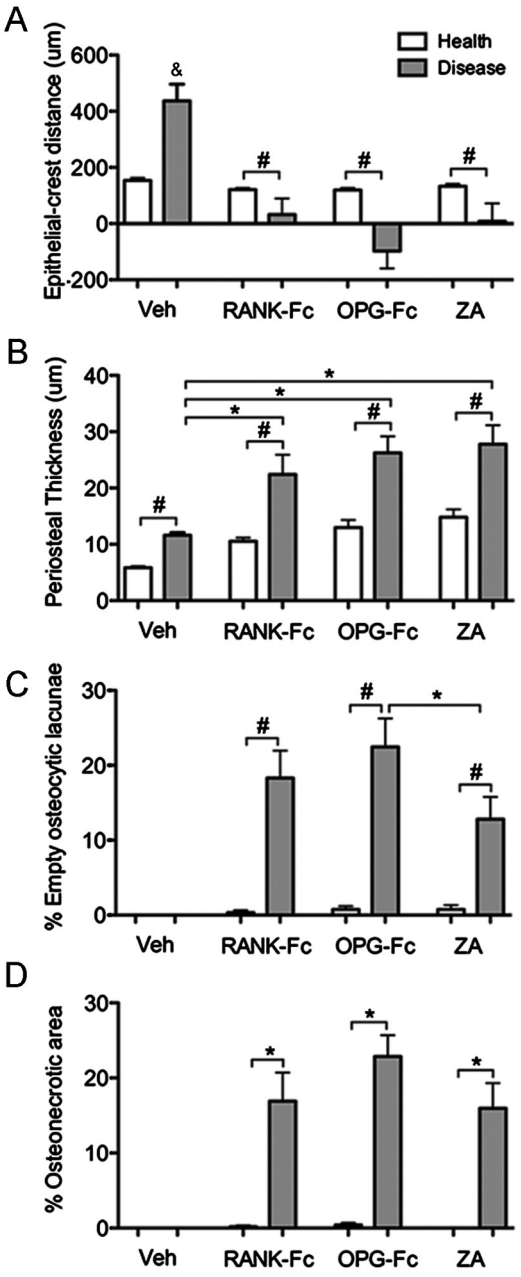

Fig. 5. Quantification of the histologic findings in the healthy and diseases sites of veh, RANK-Fc, OPG-Fc and ZA treated animals. (A) The shortest epithelial-crest distance was determined. If epithelium extended below the level of the alveolar crest, a negative value was assigned to the measurements. (B) Periosteal thickness, (C) % empty osteocytic lacunae and (D) % osteonecrotic area. &, statistically significantly different from healthy veh, diseased RANK-Fc, diseased OPG-Fc or diseased ZA, $p < 0.001$. *, statistically significantly different from indicated groups, $p < 0.05$. #, statistically significantly different from indicated groups, $p < 0.01$.

antiresorptive treatment reversed the effect on the JE-AC distance that was shorter in the diseased vs. healthy sites for RANK-Fc, OPG-Fc and ZA treated groups, likely as a result of junctional epithelium migration, but reduced bone resorption (Fig. 5A). Periosteal thickness significantly increased in the diseased vs. healthy site for all groups. However, this increase was greater for the RANK-Fc, OPG-Fc or ZA vs. veh treated animals (Fig. 5B).

To evaluate the effect of antiresorptives on osteocytes and induction of osteonecrosis, the number of empty osteocytic lacunae (Fig. 5C) and the osteonecrotic surface area (Fig. 5D) were evaluated at the area of the maxillary alveolar ridge. No empty osteocytic lacunae or areas of osteonecrosis were detected in the healthy or diseased sites of the veh treated mice. Healthy sites of RANK-Fc, OPG-Fc and ZA treated animals showed a slight increase in the number of empty osteocytic lacunae that did not reach statistical significance (Fig. 5C). In contrast, significant increase of empty osteocytic lacunae (Fig. 5C) and areas of osteonecrosis (Fig. 5D) were present in the diseased site of RANK-Fc, OPG-Fc or ZA treated mice. A small but significantly higher number of empty osteocytic lacunae was seen in the diseased site of OPG-Fc vs. ZA treated mice (Fig. 5C). However, no difference in osteonecrotic areas was noted among the three antiresorptive treatments (Fig. 5D). The osteonecrotic areas covered 16.9 %, 22.9 %, and 16.0 % of the ROI and measured 135,479 +/− 31,403, 180,368 +/− 25,106, and 139,440 +/− 39,923 μm^2 for RANK-Fc, OPG-Fc and ZA groups, respectively.

To evaluate the effect of the antiresorptive treatments on osteoclast numbers, TRAP staining was performed (Fig. 6). Few TRAP+ cells were observed at the healthy site (Fig. 6A) and were significantly increased at the diseased site (Fig. 6E) of the veh treated animals. As expected, RANK-Fc and OPG-Fc treatment nearly abolished osteoclast formation in both healthy and diseased sites (Fig. 6B, C, F, and G) Interestingly, TRAP+ cells that significantly increased in the diseased site were noted in ZA treated animals (Fig. 6D and H). However, TRAP+ cells in ZA treated animals showed a round shape with pyknotic nuclear morphology and were detached and at times moved from the bone surface (Fig. 6I). Quantification of TRAP staining revealed significant inhibition of osteoclast formation by RANK-Fc and OPG-Fc treatment compared to control and ZA groups (Fig. 6J). No statistical difference of the TRAP+ cell number between the diseased site of veh vs. ZA treated mice was found (Fig. 6I).

Discussion

ONJ occurs mainly after tooth extraction in patients treated with medications that target osteoclastic function and activity, such as BPs and denosumab, for the treatment of neoplastic or metabolic bone disease [2,36]. Several animal models have utilized tooth extraction and high-dose BPs to reproduce clinical, radiographic and histologic features of the human disease [21,24,37].

Since the great majority of tooth extractions in adults is due to advanced carious lesions or periodontal bone loss [17,18], and given that dental preventive measures reduce the risk for ONJ [38,39] and that a significant number of ONJ cases occurs in the absence of tooth extraction, we have hypothesized that dental disease plays a key role in ONJ pathogenesis [19,20,23]. Indeed, we and others have presented rat and mouse ONJ models in the absence of tooth extraction but in the presence of aggressive periodontitis or periapical disease in animals treated with high dose BPs [20,22,23,26] or RANKL inhibitors [19], thus pointing to a central role of infection/inflammation in ONJ pathophysiology [4–6].

For these ONJ animal models, established models of experimental dental disease were employed. Advantages of such approaches are the well characterized progression of dental disease, the localization of dental disease in a split-mouth design providing internal controls, and the control of onset of dental disease in relation to administration of antiresorptive medication. However, experimental induction and manipulation of disease progression does not always reflect clinical reality. To that effect, several ONJ animal models utilize extraction of healthy teeth [21,24,25,27–30], which are rarely extracted in ONJ patients. Similarly, ONJ animal models utilizing periodontitis [20,22,26] employ experimental procedures that depict some, but not necessarily all the components of the pathological process of human periodontal disease [40]. Finally, in ONJ models of antiresorptives and periapical disease drilling the crown of molars to induce pulpal exposure [22,26], although captures the pathophysiologic progression of pulp necrosis and periapical infection does not reflect the natural pulpal infection through deep carious lesions.

Naturally occurring maxillofacial abscesses have been reported in mice, including the inbred C57BL/6 strain [31–33]. The mice develop these abscesses from barbering practices including grooming, plucking,

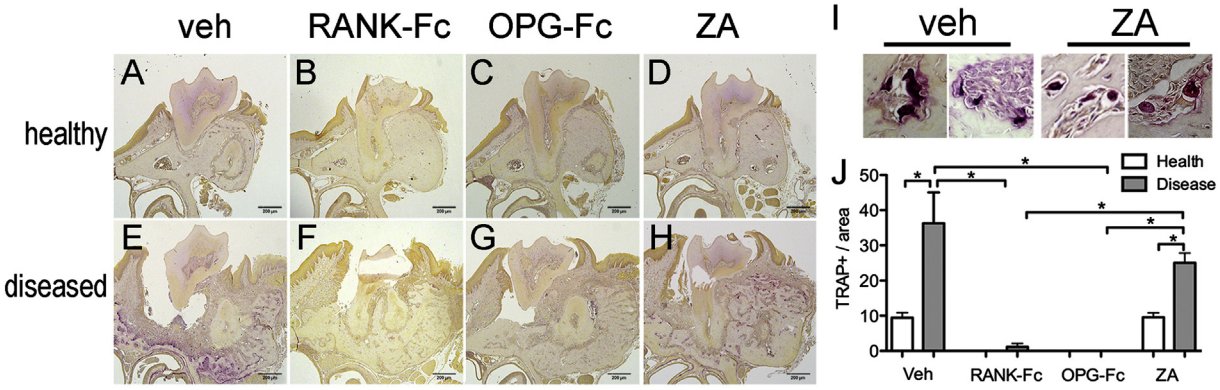

Fig. 6. TRAP staining on histologic sections from healthy (A–D) and diseased sites (E–H) from veh, RANK-Fc, OPG-Fc and ZA treated animals respectively. Select TRAP+ multinucleated cells from veh (I) and ZA (J) treated mice. Quantification TRAP+ cells in the veh, RANK-Fc, OPG-Fc and ZA treated animals (K). *Statistically significantly different, $p < 0.05$.

or eating fur or whiskers of cage-mates or oneself [41–43]. C57BL/6 mice are one of the most common rodent strains where barbering, mastication, and fragmentation of hair occur [41,43]. Here, the foreign body gets into the oral cavity, pierces the gingival sulcus, and induces dental disease [31]. After hair impaction, bacterial colonization occurs, and cultures consistently reveal Staphylococcus aureus isolated from the abscesses [31–33]. μCT of these areas demonstrates osteolysis with severe bone loss surrounding the molar roots and expansion of the alveolar bone [31]. Histologically, severe inflammatory infiltrate with presence of neutrophils and mononuclear inflammatory cells is reported [31,32]. Intrigued by this spontaneous occurrence of peri-radicular infection and resultant extensive inflammation, we investigated the potential development of ONJ-like lesions in the maxillae of mice that had been treated with high-dose antiresorptive medications, thus establishing a novel ONJ animal model. An advantage of this model is the natural occurrence or peri-radicular infection/inflammation, without the need of experimental interventions.

We utilized two classes of antiresorptive agents with distinct pharmacologic actions. RANK-Fc and OPG-Fc bind and inhibit RANKL function and were used as a surrogate for denosumab, since denosumab recognizes the human but not mouse RANKL [34]. Both RANK-Fc and OPG-Fc bind RANKL and potently inhibit bone resorption and increase bone volume in animal models [34,35]. The second type of antiresorptive was zoledronic acid (ZA), a potent nitrogen-containing bisphosphonate widely used in the management of bone malignancy [44]. Utilizing the employed treatment regimens for these antiresorptives, we have previously reported the successful inhibition of osteoclastic function and development of ONJ-like lesions in the mandible of mice around mandibular molars with experimental periapical disease [19,23].

Similar to published data [31,32], μCT assessment of the alveolar bone revealed significant peri-radicular osteolysis and expansion of the buccal and palatal cortices of the alveolar ridge in several veh treated mice. Antiresorptives attenuated interproximal and furcational bone loss and increased overall alveolar bone volume at the diseased sites. These observations are in agreement with findings around experimental periodontal or periapical disease in rats or mice [19,20,23] and parallel clinical findings that demonstrate diffuse osteosclerosis with increased trabecular density and thickening of cortical outlines in areas of ONJ [45].

Histologically, the presence of intense inflammation, significant osteolysis and epithelial migration was seen in the periodontal tissues of several control (veh treated) mice, similar to previous reports [31,32]. Presence of inflammation was also noted on antiresorptive-treated groups. However, loss of osteocytes and presence of empty osteocytic lacunae consistent with osteonecrosis were also present in these animals. Presence of osteonecrosis has been described in animals on antiresorptives after tooth extraction or experimental disease, emphasizing the resemblance of the spontaneous ONJ-like lesions observed in our studies with other ONJ-animal models [19–30]. The similar radiographic and histologic disease presentation between this and other ONJ models [19–30], which parallels findings in ONJ patients, validates such animal models as capturing essential features of disease pathophysiology that lead to alveolar bone osteonecrosis.

A noteworthy observation in our studies was the great similarity in the radiographic and histologic findings among the RANK-Fc, OPG-Fc and ZA treated groups, including the incidence of osteonecrosis and bone exposure. Indeed, to the best of our knowledge, this is the second report of antiresorptive treatment, other than bisphosphonates, inducing ONJ-like lesions in an animal model [19] and the first direct comparison of these different antiresorptive categories. Our findings parallel human data from BP vs. denosumab treated patients reporting a similar incidence of ONJ [12–14] and strongly point to a central role of osteoclastic inhibition in ONJ pathogenesis.

Utilizing this ONJ mouse model, we observed three histologic patterns at sites of disease that were similar for all three antiresorptives (Fig. 4 and Table 1). In the first pattern, significant inflammation throughout the alveolar ridge and varying amount of osteolysis were noted. However, similar to the veh treated group, no osteonecrosis was present. In the clinical setting, these animals could potentially parallel patients on antiresorptive medications and jaw inflammation but without any clinical or radiographic signs of ONJ. In the second pattern, osteonecrotic areas were present within the alveolar bone but were covered by oral mucosa. This disease appearance appears to parallel Stage 0 ONJ in patients with bone necrosis, but without clinical bone exposure [2]. Finally, in the third pattern the necrotic alveolar bone was not covered by oral mucosa but was exposed to the oral environment. This presentation is in line with the classic manifestation of clinical ONJ with varying degree of bone exposure and associated infection/inflammation (Stage 1–3 ONJ) [2]. Our present studies cannot address whether a transition from less towards higher stage ONJ exists, since we only examined the animals at a single time point. However, clinical data reporting 50% of patients with stage 0 disease developing clinical ONJ within 5 months of initial diagnosis [46] would argue for the progression of the less severe histologic osteonecrosis without bone exposure to the more severe presentation of bone necrosis and clinical exposure.

A surprising and interesting finding was the difference on osteonecrosis incidence in this ONJ mouse model with spontaneous maxillary infection vs. studies utilizing experimental periapical disease [19,23], although treatment regimens for various antiresorptives were the same. In the current study, approximately 50% of the animals with peri-radicular disease presented with areas of osteonecrosis. In contrast, 88% of ZA [23] or 100% of RANK-Fc or OPG-Fc [19] treated mice with experimental periapical disease showed osteonecrotic areas histologically.

A possible explanation for this finding is that maxilla (in the current study) vs. mandible [19,23] respond differently to bone turnover

suppression. In contrast to osteoradionecrosis that almost exclusively localizes to the mandible [47], ONJ appears to affect both jaws with high frequency. However, even in the case of ONJ the mandible appears to be more frequently affected, particularly in patients treated with antiresorptives for the treatment of osteoporosis [2,48,49]. The predilection of the mandible for osteonecrosis could be due to the decreased vascularity, thicker cortical borders and smaller percentage of trabecular bone [50,51].

A second possible explanation for this observation is the relation of antiresorptive administration with the disease onset. Maxillary lesions developed spontaneously without any intervention. Thus, some animals developed maxillary inflammatory lesions prior to, while others after the commencement of antiresorptives. In contrast, experimental periodontitis or periapical disease was induced after antiresorptive medications were administered [19,20,23,26]. Possibly the early stages of infection and resultant inflammatory response could play a crucial role in the alveolar bone response to turnover suppression. Such a premise would be significant from a clinical perspective, since it points to the potential association between antiresorptive administration and time of peri-radicular infection.

Interestingly, although osteonecrosis incidence was lower in the current ONJ model, bone exposure was more frequent and extensive compared to published studies [19,20,23]. Here, nearly 75% of animals with osteonecrosis showed bone exposure that at times involved a significant part of the maxillary alveolar bone. In contrast, only 28% of animals with osteonecrosis presented bone exposure that was mostly localized to the marginal periodontium when experimental periapical disease was induced [19,23]. The most likely explanation for these observations is the degree of infection and resultant inflammatory changes that in the current study extended to the whole alveolus and caused significant buccal and palatal bone deposition and marked ridge expansion.

Our findings have potentially significant implications for studies on ONJ animal models utilizing maxillary molar extraction, particularly if the C57BL6 strain of mice was used [21,24]. Since in many of these studies animals were pretreated with bisphosphonates prior to tooth extraction, the possible presence of naturally occurring peri-radicular lesions in some sites could complicate socket healing and confound ONJ incidence and severity.

In conclusion, our data offer potentially important insights into the mechanisms of ONJ. The nearly identical radiographic and histologic features of alveolar bone morphology and ONJ-like appearance between the RANKL inhibitors OPG-Fc and RANK-Fc, and the potent bisphosphonate ZA parallel clinical findings and strongly indicate a central role of osteoclasts in ONJ pathophysiology. The reduced incidence of osteonecrosis compared to previously published reports suggests the significance of the onset of infection/inflammation in relation to the commencement of antiresorptive treatment, while the increased frequency and extent of alveolar bone exposure points to the link between the severity of inflammation and clinical ONJ severity. From a practical point of view, our observations caution the design and interpretation of experimental findings utilizing interventional approaches, as they might be compounded by the occurrence of spontaneous ONJ lesions around naturally occurring maxillary lesions of animals treated with antiresorptives. Finally, this novel model of spontaneous ONJ validates, compliments and enhances published ONJ models that utilize tooth extraction or experimental induction of dental disease and strongly supports the central importance of infection/inflammation in combination with inhibition of osteoclastic function in ONJ pathogenesis.

Disclosures

Dr. Tetradis has served as a paid consultant for and has received grant support from Amgen Inc. All other authors state that they do not have any conflicts of interest.

Acknowledgments

This work was supported by grant support from Amgen Inc. and by NIH/NIDCR DE019465. de Molon RS was supported by fellowships from the State of Sao Paulo Research Foundation #2012/09968-5 and the Coordination for the Improvement of Higher Level -or Education-Personnel - #11575/13-1.

Authors' roles: All authors participated in the design, execution and analyses of the studies. TA, RSM, SC, and ST drafted the manuscript. All authors made revisions to the manuscript and approved the final version.

References

[1] Lipton A, Fizazi K, Stopeck AT, Henry DH, Brown JE, Yardley DA, et al. Superiority of denosumab to zoledronic acid for prevention of skeletal-related events: a combined analysis of 3 pivotal, randomised, phase 3 trials. Eur J Cancer 2012;48:3082–92.
[2] Ruggiero SL, Dodson TB, Assael LA, Landesberg R, Marx RE, Mehrotra B. American Association of Oral and Maxillofacial Surgeons position paper on bisphosphonate-related osteonecrosis of the jaws—2009 update. J Oral Maxillofac Surg 2009;67:2–12.
[3] Khosla S, Burr D, Cauley J, Dempster DW, Ebeling PR, Felsenberg D, et al. Bisphosphonate-associated osteonecrosis of the jaw: report of a task force of the American Society for Bone and Mineral Research. J Bone Miner Res 2007;22:1479–91.
[4] Allen MR, Burr DB. The pathogenesis of bisphosphonate-related osteonecrosis of the jaw: so many hypotheses, so few data. J Oral Maxillofac Surg 2009;67:61–70.
[5] Landesberg R, Woo V, Cremers S, Cozin M, Marolt D, Vunjak-Novakovic G, et al. Potential pathophysiological mechanisms in osteonecrosis of the jaw. Ann N Y Acad Sci 2011;1218:62–79.
[6] Yamashita J, McCauley LK. Antiresorptives and osteonecrosis of the jaw. J Evid Based Dent Pract 2012;12:233–47.
[7] Aghaloo TL, Felsenfeld AL, Tetradis S. Osteonecrosis of the jaw in a patient on denosumab. J Oral Maxillofac Surg 2010;68:959–63.
[8] Luckman SP, Hughes DE, Coxon FP, Graham R, Russell G, Rogers MJ. Nitrogen-containing bisphosphonates inhibit the mevalonate pathway and prevent post-translational prenylation of GTP-binding proteins, including Ras. J Bone Miner Res 1998;13:581–9.
[9] Kimmel DB. Mechanism of action, pharmacokinetic and pharmacodynamic profile, and clinical applications of nitrogen-containing bisphosphonates. J Dent Res 2007;86:1022–33.
[10] Suzuki K, Takeyama S, Sakai Y, Yamada S, Shinoda H. Current topics in pharmacological research on bone metabolism: inhibitory effects of bisphosphonates on the differentiation and activity of osteoclasts. J Pharmacol Sci 2006;100:189–94.
[11] Baron R, Ferrari S, Russell RG. Denosumab and bisphosphonates: different mechanisms of action and effects. Bone 2011;48:677–92.
[12] Dranitsaris G, Hatzimichael E. Interpreting results from oncology clinical trials: a comparison of denosumab to zoledronic acid for the prevention of skeletal-related events in cancer patients. Support Care Cancer 2012;20:1353–60.
[13] Saad F, Brown JE, Van Poznak C, Ibrahim T, Stemmer SM, Stopeck AT, et al. Incidence, risk factors, and outcomes of osteonecrosis of the jaw: integrated analysis from three blinded active-controlled phase III trials in cancer patients with bone metastases. Ann Oncol 2012;23:1341–7.
[14] Smith MR, Saad F, Coleman R, Shore N, Fizazi K, Tombal B, et al. Denosumab and bone-metastasis-free survival in men with castration-resistant prostate cancer: results of a phase 3, randomised, placebo-controlled trial. Lancet 2012;379:39–46.
[15] Ficarra G, Beninati F, Rubino I, Vannucchi A, Longo G, Tonelli P, et al. Osteonecrosis of the jaws in periodontal patients with a history of bisphosphonates treatment. J Clin Periodontol 2005;32:1123–8.
[16] Marx RE, Sawatari Y, Fortin M, Broumand V. Bisphosphonate-induced exposed bone (osteonecrosis/osteopetrosis) of the jaws: risk factors, recognition, prevention, and treatment. J Oral Maxillofac Surg 2005;63:1567–75.
[17] Chrysanthakopoulos NA. Reasons for extraction of permanent teeth in Greece: a five-year follow-up study. Int Dent J 2011;61:19–24.
[18] Phipps KR, Stevens VJ. Relative contribution of caries and periodontal disease in adult tooth loss for an HMO dental population. J Public Health Dent 1995;55:250–2.
[19] Aghaloo TL, Cheong S, Bezouglaia O, Kostenuik P, Atti E, Dry SM, et al. RANK-L inhibitors induce osteonecrosis of the jaw in mice with periapical disease. J Bone Miner Res 2013;29:843–54.
[20] Aghaloo TL, Kang B, Sung EC, Shoff M, Ronconi M, Gotcher JE, et al. Periodontal disease and bisphosphonates induce osteonecrosis of the jaws in the rat. J Bone Miner Res 2011;26:1871–82.
[21] Bi Y, Gao Y, Ehirchiou D, Cao C, Kikuiri T, Le A, et al. Bisphosphonates cause osteonecrosis of the jaw-like disease in mice. Am J Pathol 2010;177:280–90.
[22] Gotcher JE, Jee WS. The progress of the periodontal syndrome in the rice cat. II. The effects of a diphosphonate on the periodontium. J Periodontal Res 1981;16:441–55.
[23] Kang B, Cheong S, Chaichanasakul T, Bezouglaia O, Atti E, Dry SM, et al. Periapical disease and bisphosphonates induce osteonecrosis of the jaws in mice. J Bone Miner Res 2013;28:1631–40.
[24] Kikuiri T, Kim I, Yamaza T, Akiyama K, Zhang Q, Li Y, et al. Cell-based immunotherapy with mesenchymal stem cells cures bisphosphonate-related osteonecrosis of the jaw-like disease in mice. J Bone Miner Res 2010;25:1668–79.

[25] Sonis ST, Watkins BA, Lyng GD, Lerman MA, Anderson KC. Bony changes in the jaws of rats treated with zoledronic acid and dexamethasone before dental extractions mimic bisphosphonate-related osteonecrosis in cancer patients. Oral Oncol 2009; 45:164–72.
[26] Aguirre JI, Akhter MP, Kimmel DB, Pingel JE, Williams A, Jorgensen M, et al. Oncologic doses of zoledronic acid induce osteonecrosis of the jaw-like lesions in rice rats (Oryzomys palustris) with periodontitis. J Bone Miner Res 2012;27:2130–43.
[27] Lopez-Jornet P, Camacho-Alonso F, Martinez-Canovas A, Molina-Minano F, Gomez-Garcia F, Vicente-Ortega V. Perioperative antibiotic regimen in rats treated with pamidronate plus dexamethasone and subjected to dental extraction: a study of the changes in the jaws. J Oral Maxillofac Surg 2011;69:2488–93.
[28] Allen MR, Burr DB. Mandible matrix necrosis in beagle dogs after 3 years of daily oral bisphosphonate treatment. J Oral Maxillofac Surg 2008;66:987–94.
[29] Hokugo A, Christensen R, Chung EM, Sung EC, Felsenfeld AL, Sayre JW, et al. Increased prevalence of bisphosphonate-related osteonecrosis of the jaw with vitamin D deficiency in rats. J Bone Miner Res 2010;25:1337–49.
[30] Kuroshima S, Yamashita J. Chemotherapeutic and antiresorptive combination therapy suppressed lymphangiogenesis and induced osteonecrosis of the jaw-like lesions in mice. Bone 2013;56:101–9.
[31] Lawson GW. Etiopathogenesis of mandibulofacial and maxillofacial abscesses in mice. Comp Med 2010;60:200–4.
[32] Clarke MC, Taylor RJ, Hall GA, Jones PW. The occurrence in mice of facial and mandibular abscesses associated with Staphylococcus aureus. Lab Anim 1978;12: 121–3.
[33] Grant N, Jackson K, Lee R, Scharf B. Mandibular mass in a young Swiss-Webster mouse. Lab Anim (NY) 2002;31:25–6.
[34] Kostenuik PJ, Nguyen HQ, McCabe J, Warmington KS, Kurahara C, Sun N, et al. Denosumab, a fully human monoclonal antibody to RANKL, inhibits bone resorption and increases BMD in knock-in mice that express chimeric (murine/human) RANKL. J Bone Miner Res 2009;24:182–95.
[35] Lacey DL, Boyle WJ, Simonet WS, Kostenuik PJ, Dougall WC, Sullivan JK, et al. Bench to bedside: elucidation of the OPG-RANK-RANKL pathway and the development of denosumab. Nat Rev Drug Discov 2012;11:401–19.
[36] Barasch A, Cunha-Cruz J, Curro FA, Hujoel P, Sung AH, Vena D, et al. Risk factors for osteonecrosis of the jaws: a case–control study from the CONDOR dental PBRN. J Dent Res 2011;90:439–44.
[37] Ali-Erdem M, Burak-Cankaya A, Cemil-Isler S, Demircan S, Soluk M, Kasapoglu C, et al. Extraction socket healing in rats treated with bisphosphonate: animal model for bisphosphonate related osteonecrosis of jaws in multiple myeloma patients. Med Oral Patol Oral Cir Bucal 2011;16:e879–83.
[38] Dimopoulos MA, Kastritis E, Bamia C, Melakopoulos I, Gika D, Roussou M, et al. Reduction of osteonecrosis of the jaw (ONJ) after implementation of preventive measures in patients with multiple myeloma treated with zoledronic acid. Ann Oncol 2009;20:117–20.
[39] Ripamonti CI, Maniezzo M, Campa T, Fagnoni E, Brunelli C, Saibene G, et al. Decreased occurrence of osteonecrosis of the jaw after implementation of dental preventive measures in solid tumour patients with bone metastases treated with bisphosphonates. The experience of the National Cancer Institute of Milan. Ann Oncol 2009;20:137–45.
[40] Graves DT, Kang J, Andriankaja O, Wada K, Rossa Jr C. Animal models to study host-bacteria interactions involved in periodontitis. Front Oral Biol 2012;15:117–32.
[41] Kalueff AV, Minasyan A, Keisala T, Shah ZH, Tuohimaa P. Hair barbering in mice: implications for neurobehavioural research. Behav Processes 2006;71:8–15.
[42] Sarna JR, Dyck RH, Whishaw IQ. The Dalila effect: C57BL6 mice barber whiskers by plucking. Behav Brain Res 2000;108:39–45.
[43] Long SY. Hair-nibbling and whisker-trimming as indicators of social hierarchy in mice. Anim Behav 1972;20:10–2.
[44] Russell RG, Rogers MJ. Bisphosphonates: from the laboratory to the clinic and back again. Bone 1999;25:97–106.
[45] Arce K, Assael LA, Weissman JL, Markiewicz MR. Imaging findings in bisphosphonate-related osteonecrosis of jaws. J Oral Maxillofac Surg 2009;67:75–84.
[46] Fedele S, Porter SR, D'Aiuto F, Aljohani S, Vescovi P, Manfredi M, et al. Nonexposed variant of bisphosphonate-associated osteonecrosis of the jaw: a case series. Am J Med 2010;123:1060–4.
[47] Marx RE. Osteoradionecrosis: a new concept of its pathophysiology. J Oral Maxillofac Surg 1983;41:283–8.
[48] Ruggiero SL, Mehrotra B, Rosenberg TJ, Engroff SL. Osteonecrosis of the jaws associated with the use of bisphosphonates: a review of 63 cases. J Oral Maxillofac Surg 2004;62:527–34.
[49] Marx R. Oral and intravenous bisphosphonate induced osteonecrosis of the jaws: history, etiology, prevention, and treatment2nd ed. ; 2007.
[50] Devlin H, Horner K, Ledgerton D. A comparison of maxillary and mandibular bone mineral densities. J Prosthet Dent 1998;79:323–7.
[51] Kingsmill VJ, Gray CM, Moles DR, Boyde A. Cortical vascular canals in human mandible and other bones. J Dent Res 2007;86:368–72.

ORIGINAL ARTICLE

JBMR®

OPG-Fc but Not Zoledronic Acid Discontinuation Reverses Osteonecrosis of the Jaws (ONJ) in Mice

Rafael Scaf de Molon,[1,2] Hiroaki Shimamoto,[3] Olga Bezouglaia,[1] Flavia Q Pirih,[4] Sarah M Dry,[5] Paul Kostenuik,[6] Rogely W. Boyce,[7] Denise Dwyer,[7] Tara L Aghaloo,[1] and Sotirios Tetradis[1,8]

[1]Division of Diagnostic and Surgical Sciences, UCLA School of Dentistry, Los Angeles, CA, USA
[2]Department of Diagnosis and Surgery, School of Dentistry at Araraquara, S, ã, o Paulo State University, Araraquara, Brazil
[3]Department of Oral and Maxillofacial Radiology, Osaka University Graduate School of Dentistry, Osaka, Japan
[4]Division of Associated Specialties, UCLA School of Dentistry, Los Angeles, CA, USA
[5]Department of Pathology and Laboratory Medicine, David Geffen School of Medicine at UCLA, Los Angeles, CA, USA
[6]Department of Periodontics and Oral Medicine, School of Dentistry, University of Michigan, Ann Arbor, MI, USA
[7]Department of Comparative Biology and Safety Sciences, Amgen Inc., Thousand Oaks, CA, USA
[8]Molecular Biology Institute, UCLA, Los Angeles, CA, USA

ABSTRACT

Osteonecrosis of the jaws (ONJ) is a significant complication of antiresorptive medications, such as bisphosphonates and denosumab. Antiresorptive discontinuation to promote healing of ONJ lesions remains highly controversial and understudied. Here, we investigated whether antiresorptive discontinuation alters ONJ features in mice, employing the potent bisphosphonate zoledronic acid (ZA) or the receptor activator of NF-κB ligand (RANKL) inhibitor OPG-Fc, utilizing previously published ONJ animal models. Mice were treated with vehicle (veh), ZA, or OPG-Fc for 11 weeks to induce ONJ, and antiresorptives were discontinued for 6 or 10 weeks. Maxillae and mandibles were examined by μCT imaging and histologically. ONJ features in ZA and OPG-Fc groups included periosteal bone deposition, empty osteocyte lacunae, osteonecrotic areas, and bone exposure, each of which substantially resolved 10 weeks after discontinuing OPG-Fc but not ZA. Full recovery of tartrate-resistant acid phosphatase-positive (TRAP+) osteoclast numbers occurred after discontinuing OPG-Fc but not ZA. Our data provide the first experimental evidence demonstrating that discontinuation of a RANKL inhibitor, but not a bisphosphonate, reverses features of osteonecrosis in mice. It remains unclear whether antiresorptive discontinuation increases the risk of skeletal-related events in patients with bone metastases or fracture risk in osteoporosis patients, but these preclinical data may nonetheless help to inform discussions on the rationale for a "drug holiday" in managing the ONJ patient. © 2015 American Society for Bone and Mineral Research.

KEY WORDS: OSTEONECROSIS OF THE JAW (ONJ); ANTIRESORPTIVES; BISPHOSPHONATES; ZOLEDRONIC ACID; DENOSUMAB; ALVEOLAR BONE; OSTEOCLASTS

Introduction

Antiresorptive medications, such as bisphosphonates (BPs) and the receptor activator of NF-κB ligand (RANKL) inhibitor denosumab impede osteoclastic bone resorption and are used in the clinic to manage bone diseases, such as primary or metastatic bone malignancy and osteoporosis. These medications, studied in cancer and postmenopausal women with osteoporosis populations, reduce skeletal-related events (SREs), decrease tumor burden, reduce bone pain, decrease incidence of osteoporotic fractures, and help improve patients' quality of life.[1–4] Despite their distinctly different pharmacologic mechanism of action, BPs and denosumab are each associated with osteonecrosis of the jaw (ONJ), an infrequent but serious adverse effect, particularly when administered at high doses.[5] Antiresorptive-related ONJ is defined as exposed bone or bone that can be probed through an intraoral or extraoral fistula in the maxillofacial region that has persisted for more than 8 weeks in patients on current or previous treatment with antiresorptive agents and no history of radiation therapy to the jaws or obvious metastatic disease to the jaws.[6–8] The term medical-related ONJ (MRONJ) was recently introduced to include ONJ cases associated with antiangiogenic therapies.[7]

Although ONJ has been described for more than a decade,[9,10] the etiology and pathogenesis of the disease remain largely unknown.[5,11–13] Osteoclast inhibition and bone remodeling suppression, inflammation and/or infection, inhibition of angiogenesis, soft tissue toxicity, and altered immune cell

Received in original form January 26, 2015; revised form February 20, 2015; accepted February 24, 2015; accepted manuscript online Month 00, 2015.
Address correspondence to: Sotirios Tetradis, DDS, PhD, UCLA School of Dentistry, 10833 Le Conte Avenue, CHS Room 53-068, Los Angeles, CA 90095-1668, USA. E-mail: stetradis@dentistry.ucla.edu. Tara L Aghaloo, DDS, MD, PhD, UCLA School of Dentistry, 10833 Le Conte Avenue, CHS Room 53-009, Los Angeles, CA 90095-1668, USA. E-mail: taghaloo@dentistry.ucla.edu
Additional Supporting Information may be found in the online version of this article.

Journal of Bone and Mineral Research, Vol. xx, No. xx, Month 2015, pp 1–14
DOI: 10.1002/jbmr.2490
© 2015 American Society for Bone and Mineral Research

function are among the hypotheses proposed to underlie ONJ development and progression.[5,11–13] Clinical observations and experimental findings provide support for several of these hypotheses, suggesting that ONJ is probably a multifactorial disease influenced by many variables.[7]

Because antiresorptive medications with distinct pharmacologic function induce similar incidence of ONJ, osteoclastic inhibition and bone turnover suppression appear central in antiresorptive-related ONJ.[5,11–13] To that effect, discontinuation of antiresorptive treatment before tooth extraction or other dental surgical intervention or after ONJ development has been proposed as potentially beneficial in improving osteoclast function recovery, which could, in turn, increase bone turnover and improve bone healing.[7,14–16] However, such recommendations have only a theoretical basis, and clinical or experimental data supporting the benefit of antiresorptive drug withdrawal in preventing ONJ development or promoting resolution are lacking.[7,17] Furthermore, the consequences of such "drug holidays" on the progression of SREs in cancer patients or fragility fractures in osteoporosis patients remain unclear. As such, an important first step in informing treatment planning decisions is to understand whether discontinuation of antiresorptive treatments mitigates the risk of developing ONJ or fosters the resolution of established ONJ.[7,8]

Animal models recapitulating ONJ-like lesions in mice, rats, minipigs, and dogs treated with bisphosphonates have provided important insights into ONJ pathophysiology.[18–29] Moreover, utilizing OPG-Fc and RANK-Fc as surrogates for denosumab,[30] we reported for the first time ONJ-like lesions in the presence of periapical disease or spontaneous periradicular inflammation in mice treated with the RANKL inhibitors,[31,32] thus supporting the central role of osteoclastic inhibition in ONJ pathogenesis. Similar ONJ-like changes were reported more recently in mice that underwent tooth extractions and were treated with an antibody against mouse RANKL.[33]

In this study, utilizing ONJ animal models, we explored the effects of zoledronic acid (ZA) or OPG-Fc discontinuation on radiographic and histologic features of established ONJ in mice. Our findings indicate that, within the experimental time frame, OPG-Fc but not ZA discontinuation reversed features of osteonecrosis in ONJ animal models.

Materials and Methods

Animal care

Mice and surgical procedures were handled according to the guidelines of the Institutional Animal Care and Use Committee of the University of California, Los Angeles. We followed a randomized, prospective, controlled, animal model design following all the recommendations of the ARRIVE (Animal Research: Reporting In Vivo Experiments) guidelines for the execution and submission of studies in animals (Kilkenny and colleagues). Mice were kept in the animal facilities with controlled temperature (23°C ± 2°C), humidity, and a 12-hour light/dark cycle. Throughout the experimental period, mice were housed in plastic cages, fed a standard laboratory

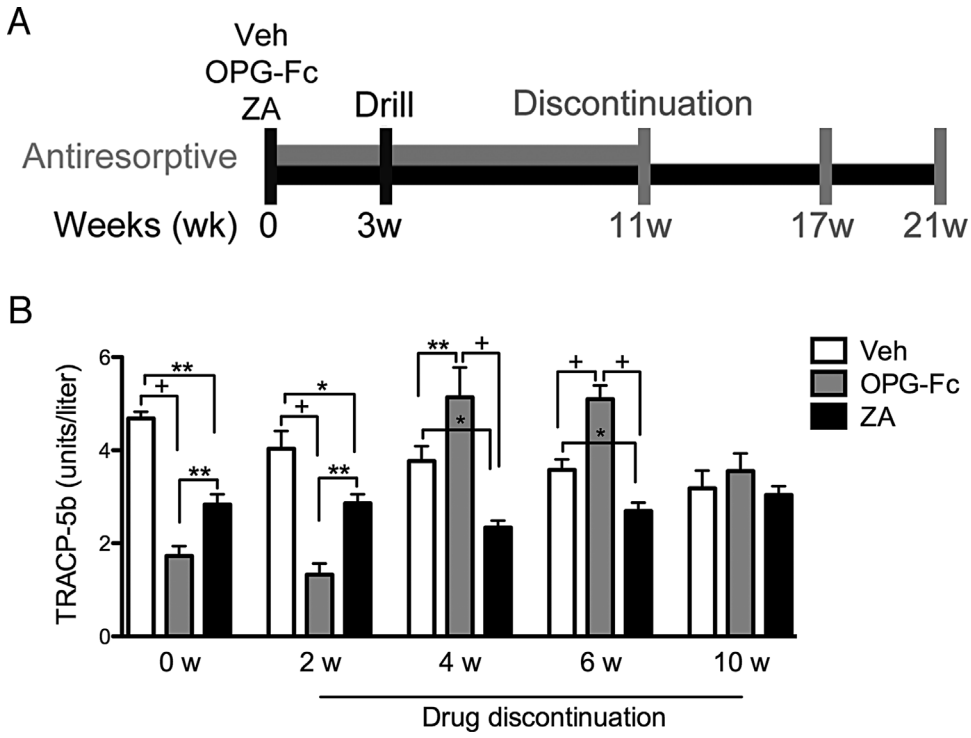

Fig. 1. Serum TRACP-5b levels increase after OPG-Fc but not after ZA discontinuation. TRACP-5b serum levels were measured at the end of treatment (0 weeks) and 2, 4, 6, and 10 weeks after drug discontinuation (13, 15, 17, and 21 weeks after the first injection) ($n = 16$/group per period). $^{+}$Statistically significantly different from indicated groups, $p < 0.0001$. **Statistically significantly different from indicated groups, $p < 0.001$. *Statistically significantly different from indicated groups, $p < 0.05$.

Table 1. Summary of Radiographic and Histologic Findings on Various Groups and Experimental Time Points

Group	Total no. of hemimandible and hemimaxillae	Healthy (%)	Diseased (%)	Osteonecrosis (%)	Bone exposure (%)
Veh 11w	64	34 (53)[a]	30 (47)[a]	0[d] (0)[a] (0)[b]	0[f] (0)[a] (0)[b] (0)[+]
Veh 17w	64	31 (48)[a]	33 (52)[a]	2[e] (3.1)[a] (6)[b]	0[d] (0)[a] (0)[b] (0)[c]
Veh 21w	64	26 (40)[a]	38 (60)[a]	1[e] (1.5)[a] (2.6)[b]	0[d] (0)[a] (0)[b] (0)[c]
OPG-Fc 11w	64	32 (50)[a]	32 (50)[a]	24 (37.5)[a] (75)[b]	13 (20.3)[a] (40.6)[b] (54.2)[c]
OPG-Fc 17w	64	26 (40)[a]	38 (60)[a]	16[g] (25)[a] (42.1)[b]	3[d] (4.7)[a] (7.9)[b] (18.7)[c]
OPG-Fc 21w	64	24 (37)[a]	40 (63)[a]	13[g] (20.3)[a] (32.5)[b]	0[d] (0)[a] (0)[b] (0)[c]
ZA 11w	64	34 (53)[a]	30 (47)[a]	19 (29.7)[a] (63.4)[b]	10 (15.6)[a] (33.3)[b] (52.6)[c]
ZA 17w	64	27 (42)[a]	37 (58)[a]	32 (50)[a] (86.5)[b]	19 (29.7)[a] (51.4)[b] (59.3)[c]
ZA 21w	64	23 (36)[a]	41 (64)[a]	31 (48.4)[a] (75.6)[b]	21 (32.8)[a] (51.2)[b] (67.7)[c]

[a]Percent of total hemimaxillae and hemimandible.
[b]Percent of diseased hemimaxillae and hemimandible.
[c]Percent of hemimaxillae and hemimandible with osteonecrosis.
[d]Statistically significantly different, $p < 0.05$ compared with OPG-Fc and ZA.
[e]Statistically significantly different, $p < 0.0001$ compared with OPG-Fc and ZA.
[f]Statistically significantly different, $p < 0.005$ compared with OPG-Fc and ZA.
[g]Statistically significantly different, $p < 0.0001$ compared with ZA.

diet, and given water *ad libitum*. A total of 144 10-week-old C57BL/6J wild-type male mice (Jackson Laboratories, Bar Harbor, ME, USA) with average weight of 25 g were randomly divided into three experimental groups of 48 animals that received intraperitoneal (ip) injections of endotoxin-free saline (group veh) two times per week, 10 mg/kg rat OPG-Fc (composed of the RANKL-binding domains of osteoprotegerin linked to the Fc portion of IgG,[32,34,35] kindly provided by Amgen, Inc, Thousand Oaks, CA, USA) twice per week (group OPG-Fc), or 200 μg/kg zoledronic acid (Z-5744, LKT Laboratories, St. Paul, MN, USA) twice per week (group ZA). These doses were used to increase the incidence of ONJ-like lesions in the mice, as described previously.

Periapical disease induction

Experimental periapical disease was performed as described.[29,32,36,37] Briefly, the crowns of the right mandibular 1st and 2nd molars were drilled utilizing a stainless-steel ¼ size round bur in a high-speed handpiece, avoiding furcal perforation, and the root canals were left exposed to the oral environment, resulting in pulpal necrosis and subsequent

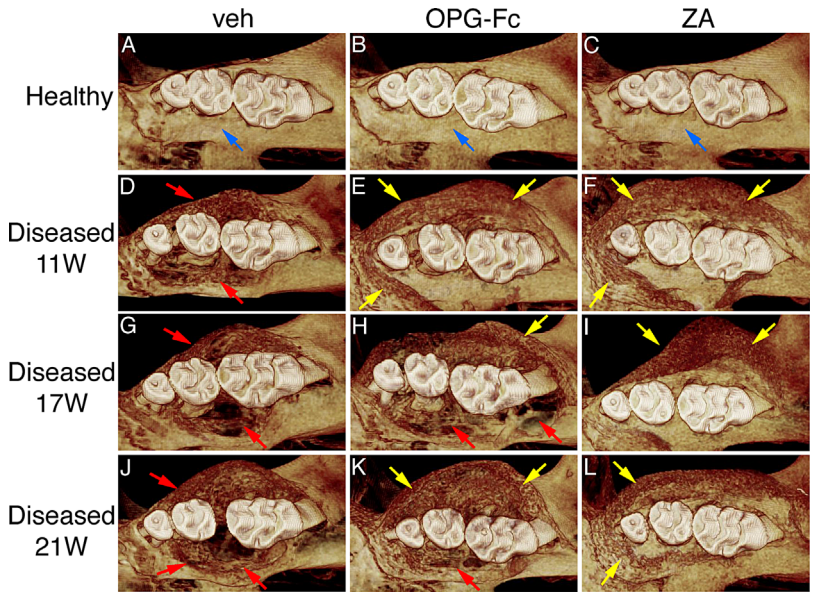

Fig. 2. Three-dimensional μCT reconstructed images of maxilla. (*A–C*) Healthy site in veh, OPG-Fc, and ZA, respectively. (*D, E*) Diseased site after 11 weeks of treatment. (*G–L*) Diseased site at 6 and 10 weeks after drug discontinuation. Blue arrows point to normal alveolar bone crest in the interproximal area between the distal root of the first molar and mesial root of the second molar. Red arrows point to periodontal bone loss and areas of osteolysis in the diseased site of OPG-Fc- and veh-treated mice. Yellow arrows point to increased bone deposition.

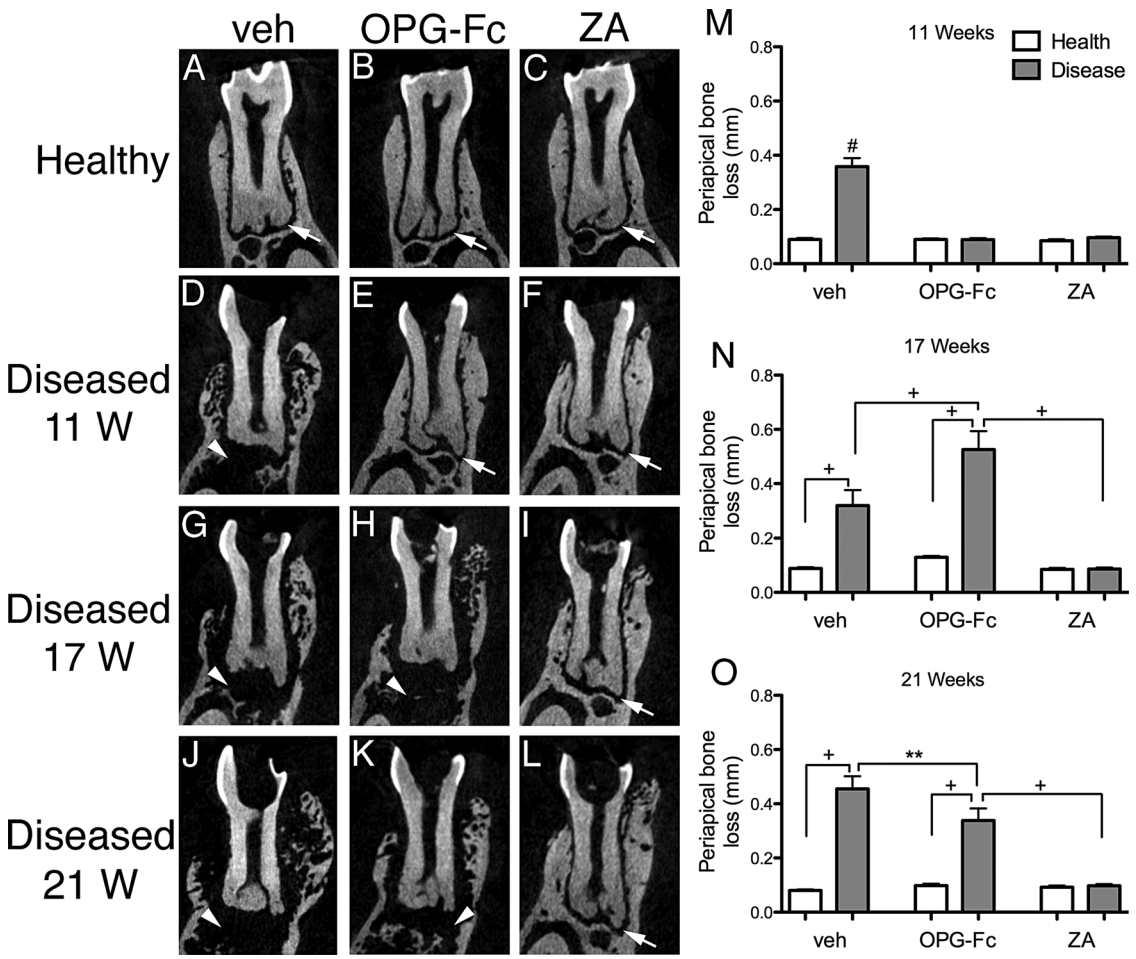

Fig. 3. μCT cross sections of the periapical area of first molars from animals treated with veh, OPG-Fc, and ZA followed by drug discontinuation. (*A–C*) Nondrilled molars at 11 weeks. (*D–F*) Drilled molars at 11 weeks. (*G–I*) Drilled molars 6 weeks after drug discontinuation. (*J–L*) Drilled molars 10 weeks after drug discontinuation ($n = 16$/group per period). Thin arrows point to normal PDL space. Arrowheads point to periapical bone loss. (*M–O*) Quantification of periapical bone loss at the distal root of the first molar and mesial root of the second molar. $^{\#}$Statistically significantly different compared with all other groups, $p < 0.0001$. $^{+}$Statistically significantly different from indicated groups, $p < 0.0001$. **Statistically significantly different from indicated groups, $p < 0.001$.

periapical infection. The crowns of the left 1st and 2nd molars were kept intact.

Spontaneous naturally occurring maxillofacial abscesses

Naturally occurring, spontaneous maxillofacial abscesses have been described in mice.[38] Hair inserts into the gingival sulcus and results in bacterial colonization and reproducible, severe periradicular osteolysis.[38–40] Such diseased maxillary sites, identified by periradicular osteolysis by μCT imaging, were compared with sites with healthy dento-alveolar structures.[31]

Antiresorptive administration and serum TRACP-5b measurement

Mice were pretreated with veh, OPG-Fc, or ZA for 3 weeks, and periapical disease was induced. Animals continued to receive veh, OPG-Fc, and ZA for 8 additional weeks, after which antiresorptives were discontinued (Fig. 1*A*). Blood was collected via retro-orbital bleeding after 11 weeks of the experiment (at the end of antiresorptives treatment) and 2, 4, 6, and 10 weeks after antiresorptive withdrawal. Serum tartrate-resistant acid phosphatase 5b (TRACP-5b) was measured by enzyme immunoassay (RatTRAP; JDS, Gaithersburg, MD, USA).

Animal euthanization and analyses

Sixteen mice from each of the veh, OPG-Fc, and ZA groups were euthanized via isoflurane overdose at 11 weeks (time of antiresorptive discontinuation), at 17 weeks (6 weeks after discontinuation), and at 21 weeks (10 weeks after antiresorptive discontinuation). The maxillae, mandibles, and femurs were fixed in 4% paraformaldehyde for 48 hours and stored in 70% ethanol.

Micro-computed tomography (μCT) scanning

Maxillae and mandibles were imaged using a μCT scanner (μCT Skyscan 1172; Skyscan, Kontich, Belgium) at 10 μm resolution, as described.[29,32] For linear measurements, axial slices were converted to DICOM format and imported in the Dolphin

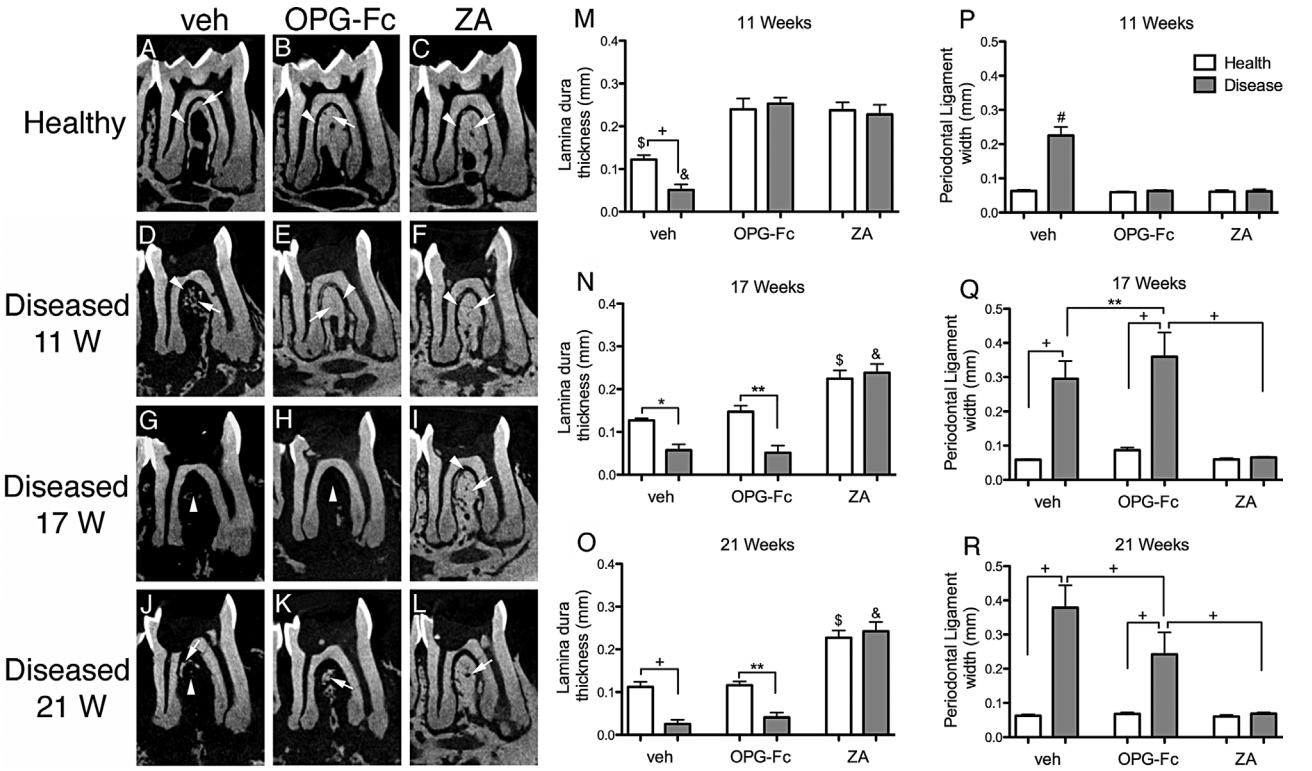

Fig. 4. Sagittal μCT sections through the furcational periodontium of veh-, OPG-Fc-, and ZA-treated animals. (*A–C*) Nondrilled molars at 11 weeks. (*D–F*) Drilled molars at 11 weeks. (*G–I*) Drilled molars 6 weeks after drug discontinuation. (*J–L*) Drilled molars 10 weeks after drug discontinuation ($n = 16$/group per period). Thin arrows point to lamina dura and arrowheads point to PDL space. (*M–R*) Quantification of changes in the furcational periodontium was performed measuring the thickness of lamina dura and width of the PDL space. $^{\$}$Statistically significantly different compared with healthy mice, $p < 0.0001$. $^{\&}$Statistically significantly different compared with diseased mice, $p < 0.0001$. $^{+}$Statistically significantly different from indicated groups, $p < 0.0001$. **Statistically significantly different from indicated groups, $p < 0.001$. *Statistically significantly different from indicated groups, $p < 0.05$.

Imaging software (Chatsworth, CA, USA). Periapical bone loss, lamina dura thickness, periodontal ligament (PDL) space width, lingual bone thickness, and cemento-enamel junction (CEJ) to alveolar bone crest (ABC) distance were measured as described.[29,31,32] Bone volume (BV), tissue volume (TV), and bone volume fraction (BV/TV) of the alveolar were measured using the CTAn software (Skyscan).

Femurs were imaged utilizing the μCT scanner at 12 μm resolution. Starting 100 μm proximal to the distal growth plate, 200 axial slices were selected. BV, TV, BV/TV, trabecular number (Tb.N), trabecular thickness (Tb.Th), and trabecular spacing (Tb.Sp) were determined using the CTAn software. The measurement terminology and units used for μCT analysis were those recommended by the Nomenclature Committee of the American Society for Bone and Mineral Research.[41]

Histology and TRAP staining

Mandibles, maxillae, and femurs were decalcified in 14.5% EDTA for 3 weeks and paraffin embedded, and 5 μm sections were obtained. Hematoxylin and eosin (H&E)-stained sections were digitally scanned using the Aperio AT automated slide scanner (Aperio Technologies, Inc, Vista, CA, USA). Using the ruler tool in Aperio ImageScope software, the crestal 1 mm of the alveolar bone was marked and all measurements were performed in this area for mandible and maxilla.

The epithelium to alveolar crest distance was measured in the palatal side of the maxilla and in the lingual side of the mandible. The number of osteocytic lacunae and empty osteocytic lacunae and the total bone area and osteonecrotic area (defined as five or more contiguous empty osteocytic lacunae) were measured. To quantify periosteal bone thickness, the Aperio ruler tool was used to measure the three greatest areas of the buccal periosteal thickness that were then averaged.

To quantify osteoclast number, sections of the mandible, maxilla, and femur were stained using the leukocyte acid phosphatase kit (Sigma-Aldrich, St. Louis, MO, USA) and TRAP+ cells adjacent to the bone surface were counted. TRAP+ cells were measured for 8 mice per group. All histology and digital imaging were performed at the Translational Pathology Core Laboratory (TPCL) at UCLA.

Statistics

Analyses were performed using GraphPad Prism Software (GraphPad Software, Inc, La Jolla, CA, USA). Group measures were expressed as mean ± the standard error of the mean (SEM). Statistical significance was assessed using one-way analysis of variance (ANOVA) followed by post hoc Tukey's test for multiple comparisons among groups. Data between groups (healthy versus diseased) were compared using the Student's *t* test. Categorical data (Table 1) were analyzed using the Fisher's exact test.

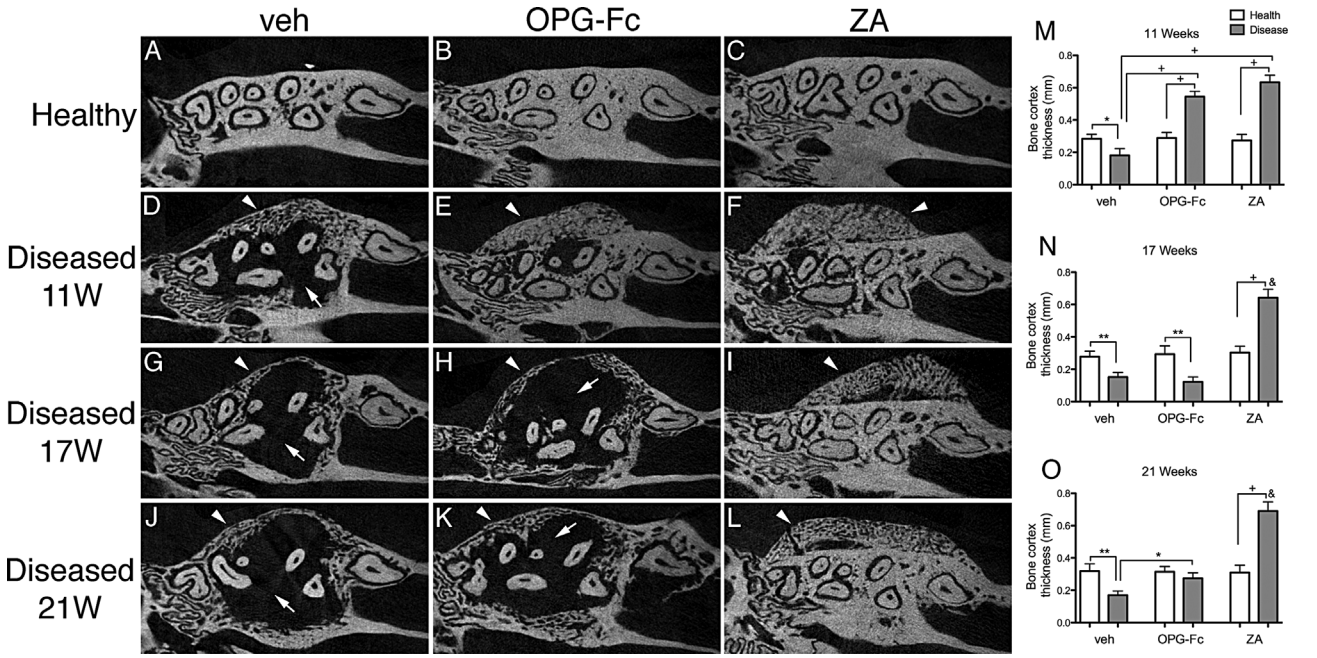

Fig. 5. Axial μCT sections through the maxillary alveolar ridge. (*A–C*) Healthy maxillae at 11 weeks. (*D–F*) Diseased maxillae at 11 weeks. (*G–I*) Diseased maxillae 6 weeks after drug discontinuation. (*J–L*) Diseased maxillae 10 weeks after drug discontinuation ($n = 16$/group per period). Thin arrows point to areas of osteolysis. Arrowheads point to bone deposition and bone expansion. (*M–O*) Quantification of buccal bone thickness. $^{\&}$Statistically significantly different compared with diseased mice, $p < 0.0001$. $^{+}$Statistically significantly different from indicated groups, $p < 0.0001$. **Statistically significantly different from indicated groups, $p < 0.001$. *Statistically significantly different from indicated groups, $p < 0.05$.

Results

Serum TRACP-5b levels increased after OPG-Fc but not after ZA discontinuation

Serum TRACP-5b levels were measured at the end of antiresorptive treatment (0 weeks: immediately after the last injection and 11 weeks after the beginning of the experiment), and 2, 4, 6, and 10 weeks after drug discontinuation (13, 15, 17, and 21 weeks after the beginning of the experiment). For the veh group, serum TRACP-5b levels remained relatively steady with a slight decline over time. After 11 weeks of treatment, ZA or OPG-Fc significantly decreased serum TRACP-5b levels in all animals, confirming the inhibition of osteoclastic function and absence of neutralizing antibody production to OPG-Fc.[42] These TRACP-5b levels remained unchanged for all groups 2 weeks after antiresorptive discontinuation. Interestingly, by 4 to 6 weeks post-OPG-Fc discontinuation, TRACP-5b rose above baseline and then returned to baseline by 10 weeks. TRACP-5b post-ZA discontinuation remained at reduced levels for 4 to 6 weeks and progressively returned to baseline by 10 weeks (Fig. 1*B*).

OPG-Fc but not ZA discontinuation reversed radiographic features of ONJ

The effect of antiresorptives and drug discontinuation on maxilla, mandible, and femur was assessed by μCT. Healthy maxillae in all groups showed normal alveolar crest extending immediately below the cemento-enamel junction (CEJ), covering most of the root and the 1st and 2nd molar root furcation and absence of bone resorption and/or bone expansion (Fig. 2*A–C*; Supplemental Fig. S1*A–C*). In contrast, diseased veh-treated mice showed altered alveolar bone morphology with large loss of alveolar crest height; bone loss covering the 1st, 2nd, and 3rd molars that in the majority of animals extended almost to the root apex surrounding the entire root; and significant buccal and palatal bone expansion of the alveolar ridge. These changes were similar for all time points (Fig. 2*D, G, J*; Supplemental Fig. S1*D, G, J*). In the diseased site of OPG-Fc- and ZA-treated mice, bone loss was also present. However, the extent of bone loss was significantly decreased and was associated with large areas of periosteal bone apposition in the buccal and palatal side of the maxillae that resulted in substantial bone expansion (Fig. 2*E, F*; Supplemental Fig. S1*E, F*). Discontinuation for 6 or 10 weeks of OPG-Fc but not ZA reversed these effects, such that the OPG-Fc and veh groups appeared similar and distinct from the ZA group (Fig. 2*H, I, K, L*; Supplemental Fig. S1*H, I, K, L*). Similar findings were observed for the mandibular alveolar ridge in nondrilled and drilled sites of veh, OPG-Fc-, and ZA-treated animals (Supplemental Fig. S2).

We then quantified radiographic changes among the various groups.[29,32] In the nondrilled side of all animals, a short apex to bone distance was observed (Fig. 3*A–C*). Significant distance was observed for the drilled site of veh animals at 11 weeks that continued to increase over time (Fig. 3*D, G, J, M*, arrowheads). As expected, OPG-Fc and ZA at 11 weeks reduced periapical bone loss, reflected by shorter apex to bone distance (Fig. 3*E, F, M*). Discontinuation of OPG-Fc reversed this effect, evidenced by a significant increase of the apex to bone distance at 17 and 21 weeks (Fig. 3*H, K, N, O*, arrowheads). On the other hand, ZA discontinuation had no effect in periapical bone loss (Fig. 3*I, L, N, O*). Similar observations were found in maxillae with spontaneous periradicular bone loss. Both antiresorptive treatments

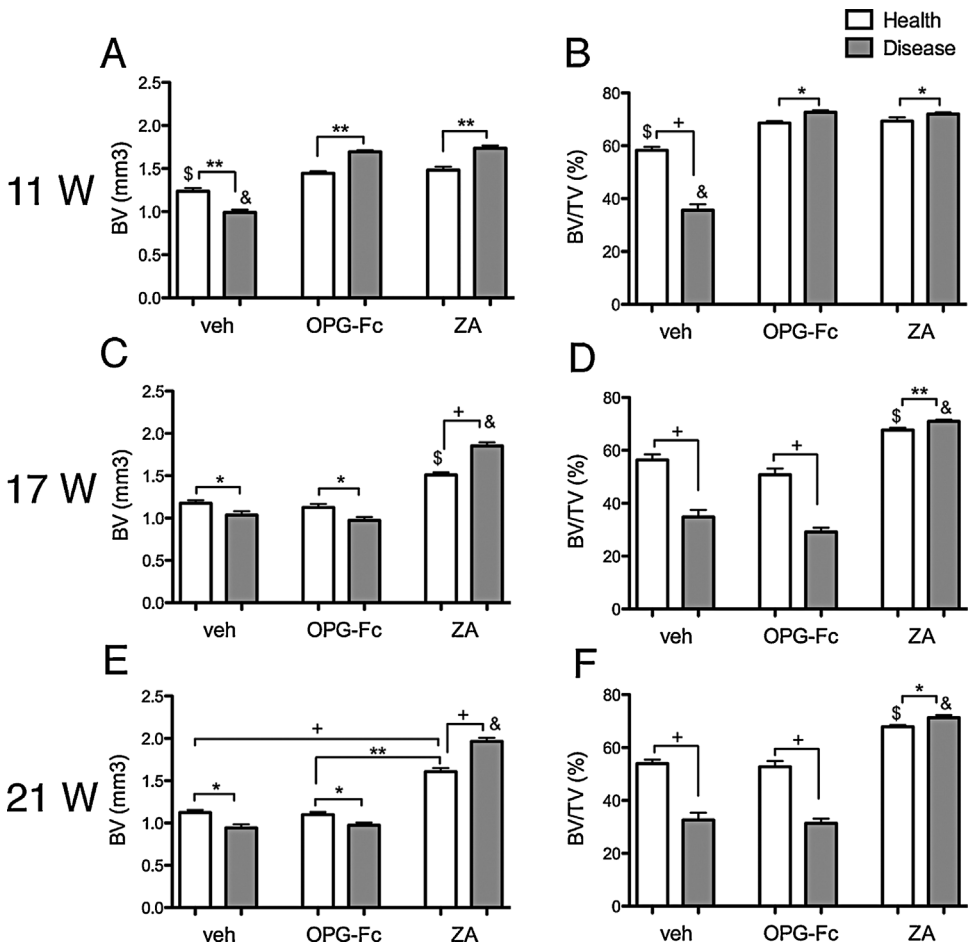

Fig. 6. Quantification of BV and BV/TV in the mandible of all mice. Eleven weeks of treatment (*A, B*) and 6 weeks (*C, D*) and 10 weeks (*E, F*) after drug discontinuation ($n = 16$/group per period). $^{\$}$Statistically significantly different compared with healthy mice, $p < 0.0001$. $^{\&}$Statistically significantly different compared with diseased mice, $p < 0.0001$. $^{+}$Statistically significantly different from indicated groups, $p < 0.0001$. **Statistically significantly different from indicated groups, $p < 0.001$. *Statistically significantly different from indicated groups, $p < 0.05$.

attenuated alveolar bone loss at 11 weeks. Six and 10 weeks of OPG-Fc, but not ZA, discontinuation reversed the protection of alveolar bone loss that was similar to veh-treated mice (Supplemental Fig. S3).

Next, we examined changes of the PDL space width and lamina dura thickness at the furcation area of the mandibular molars.[29,32] In nondrilled teeth of veh-, OPG-Fc-, and ZA-treated animals, a continuous PDL space and uniform lamina dura that increased in thickness with antiresorptive treatment were present (Fig. 4*A–C*, thin arrows and arrowheads). In the drilled side of veh-treated mice, there was increased width of the PDL space and loss of lamina dura that progressed over time (Fig. 4*D, G, J*, thin arrows and arrowheads, and Fig. 4*M, P*). Both antiresorptive treatments preserved PDL space width and thickened lamina dura at 11 weeks (Fig. 4*E, F, M–R*). OPG-Fc versus ZA discontinuation resulted in a significant reduction in the thickness of lamina dura and increase in PDL space width at 17 and 21 weeks (Fig. 4*H, K, N, O, Q, R*, thin arrows and arrowheads). ZA discontinuation had no effect compared with the week 11 measurements (Fig. 4*I, L, N, O, Q, R*).

The bone changes appeared to extend beyond the confines of the periodontal area to the adjacent alveolar bone (Fig. 5). Significant osteolysis with exuberant expansion of the alveolar bone that increased over the time was noted in the diseased versus healthy site of veh mice (Fig. 5*A, D, G, J, M–O*, thin arrows). As previously reported,[29,32] antiresorptive treatment inhibited bone osteolysis at 11 weeks (Fig. 5*B, C, E, F, M*), with an associated exuberant bone deposition on the buccal and palatal side of the alveolar ridge (Fig. 5*B, C, E, F, M*, arrowheads). Importantly, 6 and 10 weeks of OPG-Fc discontinuation reduced bone buccal and palatal thickness to levels similar to the veh group (Fig. 5). In contrast, ZA discontinuation had no effect on alveolar bone structure compared with the prediscontinuation levels (Fig. 5*H, I, K, L, N, O*). Similar findings were observed at the mandibular alveolar ridge (Supplemental Fig. S4).

Periapical disease decreased BV and BV/TV compared with the healthy site, and antiresorptives significantly increased BV and BV/TV compared with the veh group at 11 weeks. Significant increase in BV and BV/TV was observed between diseased versus healthy sites in OPG-Fc and ZA mice (Fig. 6*A, B*). OPG-Fc discontinuation decreased BV and BV/TV in the drilled site that returned to values similar to the veh group (Fig. 6*C–F*). In contrast, ZA discontinuation at 6 and 10 weeks

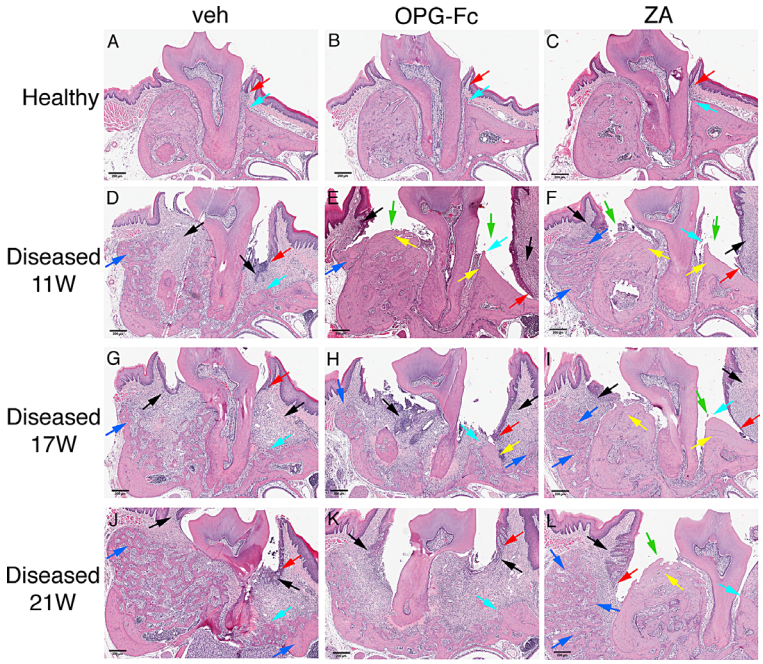

Fig. 7. Representative H&E-stained images from maxilla of all groups. (*A–C*) Healthy site of veh, OPG-Fc, and ZA animals. (*D–F*) Diseased site at 11 weeks at the end of antiresorptive treatment. (*G–I*) Diseased site of veh, OPG-Fc, and ZA 6 weeks after antiresorptive discontinuation. (*J–L*) Diseased site of veh, OPG-Fc, and ZA 10 weeks after antiresorptive discontinuation. Red arrows point to marginal gingival epithelium, turquoise arrows to alveolar crest, black arrows to areas of inflammation, blue arrows to periosteal bone deposition, yellow arrows to osteonecrotic areas, and green arrows to areas of bone exposure. Original magnification ×5.

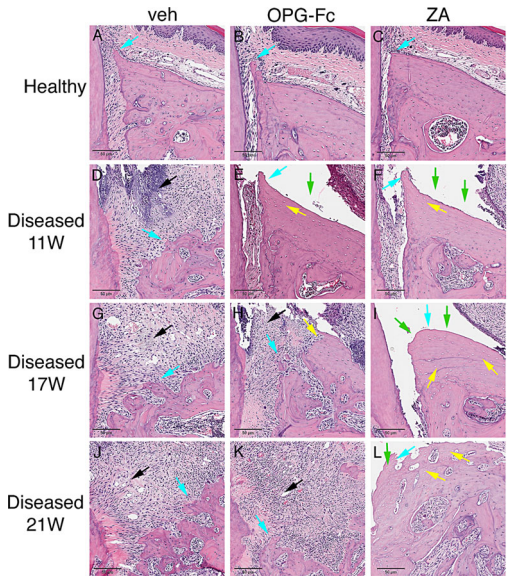

Fig. 8. Histologic appearance of periodontal and alveolar crest area of maxillae (*A–C*) Healthy site of veh, OPG-Fc, and ZA animals. (*D–F*) Diseased site at 11 weeks at the end of antiresorptive treatment. (*G–I*) Diseased site of veh, OPG-Fc, and ZA 6 weeks after antiresorptive discontinuation. (*J–L*) Diseased site of veh, OPG-Fc, and ZA 10 weeks after antiresorptive discontinuation. Turquoise arrows point to alveolar crest, black arrows to areas of inflammation, blue arrows to periosteal bone deposition, yellow arrows to osteonecrotic areas, and green arrows to areas of bone exposure. Original magnification ×10.

had no effect on the BV and BV/TV levels (Fig. 6*C–F*). Similar observations were made for the BV and BV/TV values of the maxillae (Supplemental Fig. S5).

OPG-Fc but not ZA discontinuation reverses histologic features of ONJ

As reported,[29,31,32] histologically healthy sites in all experimental groups and time points showed normal marginal epithelium (Fig. 7*A–C*; Fig. 8*A–C*, red arrows), PDL and alveolar bone (Fig. 7*A–C*; Fig. 8*A–C*, turquoise arrows). Abundant inflammatory infiltrate of the gingival and connective tissue (Fig. 7*D, G, J*, black arrows), severe destruction of the periradicular bone (Fig. 7*D, G, J*, turquoise arrows), migration of the marginal epithelium (Fig. 7*D, G, J*, red arrows), and bone expansion (Fig. 7*D, G, J*, blue arrows) were observed in the diseased site of veh-treated animals at all time points. Intense infiltration of inflammatory cells was noted in the diseased site of OPG-Fc- and ZA-treated mice at 11 weeks of treatment (Fig. 7*E, F*; Fig. 8*E, F*, black arrows); bone loss was present but appeared less compared with the veh animals (Fig. 7*E, F*; Fig. 8*E, F*, turquoise arrows). Empty osteocytic lacunae, areas of osteonecrosis (Fig. 7*E, F*; Fig. 8*E, F*, yellow arrows), and abundant periosteal bone formation (Fig. 7*E, F*; Fig. 8*E, F*, blue arrows) were found for both OPG-Fc and ZA mice. In several animals, necrotic bone was not covered by epithelium and was exposed to the oral cavity (Fig. 7*E, F*; Fig. 8*E–F*, green arrows; Table 1).

After OPG-Fc discontinuation, extensive osteolysis was noted in the maxillae, similar to the veh-treated animals (Fig. 7*H, K*; Fig. 8*H, K*). Importantly, areas of osteonecrosis and bone

exposed to the oral cavity significantly decreased by 6 weeks and were almost completely absent by 10 weeks of OPG-Fc discontinuation. Significant bone resorption and decreased areas of necrosis were associated with epithelial migration to areas of vital bone and with decreased number of animals with bone exposure (Fig. 7*H, K*; Fig. 8*H, K*; Table 1). In contrast, 6 and 10 weeks after ZA discontinuation did not alter these histologic features (Fig. 7*I, L*; Fig. 8*I, L*). Similar observations were made for healthy and drilled sites of the mandible for all experimental groups (Supplemental Fig. S6*A–L*).

In maxillae, increased marginal epithelium to alveolar bone crest (ABC) distance for diseased sites of veh animals at 11 weeks that continued to increase over time was found. As reported,[29,31,32] antiresorptive treatment significantly decreased this distance because of reduced bone resorption (Fig. 9*A–C*). After OPG-Fc discontinuation, the epithelium to ABC distance progressively increased, as a result of increased bone resorption, and was statistically different compared with healthy sites or ZA-treated diseased sites (Fig. 9*B*). Six weeks after ZA discontinuation, the epithelium to ABC distance remained low and significantly different from the other groups (Fig. 9*B*). At 10 weeks after ZA discontinuation, an increase in the epithelium to ABC distance was noted but remained statistically different compared with the other groups (Fig. 9*C*). Similar results were found for the nondrilled and drilled sites of the mandible (Supplemental Fig. S7*A–C*). A significant increase in periosteal thickness was noted in the diseased versus healthy side for all treatment groups at all experimental time points. No consistent effects were noted by antiresorptive treatment or drug discontinuation (Fig. 9*A–C*).

The number of empty osteocytic lacunae (Fig. 9*G–I*) and osteonecrotic surface area (Fig. 9*J–L*) were measured in the maxilla. No statistically significant presence of empty osteocytic lacunae was detected in healthy or diseased sites of veh mice or healthy sites of OPG-Fc or ZA mice at any time point. As previously reported,[29,31,32] significant increases in empty osteocytic lacunae (Fig. 9*G–I*) and osteonecrotic area (Fig. 9*J–L*) were present in the diseased sites of mice on antiresorptive treatment at 11 weeks. Six and 10 weeks after OPG-Fc discontinuation, a significant reduction of empty osteocytic lacunae and osteonecrotic area was noted, to levels statistically similar to those of healthy sites and significantly lower than the diseased site of the ZA group. Interestingly, at 6 and 10 weeks after ZA discontinuation, significant increases in empty osteocytic lacunae number and osteonecrotic areas were observed. Comparable findings were observed for nondrilled and drilled sites of the mandible (Supplemental Fig. S7*D–I*).

Few TRAP+ cells were found at the healthy site of veh animals but were significantly increased at the diseased site of veh animals at all time points (Fig. 10*A, D*). TRAP+ cells were absent in OPG-Fc-treated animals in both healthy and diseased sites at 11 weeks (Fig. 10*B, E, M*). As previously reported,[29,31,32] at 11 weeks TRAP+ cells in the diseased sites of ZA mice increased but demonstrated round morphology, with pyknotic nuclei, and were detached from the bone surface (Fig. 10*C, F, M*). After OPG-Fc discontinuation, TRAP+ cells in the diseased sites increased to higher levels than all other groups at 17 weeks and higher than the healthy sites of OPG-Fc animals at 21 weeks (Fig. 10*H, K, N, O*). A slight significant increase in TRAP+ cell number was found in the diseased sites after ZA discontinuation. Similar results were found for the nondrilled and drilled sites of the mandible (Supplemental Fig. S8*A–O*).

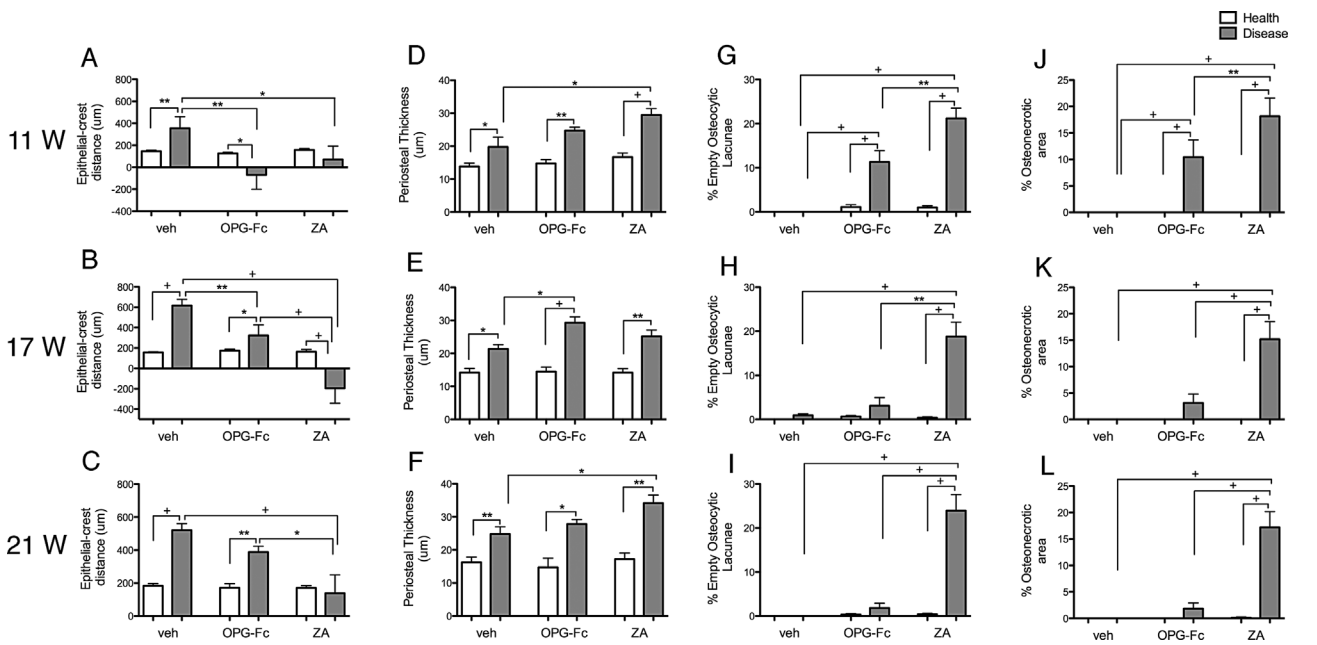

Fig. 9. Quantification of histologic findings. (*A–C*) The shortest epithelial-crest distance was determined. (*D–F*) Thickness of periosteum at the buccal side was measured. (*G–I*) Osteocytic lacunae were measured and empty lacunae were expressed as percent of total. (*J–L*) Area of osteonecrosis was measured and expressed as percent of total bone area ($n = 16$/group per period). $^{+}$Statistically significantly different from indicated groups, $p < 0.0001$. **Statistically significantly different from indicated groups, $p < 0.001$. *Statistically significantly different from indicated groups, $p < 0.05$.

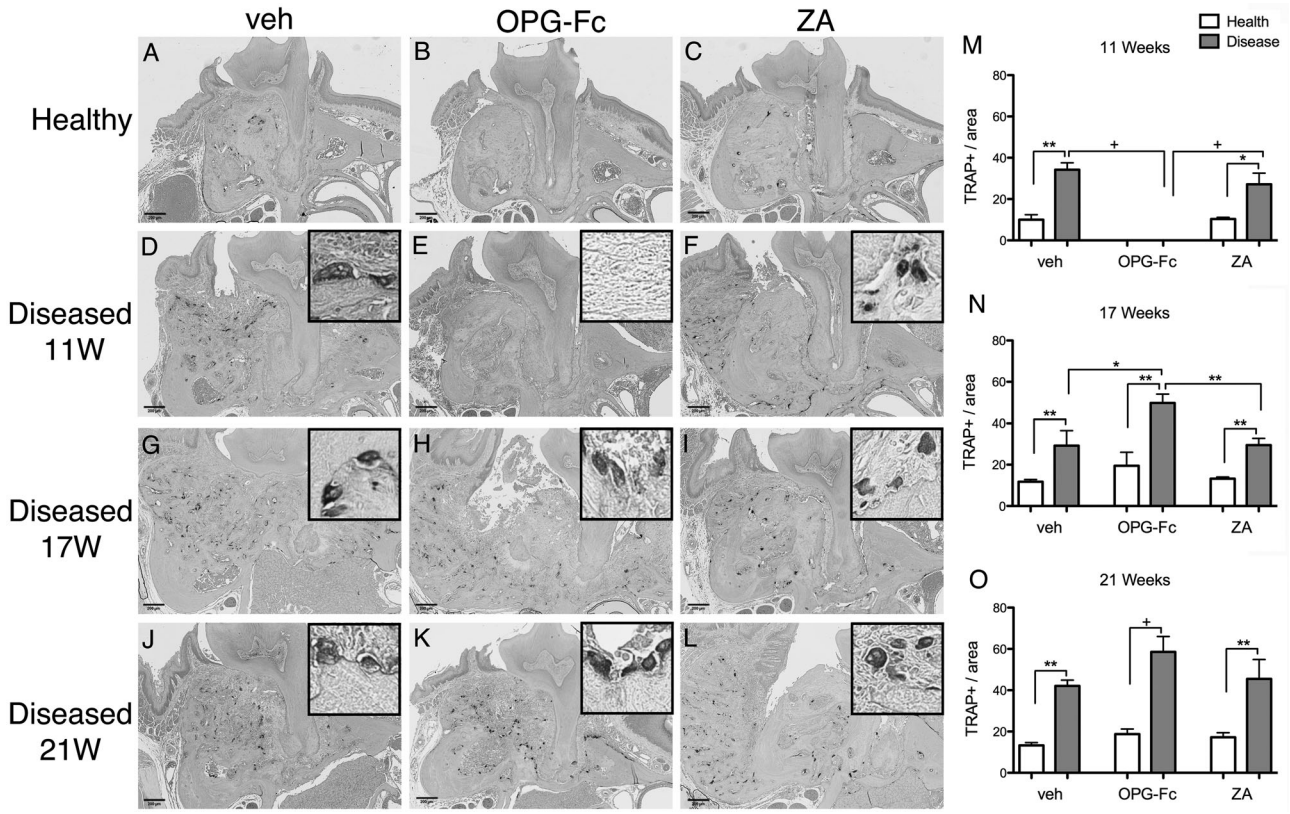

Fig. 10. Representative sections of the maxilla stained for TRAP+ cells (original magnification ×5). Insets are magnified views of individual TRAP+ cells (original magnification ×20). (*A–C*) Healthy site of veh, OPG-Fc, and ZA animals. (*D–F*) Diseased site at 11 weeks at the end of antiresorptive treatment. (*G–I*) Diseased site of veh, OPG-Fc, and ZA 6 weeks after antiresorptive discontinuation. (*J–L*) Diseased site of veh, OPG-Fc, and ZA 10 weeks after antiresorptive discontinuation. (*M–O*) Quantification of TRAP+ cell number ($n = 8$/group per period). $^{+}$Statistically significantly different from indicated groups, $p < 0.0001$. **Statistically significantly different from indicated groups, $p < 0.001$. *Statistically significantly different from indicated groups, $p < 0.05$.

Table 1 summarizes radiographic and histologic findings. Disease prevalence, which included periradicular and periapical disease, ranged from 47% to 64%, with no statistical differences among treatment groups or time points. Small areas of osteonecrosis were found in 2 veh-treated mice at 17 weeks and 1 at 21 weeks. Osteonecrosis was present in 75% of OPG-Fc and 63.4% of ZA animals at 11 weeks with no difference between antiresorptive groups but statistically different compared with veh. Bone exposure was observed only in animals on antiresorptives, ranging from 40.6% of the OPG-Fc and 52.6% of ZA-treated mice, respectively. After OPG-Fc discontinuation, areas of osteonecrosis and bone exposure were markedly diminished. Osteonecrosis incidence decreased to 42.1% and to 32.5% at 6 and 10 weeks after OPG-Fc discontinuation, respectively. Bone exposure decreased to 7.9% at 6 weeks after discontinuation. Importantly, at 10 weeks after OPG-Fc discontinuation, no animal with bone exposure was found. In contrast, 6 and 10 weeks of discontinuation in ZA-treated mice had no effect on incidence of osteonecrosis or bone exposure compared with prediscontinuation levels at 11 weeks.

To assess effects of antiresorptive discontinuation in other bones, we investigated radiographic changes in the femur of all groups and time points. As expected, after 11 weeks of treatment, antiresorptives caused an increase in all bone radiographic indices including BV, BV/TV, trabecular number, and trabecular thickness. OPG-Fc induced a slightly higher trabecular thickness and smaller trabecular number compared with ZA. OPG-Fc discontinuation resulted in a progressive decrease in all measurements to veh levels. However, ZA discontinuation showed little effect and all radiographic indices remained high at both the 17- and 21-week time points (Fig. 11*A–M*).

To explore the effects of various treatments on osteoclast inhibition in femurs, TRAP+ cells were measured in the proximal femur. The number of TRAP+ cells in veh mice did not change over time (Fig. 11*N, Q, T*). At 11 weeks, no TRAP+ cells were observed in OPG-Fc mice (Fig. 11*O*), whereas increased TRAP+ cell numbers were found in ZA mice. However, in ZA mice, the osteoclasts had a round shape and were detached from the bone surface (Fig. 11*P*), with similar morphologic features as observed in the maxilla (Fig. 10) and mandible (Supplemental Fig. S8). At 6 and 10 weeks after OPG-Fc discontinuation, the number of TRAP+ cells significantly increased compared with the veh group (Fig. 11*R, U, W*). ZA discontinuation had no effect on TRAP+ cell numbers.

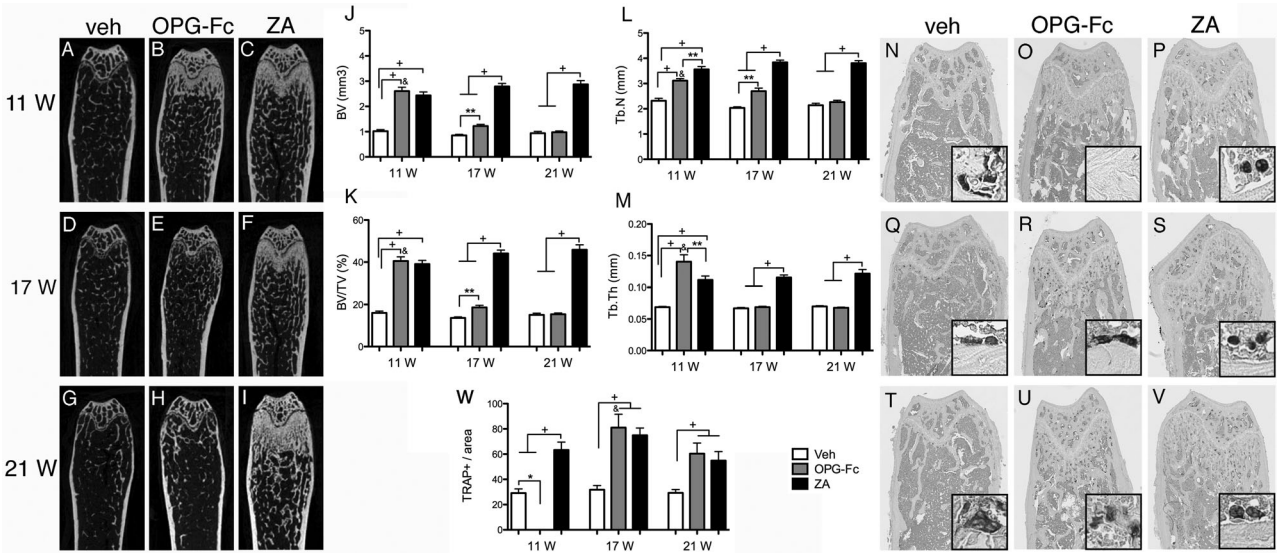

Fig. 11. Representative sagittal μCT slices of femurs. (*A–I*) Veh, OPG-Fc, and ZA at the end of treatment and after drug discontinuation. (*J–M*) Quantification of BV, BV/TV, Tb.N, and Tb.Th ($n = 16$/group per period). Representative sections of TRAP-stained sections from femurs (original magnification ×5). Insets are magnified views of individual TRAP+ cells (original magnification ×20). (*N–P*) Veh, OPG-Fc, and ZA animals at 11 weeks, (*Q–S*) 6 weeks after drug discontinuation, and (*T–V*) 10 weeks after drug discontinuation. (*W*) Quantification of TRAP+ cell number ($n = 8$/group per period). $^{\&}$Statistically significantly different compared with diseased mice, $p < 0.0001$. $^{+}$Statistically significantly different from indicated groups, $p < 0.0001$. **Statistically significantly different from indicated groups, $p < 0.001$. *Statistically significantly different from indicated groups, $p < 0.05$.

Discussion

BPs are antiresorptive agents widely used in bone diseases with elevated osteoclastic activity, such as osteoporosis, cancer metastases to bone, multiple myeloma, and hypercalcemia of malignancy. Recently, the US FDA approved denosumab, an anti-RANKL monoclonal antibody, for the prevention of skeletal-related events in patients with bone metastases from solid tumors, for the management of unresectable giant cell tumors, for increasing bone mass in nonmetastatic prostate patients with androgen deprivation therapy, breast cancer patients receiving adjuvant aromatase inhibitor therapy, and men with osteoporosis, and for the treatment of postmenopausal and male osteoporosis.[43–45] Although both BPs and denosumab target the osteoclast, their mechanism of function is distinctly different.

BPs have high affinity to bone surfaces, where they remain inactive until they are released during osteoclastic bone resorption.[46–50] Because they target bones with high turnover, BP skeletal distribution is not homogeneous. The availability of exposed hydroxyapatite, blood supply, and the ratio of bone surface to bone volume are parameters that may contribute to this uneven distribution.[51] On the other hand, denosumab, a high-affinity, highly specific monoclonal antibody for human RANKL, inhibits osteoclastic formation, function, and survival.[52,53] Upon subcutaneous injection, denosumab is absorbed via the lymphatic system, with subsequent drainage into the vasculature. Three phases of drug distribution are described: a prolonged absorption phase with maximum serum concentration at 5 to 21 days, a long duration phase with a 32-day maximum half-life, and a rapid terminal phase when serum concentrations reach levels below 1000 ng/mL.[54,55]

Given their distinct biodistribution and mechanism of action, BP versus denosumab inhibition of osteoclastic function has distinct temporal dynamics. Because of their incorporation in the bone mineral, BPs can exert their anti-osteoclastic effects long after their administration.[46] In contrast, denosumab does not require binding to bone mineral to exert its anti-osteoclastic activity[30] and demonstrates rapid reversibility of its antiresorptive effects.[43]

Here, we investigated osteoclast recovery by measuring serum TRACP-5b levels before and at various times after antiresorptive discontinuation. As expected, ZA treatment significantly attenuated TRACP-5b levels. After ZA discontinuation, TRACP-5b levels gradually returned to baseline, remaining lower than the veh group for up to 6 weeks and reaching veh group levels by 10 weeks after drug withdrawal. These findings resemble data from the FLEX randomized trial showing that in osteoporotic patients receiving alendronate for 5 years, BP discontinuation results in a gradual increase of serum bone resorption and formation markers measured at 3 and 5 years after discontinuation.[56] A faster recovery of bone turnover markers is reported at 1 year after BP discontinuation in osteoporotic patients receiving risedronate for 3 years.[57] The HORIZON-Pivotal Fracture Trial (PFT) reported that annual ZA infusions are efficacious in decreasing bone turnover and reducing fracture risk in postmenopausal women with osteoporosis.[58] Interestingly, in the HORIZON extension, discontinuation of iv ZA infusions for a period of 36 months showed that bone turnover markers increase only slightly compared with controls continuing to receive ZA.[59] These variations in resolution of bone turnover indices after BP discontinuation could reflect differences in BP biodistribution, bone mineral affinity, and mode of administration.

The RANKL inhibitor OPG-Fc was used as a surrogate to denosumab because the latter does not recognize the mouse RANKL.[30] OPG-Fc treatment significantly reduced serum TRACP-5b levels that declined to levels lower than veh- or ZA-treated animals. Interestingly, at 4 and 6 weeks after OPG-Fc discontinuation, TRACP-5b levels rose above those in the veh-treated group and declined to baseline by 10 weeks. These results parallel observations from studies in postmenopausal patients with osteoporosis, wherein denosumab discontinuation led to recovery of bone resorption markers that transiently exceeded pretreatment levels before recovering to normal.[60] At the tissue level, denosumab treatment reduces bone turnover, including eroded surfaces and tetracycline labeling.[61,62] After denosumab cessation, bone histomorphometry indices return to pretreatment levels, indicating that the effects of denosumab on bone turnover are fully reversible.[63]

Given the great importance of osteoclasts in bone healing and in periapical and periodontal disease progression[64–67] and the central role of bone remodeling suppression in ONJ pathophysiology,[5,11,12] discontinuation of oral bisphosphonates in patients with low bone turnover marker values was recommended to allow recovery of osteoclastic function before dental surgical procedures.[68] However, such recommendations have been questioned, and the significance of oral bisphosphonate discontinuation in the management of the ONJ patient remains controversial.[69]

Recommendations for discontinuation of antiresorptive medication by professional organizations are cautious and based on theoretical assumptions. For osteoporotic patients, the American Dental Association (ADA) Council on Scientific Affairs recommends that before a dental procedure, "discontinuation of antiresorptive therapy should be a medical decision based primarily on the risk of experiencing SRE secondary to low bone density, not the potential risk of developing ARONJ."[15] The AAOMS position paper reports that a theoretical benefit might exist for patients with history of prolonged bisphosphonate treatment (>4 years), [7] whereas the International Task Force opines that "it may be advisable to stop antiresorptive therapy if it is possible to do so without adverse consequences for bone health."[8] Similarly, recommendations for patients receiving oncologic doses of antiresorptives on drug discontinuation before surgical dental procedures are inconclusive. For patients who have developed ONJ, discontinuation of antiresorptive medication until closure of the soft tissue defect with well-epithelialized mucosa may be considered, depending on the systemic disease status. A potentially greater rate of ONJ resolution upon discontinuation of denosumab (40.4%) versus ZA (29.7%) in cancer patients with bone metastases has been reported.[70] However, the benefit of such drug discontinuation in ONJ healing is unclear. All reports uniformly describe the lack of evidence to support or contradict utilization of drug withdrawal in the management of patients on antiresorptives and emphasize the great importance of studies that would inform such clinical decisions.[7,8,70]

To address this void in our understanding of ONJ management as it pertains to drug holidays for resolution of existing ONJ lesions, we treated mice with high-dose OPG-Fc to inhibit RANKL-RANK signaling or with ZA to develop ONJ lesions and then discontinued drug administration for 6 or 10 weeks. Qualitative and quantitative radiographic and histologic analysis of mandibles and maxillae revealed that both antiresorptive treatments successfully induced ONJ-like lesions in mice, similar to our previous observations.[29,31,32] Upon discontinuation of OPG-Fc, radiographic indices of alveolar bone loss, such as PDL space width, lamina dura loss, and alveolar BV and BV/TV, were similar to the veh-treated animals. However, ZA cessation did not significantly alter radiographic appearance within the experimental time frame. Importantly, OPG-Fc discontinuation progressively decreased histologic features of ONJ, including number of empty osteocytic lacunae, osteonecrotic area, and presence of exposed bone. In contrast, for both time points of ZA, all histologic indices of ONJ remained similar to the prewithdrawal levels and different than both the veh and OPG-Fc groups. An interesting caveat that our studies did not address is whether ONJ incidence and severity would have progressed if antiresorptives were continuously present for the 21 weeks of the experiment. Thus, although it remained the same pre- and post-ZA withdrawal, ONJ burden could have potentially worsened if ZA were continuously present. If that were true, ZA withdrawal would have ablated this increased burden.

The reversal of ONJ radiographic and histologic findings after OPG-Fc discontinuation was paralleled by a robust recovery of osteoclastic function, indicated by the increased serum TRACP-5b levels and the increased osteoclast numbers in the femur and the diseased sites of the mandible and maxillae. Because OPG-Fc withdrawal was associated with bone loss that progressively reached similar levels to that of veh animals and with increased osteoclast numbers and activity, the reduction in osteonecrotic areas appears to be mainly attributable to removal of the necrotic bone by the recovered osteoclasts. Increased bone remodeling, although probably present in areas of inflammation, appeared less likely to play a significant role in the reduced bone necrosis and exposure.

The close association of osteoclastic recovery to ONJ burden points to the central involvement of osteoclastic function, not only for ONJ pathogenesis but also, importantly, for ONJ resolution. Our data collectively demonstrate that OPG-Fc, but not ZA, discontinuation reversed radiographic and histologic features of osteonecrosis and support theoretical predictions based on antiresorptive pharmacokinetics and mode of action hypothesizing that denosumab withdrawal leads to higher recovery rates of ONJ compared with ZA because of denosumab's reversible inhibition of osteoclastic activity.[70,71] Although our findings are potentially instructive for other settings of drug holidays, such as before tooth extractions or oral surgical interventions, future studies that directly address these scenarios would provide valuable insight into usefulness of antiresorptive withdrawal to prevent ONJ development.

In conclusion, we report that antiresorptive treatment discontinuation alters radiographic and histologic findings of ONJ in mice differently, depending on the type of antiresorptive agent. To the best of our knowledge, this is the first experimental study to illustrate and quantify such differences. Our findings provide a rationale that informs clinical decisions for drug holidays in the management of the ONJ patient. Indeed, if our findings remain translatable to the clinical setting, they would suggest that for patients receiving high-dose antiresorptives for the management of malignancy, denosumab discontinuation would offer faster and more complete resolution of ONJ compared with BPs.

Disclosures

ST has served as a paid consultant for and has received grant support from Amgen Inc. PK, RB, and DD are full-time employees and/or shareholders of Amgen Inc. All other authors state that they do not have any conflicts of interest.

Acknowledgments

This work was supported by grants from Amgen Inc, and by NIH/NIDCR R01 DE019465. RSM was supported by fellowships from the State of Sao Paulo Research Foundation (FAPESP) #2012/09968-5, the Coordination for the Improvement of Higher Level or Education Personnel (CAPES) #11575/13-1, and Lemann Foundation.

Authors' roles: Conceived and designed the experiments: RSM, FQP, SMD, PK, RWB, TLA, and ST. Performed the experiments: RSM, HS, OB, FQP, SDM, PK, DD, TLA, and ST. Analyzed the data: RSM, HS, PK, RWB, TLA, and ST. Contributed to the writing of the manuscript: RSM and ST. Contributed to editing the manuscript: RSM, HS, OB, FQP, SMD, PK, RWB, DD, TLA, and ST.

References

1. Tolia M, Zygogianni A, Kouvaris JR, et al. The key role of bisphosphonates in the supportive care of cancer patients. Anticancer Res. 2014;34:23–37.
2. Tella SH, Gallagher JC. Prevention and treatment of postmenopausal osteoporosis. J Steroid Biochem Mol Biol. 2014;142:155–70.
3. Morgans AK, Smith MR. Bone-targeted agents: preventing skeletal complications in prostate cancer. Urol Clin North Am. 2012;39: 533–46.
4. Roelofs AJ, Thompson K, Gordon S, Rogers MJ. Molecular mechanisms of action of bisphosphonates: current status. Clin Cancer Res. 2006;12:6222s–30s.
5. Allen MR, Ruggiero SL. A review of pharmaceutical agents and oral bone health: how osteonecrosis of the jaw has affected the field. Int J Oral Maxillofac Implants. 2014;29:e45–57.
6. Khosla S, Burr D, Cauley J, et al. Bisphosphonate-associated osteonecrosis of the jaw: report of a task force of the American Society for Bone and Mineral Research. J Bone Miner Res. 2007; 22:1479–91.
7. Ruggiero SL, Dodson TB, Fantasia J, et al. Medication-related osteonecrosis of the jaw-2014 update [Internet]. American Association of Oral and Maxillofacital Surgeons position paper. 2014. Available at: http://www.aaoms.org/docs/position_papers/mronj_position_paper.pdf?pdf=MRONJ-Position-Paper.
8. Khan A., Morrison A, Hanley D, et al. Diagnosis and management of osteonecrosis of the jaw: a systematic review and international consensus. J Bone Miner Res. 2015;30:3–23.
9. Marx RE. Pamidronate (Aredia) and zoledronate (Zometa) induced avascular necrosis of the jaws: a growing epidemic. J Oral Maxillofac Surg. 2003;61:1115–7.
10. Ruggiero SL, Mehrotra B, Rosenberg TJ, Engroff SL. Osteonecrosis of the jaws associated with the use of bisphosphonates: a review of 63 cases. J Oral Maxillofac Surg. 2004;62:527–34.
11. Yamashita J, McCauley LK. Antiresorptives and osteonecrosis of the jaw. J Evid Based Dent Pract. 2012;12:233–47.
12. Allen MR, Burr DB. The pathogenesis of bisphosphonate-related osteonecrosis of the jaw: so many hypotheses, so few data. J Oral Maxillofac Surg. 2009;67:61–70.
13. Allen MR. Bisphosphonates and osteonecrosis of the jaw: moving from the bedside to the bench. Cells Tissues Organs. 2009;189: 289–94.
14. Woo SB, Hellstein JW, Kalmar JR. Narrative [corrected] review: bisphosphonates and osteonecrosis of the jaws. Ann Intern Med. 2006;144:753–61.
15. Hellstein JW, Adler RA, Edwards B, et al. Managing the care of patients receiving antiresorptive therapy for prevention and treatment of osteoporosis: executive summary of recommendations from the American Dental Association Council on Scientific Affairs. J Am Dent Assoc. 2011;142:1243–51.
16. Damm DD, Jones DM. Bisphosphonate-related osteonecrosis of the jaws: a potential alternative to drug holidays. Gen Dent. 2013;61: 33–8.
17. Food and Drug Administration. Background document of meeting of Advisory Committee for Reproductive Health Drugs and Drug Safety and Risk Management Advisory Committee [Internet]. 2011. Available at: http://www.fda.gov/downloads/AdvisoryCommittees/CommitteesMeetingMaterials/drugs/DrugSafetyandRiskManagementAdvisoryCommittee/ucm270958.pdf.
18. Abtahi J, Agholme F, Sandberg O, Aspenberg P. Bisphosphonate-induced osteonecrosis of the jaw in a rat model arises first after the bone has become exposed. No primary necrosis in unexposed bone. J Oral Pathol Med. 2012;41:494–9.
19. Aghaloo TL, Kang B, Sung EC, et al. Periodontal disease and bisphosphonates induce osteonecrosis of the jaws in the rat. J Bone Miner Res. 2011;26:1871–82.
20. Aguirre JI, Akhter MP, Kimmel DB, et al. Oncologic doses of zoledronic acid induce osteonecrosis of the jaw-like lesions in rice rats (Oryzomys palustris) with periodontitis. J Bone Miner Res. 2012;27:2130–43.
21. Ali-Erdem M, Burak-Cankaya A, Cemil-Isler S, et al. Extraction socket healing in rats treated with bisphosphonate: animal model for bisphosphonate related osteonecrosis of jaws in multiple myeloma patients. Med Oral Patol Oral Cir Bucal. 2011;16:e879–83.
22. Bi Y, Gao Y, Ehirchiou D, et al. Bisphosphonates cause osteonecrosis of the jaw-like disease in mice. Am J Pathol. 2010;177:280–90.
23. Lopez-Jornet P, Camacho-Alonso F, Molina-Minano F, Gomez-Garcia F, Vicente-Ortega V. An experimental study of bisphosphonate-induced jaws osteonecrosis in Sprague-Dawley rats. J Oral Pathol Med. 2010;39:697–702.
24. Kikuiri T, Kim I, Yamaza T, et al. Cell-based immunotherapy with mesenchymal stem cells cures bisphosphonate-related osteonecrosis of the jaw-like disease in mice. J Bone Miner Res. 2010;25: 1668–79.
25. Sonis ST, Watkins BA, Lyng GD, Lerman MA, Anderson KC. Bony changes in the jaws of rats treated with zoledronic acid and dexamethasone before dental extractions mimic bisphosphonate-related osteonecrosis in cancer patients. Oral Oncol. 2009;45: 164–72.
26. Pautke C, Kreutzer K, Weitz J, et al. Bisphosphonate related osteonecrosis of the jaw: a minipig large animal model. Bone. 2012;51:592–9.
27. Allen MR, Chu TM, Ruggiero SL. Absence of exposed bone following dental extraction in beagle dogs treated with 9 months of high-dose zoledronic acid combined with dexamethasone. J Oral Maxillofac Surg. 2013;71:1017–26.
28. Gotcher JE, Jee WS. The progress of the periodontal syndrome in the rice cat. II. The effects of a diphosphonate on the periodontium. J Periodontal Res. 1981;16:441–55.
29. Kang B, Cheong S, Chaichanasakul T, et al. Periapical disease and bisphosphonates induce osteonecrosis of the jaws in mice. J Bone Miner Res. 2013;28:1631–40.
30. Kostenuik PJ, Nguyen HQ, McCabe J, et al. Denosumab, a fully human monoclonal antibody to RANKL, inhibits bone resorption and increases BMD in knock-in mice that express chimeric (muri ne/human) RANKL. J Bone Miner Res. 2009;24:182–95.
31. de Molon RS, Cheong S, Bezouglaia O, et al. Spontaneous osteonecrosis of the jaws in the maxilla of mice on antiresorptive treatment: a novel ONJ mouse model. Bone. 2014;68:11–9.
32. Aghaloo TL, Cheong S, Bezouglaia O, et al. RANKL inhibitors induce osteonecrosis of the jaw in mice with periapical disease. J Bone Miner Res. 2014;29:843–54.
33. Williams DW, Lee C, Kim T, et al. Impaired bone resorption and woven bone formation are associated with development of osteonecrosis of the jaw-like lesions by bisphosphonate and anti-receptor activator of NF-kappaB ligand antibody in mice. Am J Pathol. 2014;184:3084–93.
34. Lacey DL, Boyle WJ, Simonet WS, et al. Bench to bedside: elucidation of the OPG-RANK-RANKL pathway and the development of denosumab. Nat Rev Drug Discov. 2012;11:401–19.
35. Kostenuik PJ, Smith SY, Jolette J, Schroeder J, Pyrah I, Ominsky MS. Decreased bone remodeling and porosity are associated with improved bone strength in ovariectomized cynomolgus monkeys

treated with denosumab, a fully human RANKL antibody. Bone. 2011;49:151–61.

36. Sasaki H, Hou L, Belani A, et al. IL-10, but not IL-4, suppresses infection-stimulated bone resorption in vivo. J Immunol. 2000; 165:3626–30.
37. Wang CY, Stashenko P. Kinetics of bone-resorbing activity in developing periapical lesions. J Dent Res. 1991;70:1362–6.
38. Lawson GW. Etiopathogenesis of mandibulofacial and maxillofacial abscesses in mice. Comp Med. 2010;60:200–4.
39. Clarke MC, Taylor RJ, Hall GA, Jones W. The occurrence in mice of facial and mandibular abscesses associated with Staphylococcus aureus. Lab Anim. 1978;12:121–3.
40. Grant N, Jackson K, Lee R, Scharf B. Mandibular mass in a young Swiss-Webster mouse. Lab Anim (NY). 2002;31:25–6.
41. Bouxsein ML, Boyd SK, Christiansen BA, Guldberg RE, Jepsen KJ, Muller R. Guidelines for assessment of bone microstructure in rodents using micro-computed tomography. J Bone Miner Res. 2010;25:1468–86.
42. Ominsky MS, Li X, Asuncion FJ, et al. RANKL inhibition with osteoprotegerin increases bone strength by improving cortical and trabecular bone architecture in ovariectomized rats. J Bone Miner Res. 2008;23:672–82.
43. Silva I, Branco JC. Denosumab: recent update in postmenopausal osteoporosis. Acta Reumatol Port. 2012;37:302–13.
44. Iranikhah M, Stricker S, Freeman MK. Future of bisphosphonates and denosumab for men with advanced prostate cancer. Cancer Manag Res. 2014;6:217–24.
45. Lewin J, Thomas D. Denosumab: a new treatment option for giant cell tumor of bone. Drugs Today (Barc). 2013;49:693–700.
46. Kimmel DB. Mechanism of action, pharmacokinetic and pharmacodynamic profile, and clinical applications of nitrogen-containing bisphosphonates. J Dent Res. 2007;86:1022–33.
47. Coxon FP, Helfrich MH, Van't Hof R, et al. Protein geranylgeranylation is required for osteoclast formation, function, and survival: inhibition by bisphosphonates and GGTI-298. J Bone Miner Res. 2000;15: 1467–76.
48. Hughes DE, Wright KR, Uy HL, et al. Bisphosphonates promote apoptosis in murine osteoclasts in vitro and in vivo. J Bone Miner Res. 1995;10:1478–87.
49. Fisher JE, Rogers MJ, Halasy JM, et al. Alendronate mechanism of action: geranylgeraniol, an intermediate in the mevalonate pathway, prevents inhibition of osteoclast formation, bone resorption, and kinase activation in vitro. Proc Natl Acad Sci USA. 1999;96:133–8.
50. Luckman SP, Hughes DE, Coxon FP, Graham R, Russell G, Rogers MJ. Nitrogen-containing bisphosphonates inhibit the mevalonate pathway and prevent post-translational prenylation of GTP-binding proteins, including Ras. J Bone Miner Res. 1998;13:581–9.
51. Lin JH. Bisphosphonates: a review of their pharmacokinetic properties. Bone. 1996;18:75–85.
52. Romas E. Clinical applications of RANK-ligand inhibition. Intern Med J. 2009;39:110–6.
53. Geusens P. Emerging treatments for postmenopausal osteoporosis—focus on denosumab. Clin Interv Aging. 2009;4:241–50.
54. Lewiecki EM. Denosumab: an investigational drug for the management of postmenopausal osteoporosis. Biologics. 2008; 2:645–53.
55. Lewiecki EM. Denosumab update. Curr Opin Rheumatol. 2009;21: 369–73.
56. Black DM, Schwartz AV, Ensrud KE, et al. Effects of continuing or stopping alendronate after 5 years of treatment: the Fracture Intervention Trial Long-term Extension (FLEX): a randomized trial. JAMA. 2006;296:2927–38.
57. Watts NB, Chines A, Olszynski WP, et al. Fracture risk remains reduced one year after discontinuation of risedronate. Osteoporos Int. 2008;19:365–72.
58. Black DM, Delmas PD, Eastell R, et al. Once-yearly zoledronic acid for treatment of postmenopausal osteoporosis. N Engl J Med. 2007;356:1809–22.
59. Black DM, Reid IR, Boonen S, et al. The effect of 3 versus 6 years of zoledronic acid treatment of osteoporosis: a randomized extension to the HORIZON-Pivotal Fracture Trial (PFT). J Bone Miner Res. 2012;27:243–54.
60. Bone HG, Bolognese MA, Yuen CK, et al. Effects of denosumab treatment and discontinuation on bone mineral density and bone turnover markers in postmenopausal women with low bone mass. J Clin Endocrinol Metab. 2011;96:972–80.
61. Brown JP, Reid IR, Wagman RB, et al. Effects of up to 5 years of denosumab treatment on bone histology and histomorphometry: the FREEDOM study extension. J Bone Miner Res. 2014;29:2051–6.
62. Reid IR, Miller PD, Brown JP, et al. Effects of denosumab on bone histomorphometry: the FREEDOM and STAND studies. J Bone Miner Res. 2010;25:2256–65.
63. Brown JP, Dempster DW, Ding B, et al. Bone remodeling in postmenopausal women who discontinued denosumab treatment: off-treatment biopsy study. J Bone Miner Res. 2011;26: 2737–44.
64. Han X, Lin X, Yu X, et al. Porphyromonas gingivalis infection-associated periodontal bone resorption is dependent on receptor activator of NF-kappaB ligand. Infect Immun. 2013;81: 1502–9.
65. Yuan H, Gupte R, Zelkha S, Amar S. Receptor activator of nuclear factor kappa B ligand antagonists inhibit tissue inflammation and bone loss in experimental periodontitis. J Clin Periodontol. 2011;38:1029–36.
66. Jin Q, Cirelli JA, Park CH, et al. RANKL inhibition through osteoprotegerin blocks bone loss in experimental periodontitis. J Periodontol. 2007;78:1300–8.
67. Xiong H, Wei L, Hu Y, Zhang C, Peng B. Effect of alendronate on alveolar bone resorption and angiogenesis in rats with experimental periapical lesions. Int Endod J. 2010;43:485–91.
68. Marx RE, Cillo JE Jr, Ulloa JJ. Oral bisphosphonate-induced osteonecrosis: risk factors, prediction of risk using serum CTX testing, prevention, and treatment. J Oral Maxillofac Surg. 2007;65:2397–410.
69. American Society for Bone and Mineral Research Task Force on Osteoporosis of the Jaw, Khosla S, Burr D, et al. Oral bisphosphonate-induced osteonecrosis: risk factors, prediction of risk using serum CTX testing, prevention, and treatment. J Oral Maxillofac Surg. 2008;66:1320–1; author reply 1321–2.
70. Saad F, Brown JE, Van Poznak C, et al. Incidence, risk factors, and outcomes of osteonecrosis of the jaw: integrated analysis from three blinded active-controlled phase III trials in cancer patients with bone metastases. Ann Oncol. 2012;23:1341–7.
71. Malan J, Ettinger K, Naumann E, Beirne OR. The relationship of denosumab pharmacology and osteonecrosis of the jaws. Oral Surg Oral Med Oral Pathol Oral Radiol. 2012;114:671–6.

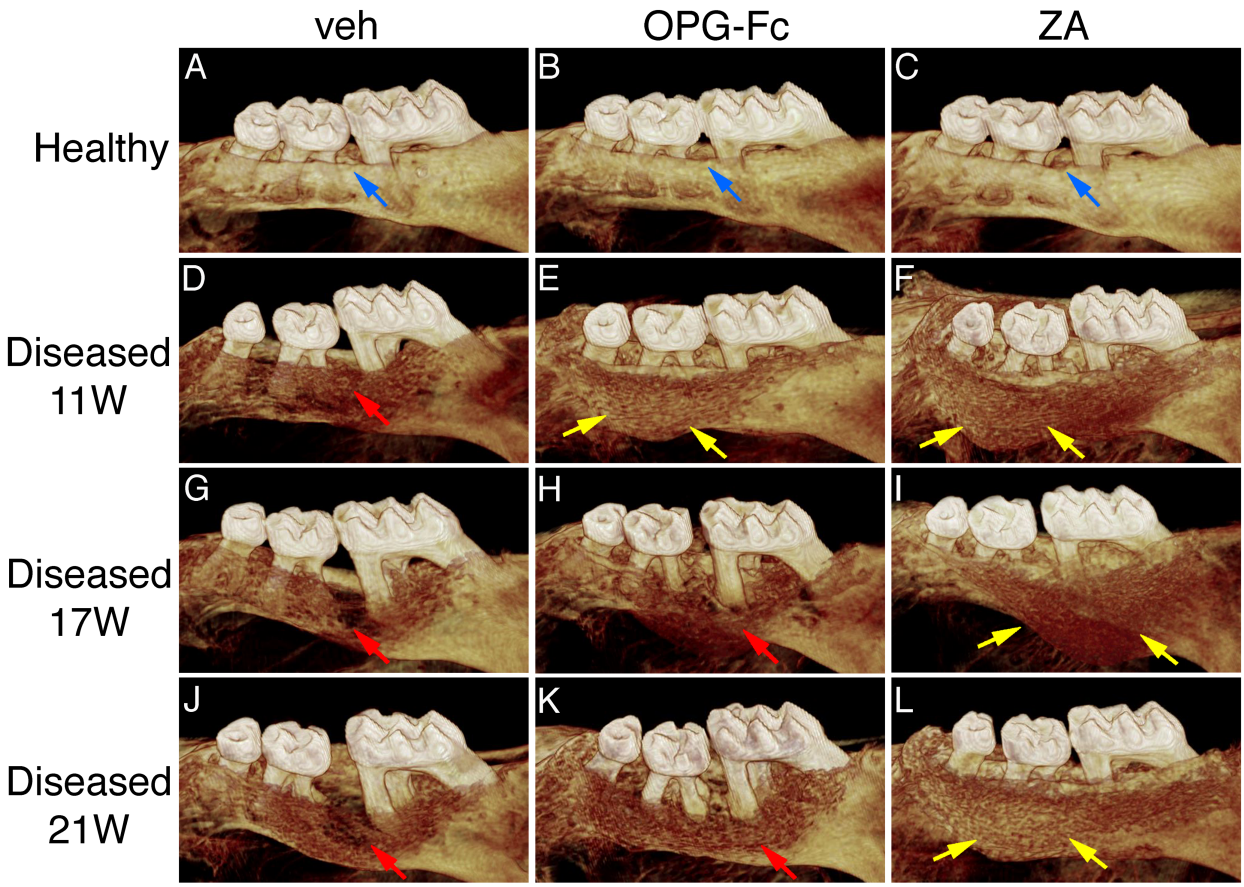

Supplemental Figure 1. 3D µCT reconstructed images of maxillae. (A-C) Healthy site in veh, OPG-Fc and ZA. (D-E) Diseased site after 11 weeks of treatment. (G-I) Diseased site after 6 weeks drug discontinuation. (J-L) Diseased site after 10 weeks discontinuation. Blue arrows point to normal alveolar bone crest in the interproximal area between the distal root of the first molar and mesial root of the second molar. Red arrow point to periodontal bone loss and areas of osteolysis. Yellow arrows point to increased bone deposition.

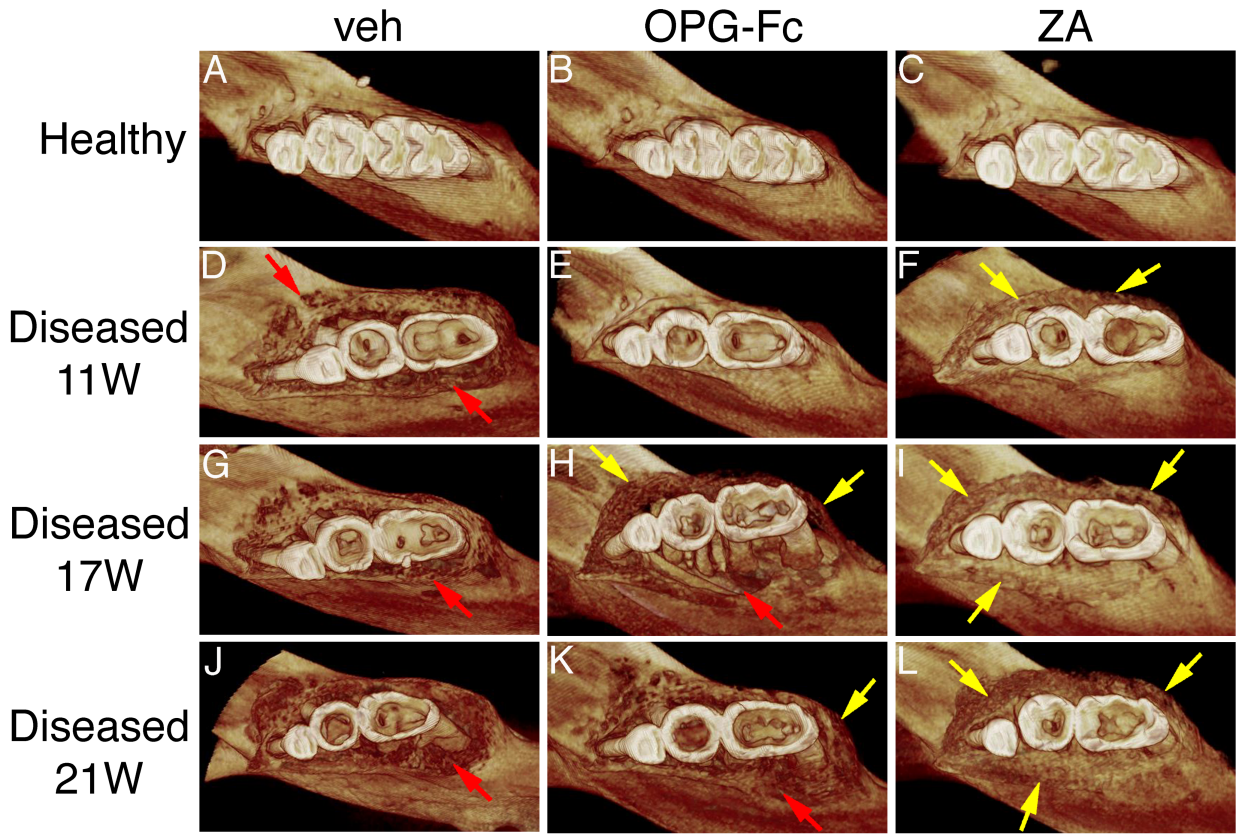

Supplemental Figure 2. 3D µCT reconstructed images of mandibles. (A-C) Healthy site in veh, OPG-Fc and ZA. (D-E) Drilled site after 11 weeks of treatment. (G-I) Drilled site site after 6 weeks of drug discontinuation. (J-L) Drilled site after 10 weeks drug discontinuation. Blue arrows point to normal alveolar bone crest in the interproximal area between the distal root of the first molar and mesial root of the second molar. Red arrow point to periodontal bone loss and areas of osteolysis. Yellow arrows point to increased bone deposition.

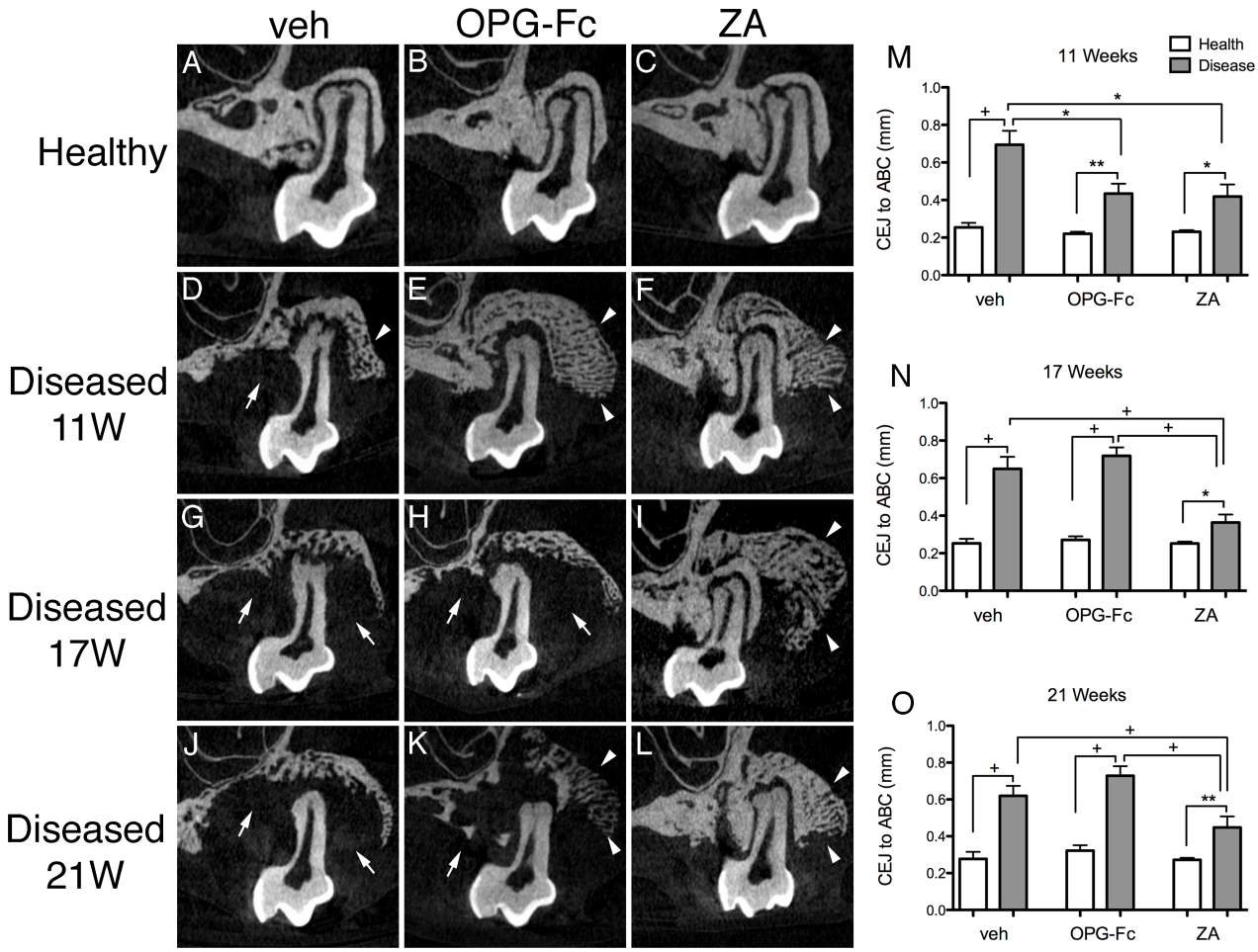

Supplemental Figure 3. Coronal µCT slices of the maxillary alveolar bone at the area of the first molars. (A-C) Healthy site in veh, OPG-Fc and ZA. (D-E) Diseased site after 11 weeks of treatment. (G-I) Diseased site after 6 weeks drug discontinuation. (J-L) Diseased site after 10 weeks discontinuation. Thin arrows point to areas of osteolysis. Arrowheads point to new bone deposition. (M-O) Quantification of the distance from the CEJ to ABC. $^{+}$Statistically significant different from indicated groups, $p < 0.0001$. **Statistically significant different from indicated groups, $p < 0.001$. *Statistically significant different from indicated groups, $p < 0.05$. Statistically significant differences were calculated using one-way ANOVA followed by post-hoc Tukey's test and using Student's t test. Data represent the mean ± SEM.

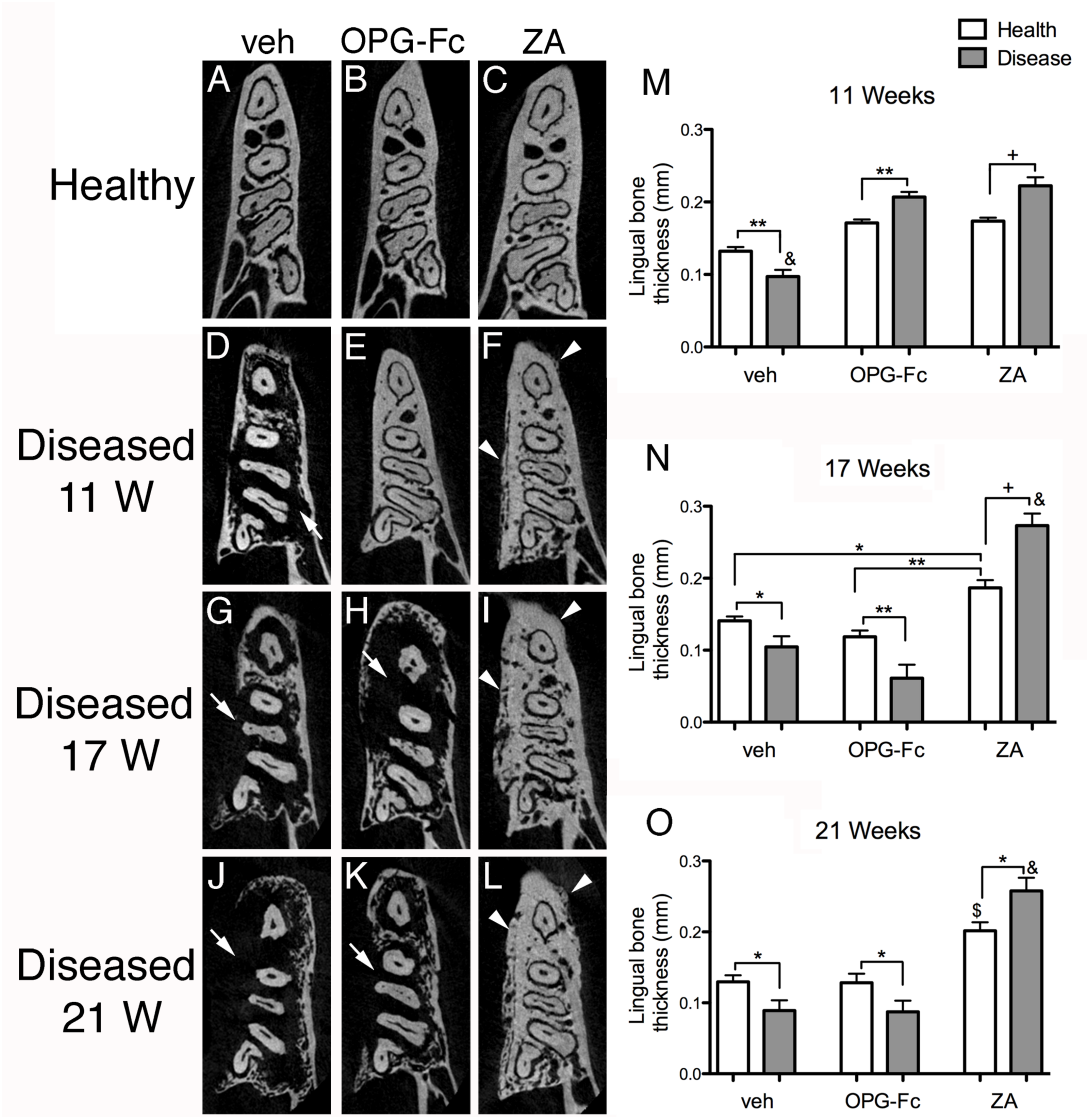

Supplemental Figure 4. Axial µCT sections of the mandibular alveolar ridge. (A-C) Healthy site in veh, OPG-Fc and ZA. (D-E) Drilled site after 11 weeks of treatment. (G-I) Drilled site after 6 weeks of drug discontinuation. (J-L) Drilled site after 10 weeks drug discontinuation. Thin arrows point to areas of osteolysis. Arrowheads point to new bone deposition. (M-O) Quantification of lingual bone thickness. $^{\$}$Statistically significant different compared to healthy mice, $p < 0.0001$. $^{\&}$Statistically significant different compared to diseased mice, $p < 0.0001$. $^{+}$Statistically significant different from indicated groups, $p < 0.0001$. **Statistically significant different from indicated groups, $p < 0.001$. *Statistically significant different from indicated groups, $p < 0.05$. Statistically significant differences were calculated using one-way ANOVA followed by post-hoc Tukey's test and using Student's t test. Data represent the mean ± SEM.

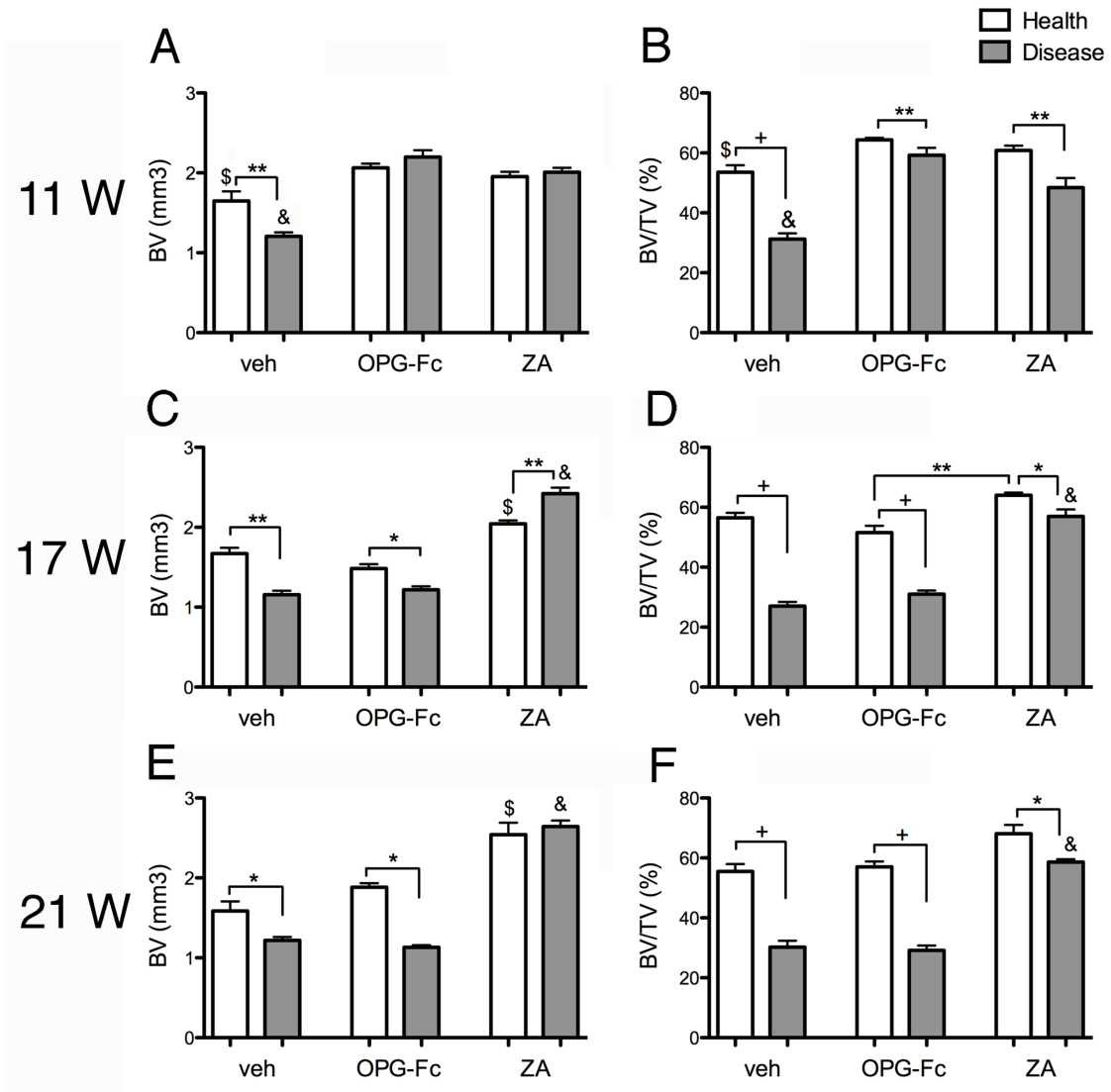

Supplemental Figure 5. Quantification of BV and BV/TV in the maxillae of all mice. 11 weeks of treatment (A, B), 6 weeks (C, D) and 10 weeks (E, F) after drug discontinuation. $^{\$}$Statistically significant different compared to healthy mice, $p < 0.0001$. $^{\&}$Statistically significant different compared to diseased mice, $p < 0.0001$. $^{+}$Statistically significant different from indicated groups, $p < 0.0001$. **Statistically significant different from indicated groups, $p < 0.001$. *Statistically significant different from indicated groups, $p < 0.05$. Statistically significant differences were calculated using one-way ANOVA followed by post-hoc Tukey's test and using Student's t test. Data represent the mean ± SEM.

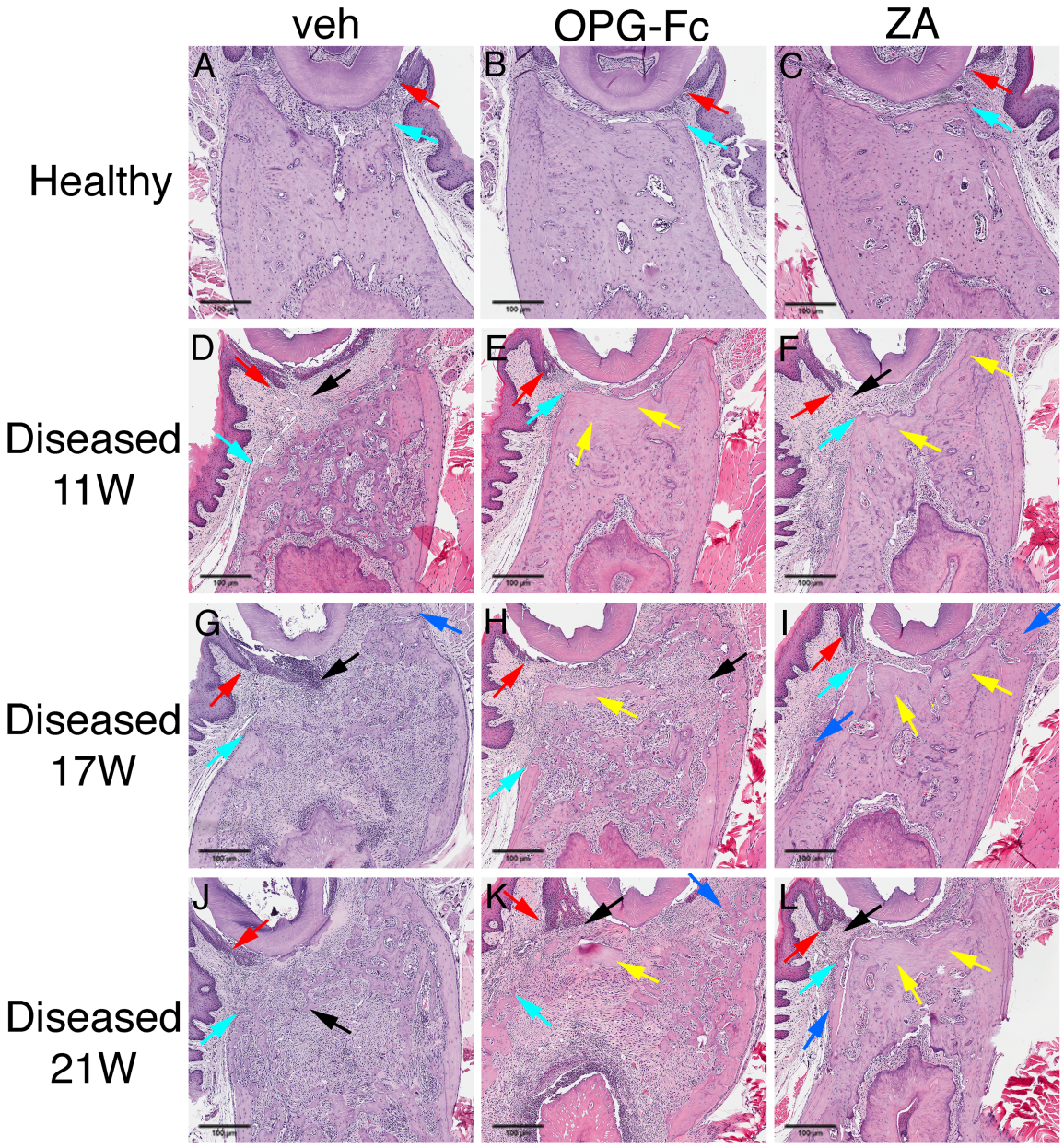

Supplemental Figure 6. Representative H&E-stained images from mandible of all groups. (A-C) Healthy site of veh, OPG-Fc and ZA animals. (D-F) Drilled site at 11 weeks at the end of antiresorptive treatment. (G-I) Drilled site 6 weeks after antiresorptive discontinuation. (J-L) Drilled site 10 weeks after antiresorptive discontinuatio. Red arrows point to marginal gingival epithelium, turquoise arrows to alveolar crest, black arrows to areas of inflammation, blue arrows to periosteal bone deposition, yellow arrows to osteonecrotic areas, and green arrows to areas of bone exposure. Original magnification, x5.

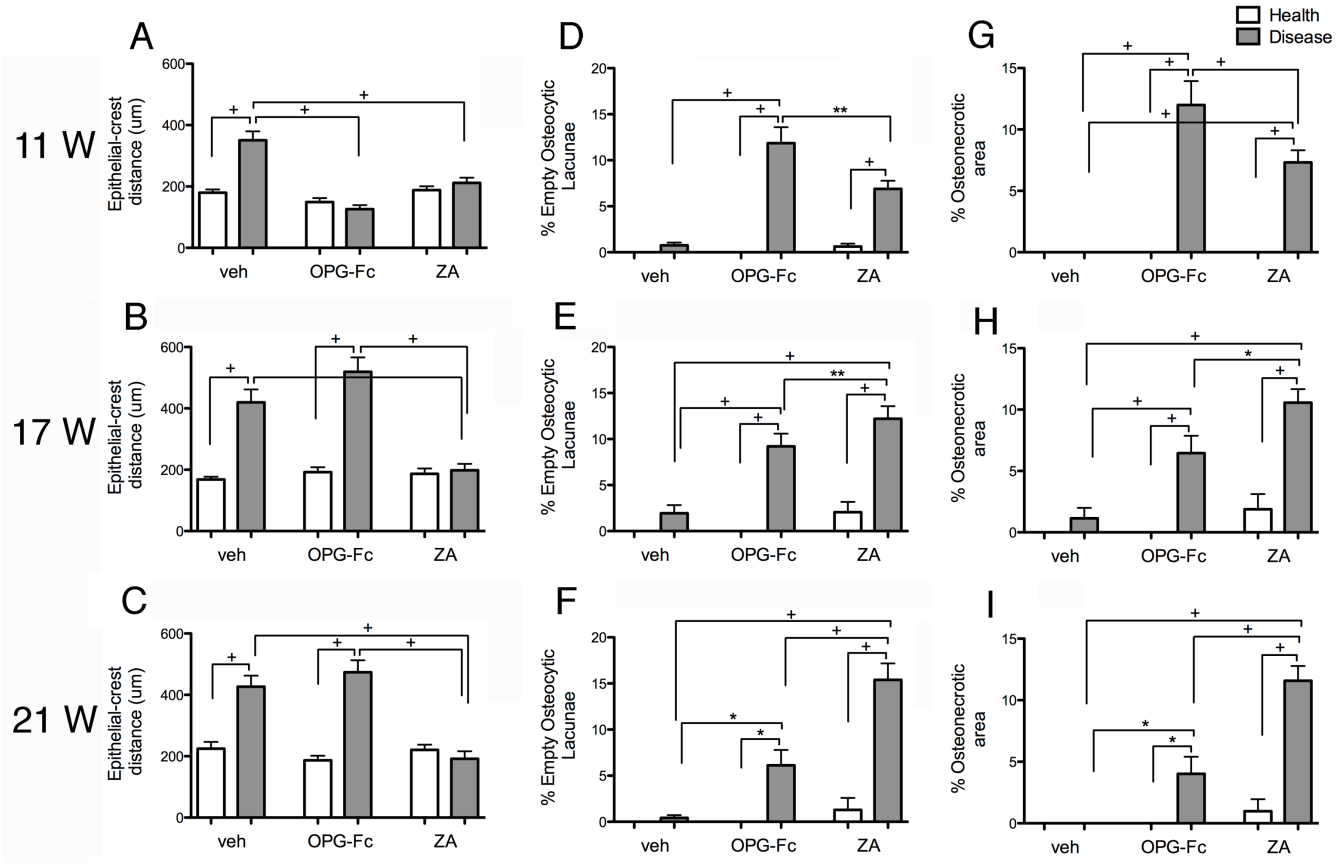

Supplemental Figure 7. Quantification of histologic findings in the mandible. (A-C) The shortest epithelial-crest distance was determined. (D-F) Osteocytic lacunae were measured and empty lacunae were expressed as percent of total. (G-I) Area of osteonecrosis was measured and expressed as % of total bone area. $^{+}$Statistically significant different from indicated groups, $p < 0.0001$. **Statistically significant different from indicated groups, $p < 0.001$. *Statistically significant different from indicated groups, $p < 0.05$. Statistically significant differences were calculated using one-way ANOVA followed by post-hoc Tukey's test and using Student's t test. Data represent the mean ± SEM.

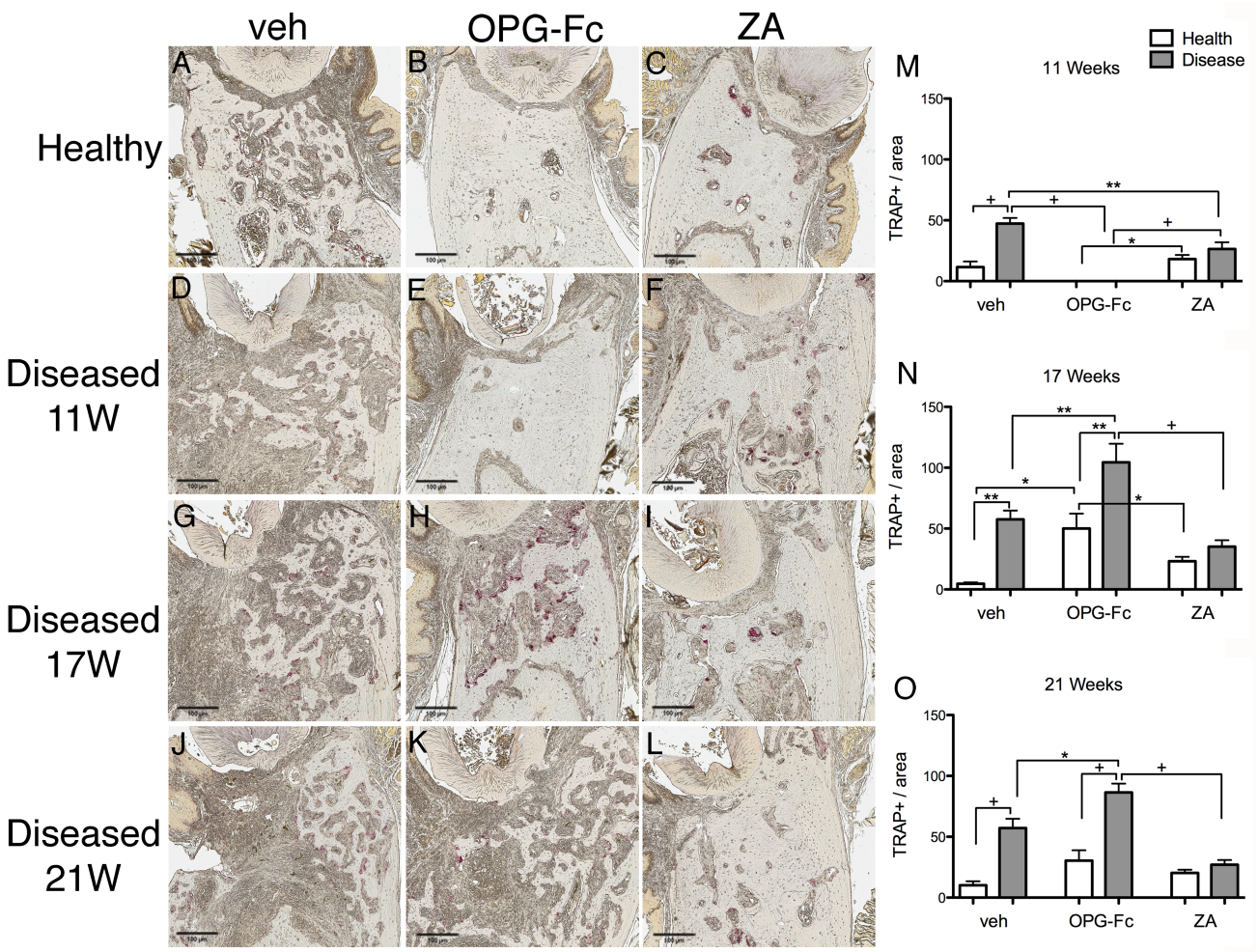

Supplemental Figure 8. Representative sections of mandibles stained for TRAP + cells. Original magnification, x5. (A-C) Healthy site of veh, OPG-Fc and ZA animals. (D-F) Drilled site at 11 weeks, at the end of antiresorptive treatment. (G-I) Drilled site of veh, OPG-Fc and ZA 6 weeks after antiresorptive discontinuation. (J-L) Drilled site of veh, OPG-Fc and ZA 10 weeks after antiresorptive discontinuation. (M-O) Quantification of TRAP + cell number. $^{+}$Statistically significant different from indicated groups, $p < 0.0001$. **Statistically significant different from indicated groups, $p < 0.001$. *Statistically significant different from indicated groups, $p < 0.05$. Statistically significant differences were calculated using one-way ANOVA followed by post-hoc Tukey's test and using Student's t test. Data represent the mean ± SEM.

Original Article

Rheumatoid arthritis exacerbates the severity of osteonecrosis of the jaws (ONJ) in mice. A randomized, prospective, controlled animal study†

Rafael Scaf de Molon,[1,2] Chingyun Hsu,[1] Olga Bezouglaia,[1] Sarah M. Dry,[3] Flavia Q. Pirih,[4] Akrivoula Soundia,[1] Fernando Queiroz Cunha,[5] Joni Augusto Cirelli,[2] Tara L. Aghaloo,[1,*] Sotirios Tetradis[1,6,*]

[1]Division of Diagnostic and Surgical Sciences, UCLA School of Dentistry, Los Angeles, CA 90095, USA
[2]Department of Diagnosis and Surgery, School of Dentistry at Araraquara, Sao Paulo State University, Araraquara 14801–903, Brazil
[3]Department of Pathology and Laboratory Medicine, David Geffen School of Medicine at UCLA, Los Angeles, CA 90095, USA
[4]Division of Constitutive & Regenerative Sciences, UCLA School of Dentistry, Los Angeles, CA 90095, USA
[5]Department of Pharmacology, School of Medicine of Ribeirao Preto, Sao Paulo 14049, Brazil
[6]Molecular Biology Institute, UCLA, Los Angeles, CA 90095, USA

* Corresponding Authors

Sotirios Tetradis DDS, PhD
UCLA School of Dentistry
10833 Le Conte Ave. CHS Rm. 53-068
Los Angeles, CA 90095-1668
Tel: (310) 825-5712, Fax: (310) 825-7232
Email: stetradis@dentistry.ucla.edu

Tara L. Aghaloo DDS, MD, PhD
UCLA School of Dentistry
10833 Le Conte Ave. CHS Rm. 53-009
Los Angeles, CA 90095-1668
Tel: (310) 794-7070, Fax: (310) 825-7232
Email: taghaloo@dentistry.ucla.edu

†This article has been accepted for publication and undergone full peer review but has not been through the copyediting, typesetting, pagination and proofreading process, which may lead to differences between this version and the Version of Record. Please cite this article as doi: [10.1002/jbmr.2827]

Additional Supporting Information may be found in the online version of this article.

Initial Date Submitted September 7, 2015; Date Revision Submitted March 1, 2016; Date Final Disposition Set March 2, 2016

Journal of Bone and Mineral Research
This article is protected by copyright. All rights reserved
DOI 10.1002/jbmr.2827

This article is protected by copyright. All rights reserved

Accepted Article

Accepted Article

ABSTRACT

Rheumatoid arthritis (RA), an autoimmune inflammatory disorder, results in persistent synovitis with severe bone and cartilage destruction. Bisphosphonates (BPs) are often utilized in RA patients to reduce bone destruction and manage osteoporosis. However, BPs, especially at high doses, are associated with osteonecrosis of the jaw (ONJ). Here, utilizing previously published ONJ animal models, we are exploring interactions between RA and ONJ incidence and severity. DBA1/J-mice were divided in 4 groups: control, zoledronic acid (ZA), collagen induced arthritis (CIA), and CIA-ZA. Animals were pre-treated with vehicle or ZA. Bovine collagen II emulsified in Freund's adjuvant was injected to induce arthritis (CIA) and the mandibular molar crowns were drilled to induce periapical disease. Vehicle or ZA treatment continued for 8-weeks. ONJ indices were measured by micro-CT and histological examination of maxillae and mandibles. Arthritis development was assessed by visual scoring of paw swelling, and by micro-CT and histology of interphalangeal and knee joints. Maxillae and mandibles of control and CIA mice showed bone loss, PDL space widening, lamina dura loss and cortex thinning. ZA prevented theses changes in both ZA and CIA-ZA groups. Epithelial to alveolar crest distance was increased in the control and CIA mice. This distance was preserved in ZA and CIA-ZA animals. Empty osteocytic lacunae and areas of osteonecrosis were present in ZA and CIA-ZA but more extensively in CIA-ZA animals, indicating more severe ONJ. CIA and CIA-ZA groups developed severe arthritis in the paws and knees. Interphalangeal and knee joints of CIA mice showed advanced bone destruction with cortical erosions and trabecular bone loss, and ZA treatment reduced these effects. Importantly, no osteonecrosis was noted adjacent to areas of articular inflammation in CIA-ZA mice. Our data suggest that ONJ burden was more pronounced in ZA treated CIA mice and that RA could be a risk factor for ONJ development. This article is protected by copyright. All rights reserved

Keywords: Collagen-induced arthritis, rheumatoid arthritis, osteonecrosis of the jaws, bisphosphonates, ONJ, osteoclasts, antiresorptive.

This article is protected by copyright. All rights reserved

Accepted Article

INTRODUCTION

Rheumatoid arthritis (RA), an immunologically driven long-term disorder is characterized by persistent synovitis, systemic inflammation, and presence of autoantibodies (particularly to rheumatoid factor and citrullinated peptide), leading to long-term joint damage, chronic pain, loss of function and disability.[1,2] An exacerbated immune response from the activation of immune, inflammatory and resident cells is responsible for most of the tissue damage observed in RA, while osteoclastic activation plays major role in joint destruction.[3,4] Several treatments for RA have been developed and include nonsteroidal anti-inflammatory drugs (NSAIDs), corticosteroids, disease-modifying antirheumatic drugs (DMARDs), biologic agents (tumor necrosis factor or interleukin inhibitors) and JAK inhibitors.[1,5] All treatment strategies aim to reduce periarticular inflammation and limit joint destruction.

A major comorbidity in RA patients is a generalized skeletal BMD reduction and micro architectural deterioration.[6-8] RA vs. non-RA patients, show a 22.1 % increased incidence of osteoporosis and 11.4 % BMD reduction, while the overall frequency of osteoporosis and BMD below the expected age range in RA vs. non-RA subjects was 1.9 and 7.8 times higher, respectively.[9]

Nitrogen-containing bisphosphonates (BPs) strong inhibitors of osteoclastic bone resorption, are widely used to manage bone diseases, such as osteoporosis[10] or bone malignancy.[11] Many patients with RA are treated with bisphosphonates for managing their osteoporosis. Furthermore, the beneficial effects of BPs in the RA mediated focal osteolysis have been shown.[12-14] Indeed, BPs are among the most frequent prescribed drugs in rheumatologic practice.[15,16]

An infrequent but serious adverse effect of BPs is osteonecrosis of the jaw (ONJ) especially during intravenous high dose administration.[17] ONJ is defined as an area of exposed bone or bone that can be probed through an intraoral fistula in the maxillofacial region that does not heal within 8 weeks in patients exposed to antiresorptive medications and without history of radiation therapy to the

This article is protected by copyright. All rights reserved

jaws.[18,19] ONJ is most frequently observed after dental interventions such as tooth extraction, periodontal disease and in patients receiving corticosteroid treatment.[18,20,21] Recently, the term medication-related ONJ (MRONJ) was proposed[21] to include ONJ cases related to antiangiogenic therapies.

Despite described in 2004, pathophysiology of ONJ remains largely unknown.[22] Parameters that increase the risk for ONJ include dose and duration of antiresorptives, dentoalveolar surgery, concomitant dental disease, corticosteroid and anti-angiogenic treatment, and diabetes.[23-26] Interestingly, clinical studies point to an increased incidence of ONJ in RA patients and suggest that RA may represent a significant risk factor for the development of ONJ when BPs are administered to manage osseous complications.[8,20,27-29] However, the validity of this conclusion has been questioned, since almost all patients were receiving steroids, DMARDs, or a combination of these immunosuppressive agents that could alone increase ONJ risk.[28] Experimental data that directly explore the incidence and severity of ONJ in the absence or presence of RA are lacking.

Here, we employed two previously published ONJ mouse models utilizing either experimental periapical disease of mandibular teeth or naturally occurring periradicular inflammation of maxillary teeth [30-33] with a well-established model of collagen-induced arthritis (CIA) to explore the interplay between RA and ONJ. Our findings indicate that, jaw osteonecrosis was more extensive in ZA treated CIA mice in both maxilla and mandible, suggesting that systemic inflammation in RA compounds ONJ severity. ZA reduced bone resorption and cartilage destruction but not synovial inflammation in the hind paws and knee joints. Importantly, no osteonecrosis was noted adjacent to areas of articular inflammation in ZA treated mice with CIA.

This article is protected by copyright. All rights reserved

Accepted Article

MATERIALS AND METHODS

Animal care

Mice and surgical procedures were handled according to the guidelines of the Institutional Animal Care and Use Committee of UCLA. 10-week old DBA1/J male mice (Jackson Laboratories, Bar Harbor, ME, USA) were randomly divided into four experimental groups of 6 animals each: control (vehicle), ZA, CIA and CIA-ZA. Animals were pre-treated with *i.p*. injections of endotoxin free saline (vehicle) or 200 μg/kg zoledronic acid (ZA, Z-5744 LKT laboratories, St. Paul, MN) two times per week, for 1 week prior to periapical disease and CIA induction. The rationale for this 1-week pre-treatment was to induce bone turnover suppression at the time of dental intervention. Vehicle or ZA treatment continued for 8 additional weeks for a total duration of nine weeks for the experiment. Also, at week 4 of the experiment, and three weeks after the original injection to induce CIA, a booster injection of type-II collagen in IFA was performed (see bellow). ZA dose was used to increase the incidence of ONJ-like lesions in mice, as described previously.[30] The protocol followed all recommendations of the ARRIVE (Animal Research: Reporting in Vivo Experiments) guidelines for execution and submission of studies in animals.[34]

Induction of periapical disease

We have established an ONJ mouse model employing experimental periapical disease.[30,33] To induce periapical disease, the pulp chamber of the right 1st and 2nd mandibular molars were accessed utilizing a stainless-steel ¼ size round bur in a high speed handpiece, avoiding furcal perforation, and the root canals were left exposed to the oral environment for lesion induction. The crowns of the left 1st and 2nd molars were kept intact.

Spontaneous naturally occurring peri-radicular disease

This article is protected by copyright. All rights reserved

Accepted Article

Naturally and spontaneously occurring peri-radicular disease have been reported in mice.[35-37] We have observed ONJ like lesions around such lesions in mice treated with high doses of antiresorptives [31] Such diseased maxillary sites, identified by periradicular osteolysis and/or periosteal bone formation by μCT imaging, were compared to sites with healthy dento-alveolar structures, as previously described.[31]

Induction of collagen-induced arthritis (CIA)

CIA was established following precisely previous published protocol.[38] Briefly, bovine type-II collagen (Chondrex 20021; BD Biosciences, San Jose, CA, USA) was dissolved at 4 mg/mL in 0.1 M acetic acid at 4°C. Complete Freund's adjuvant (CFA) was composed of incomplete Freund's adjuvant (IFA) (Sigma Aldrich – F5506) and freshly ground heat-killed *Mycobacterium tuberculosis* strain H37Ra (BD Biosciences, San Jose, CA, USA). A 1:1 (v/v) emulsion consisting of collagen (100 μg) and CFA (100 μg of *M. tuberculosis*) was prepared. DBA1/J male mice were immunized via intradermal injection with 50 μL of the emulsion about 1.5 cm distal from the base of the tail, being careful to choose a tissue site and not a vessel. Three weeks after the primary immunization, a booster injection with 100 μg bovine type-II collagen in IFA was given in the tail at a site proximal to the first injection, about 1 cm distal from the tail base.

Clinical assessment of RA

Mice were scored for arthritis every other day from day 21 after the first immunization until the time of sacrifice using the following criteria: 0 = no joint swelling, 1 = swelling of one finger joint, 2 = mild swelling of the wrist or ankle, or 3 = severe swelling of the wrist or ankle, as described.[39] The scores for all fingers of forepaws and hind paws, wrists and ankles were totaled for each mouse (with a maximum possible score of 12 for each mouse).

This article is protected by copyright. All rights reserved

Accepted Article

Animal sacrifice and analyses

After 9 weeks of treatment, six animals from the control and experimental groups were sacrificed via isoflurane overdose. The mandibles, maxillae, tibias, femurs and hind paws were carefully harvested, and the block samples were fixed in 4% paraformaldehyde for 48 hours and stored in 70% ethanol at room temperature until they were scanned using a μCT system.

Micro-computed tomography scanning (*μ*CT scanning)

Maxillae, mandibles, femurs, tibiae and hind paws were scanned using a μCT imaging system (μCT Skyscan 1172; Skyscan, Kontich, Belgium) as described.[30-33] For linear measurements, volumetric image data were converted to Digital Imaging and Communications in Medicine (DICOM) format and imported in the Dolphin Imaging software (Chatsworth, CA) to generate 3D and multiplanar reconstructed images.

In the mandible, periapical bone loss (the distance from the root apex to the periapical alveolar bone) was measured at the distal root of the first and the mesial root of the second molars in a sagittal slice. The lamina dura thickness and the width of the periodontal ligament (PDL) space were quantified through the middle of the furcation area of the first molar along the mesial-distal axis of the tooth, in a sagittal slice. The lingual and buccal bone thickness was measured in an axial slice at the level of the apical third or the root for the first and second molar comprising the shortest distance from the lingual surface of the root to the outline of the alveolar ridge. In the maxilla, the cement-enamel junction (CEJ) to the alveolar bone crest (ABC) distance was measured at the distal surface of the first molar. The lamina dura thickness, width of the PDL space and lingual bone thickness were measure in the same manner as in the mandible. All measurements were performed according to previous studies.[30-33]

This article is protected by copyright. All rights reserved

Accepted Article

Alveolar bone volume (BV), tissue volume (TV) and BV/TV analysis were assessed using the CTAn software (Skyscan, Kontich, Belgium). A region of interest (ROI) was delimitated from the root apices to the alveolar crest, and from the mesial root of the first molar to the distal root of the third molar. Teeth roots and periodontal ligament were excluded from the ROI.

Analysis in the femurs and tibiae was performed using CTAn on transaxial datasets for the proximal epiphyseal bone. ROIs of distal femur metaphysis and proximal tibia metaphysis included the trabecular but excluded the cortical bone. Greyscale thresholds for quantitation of structural parameters were determined using the thresholding algorithm within CTAn software. BV, TV, BV/TV, trabecular number (Tb.N), trabecular thickness (Tb.Th), and trabecular separation (Tb.Sp) were determined.

Histologic analyses

Mandible, maxilla, femur, tibia and hind paws were decalcified in 14.5% EDTA. Samples were paraffin embedded, 4 μm thick serial sections were obtained and stained with hematoxylin and eosin (H&E). All H&E stained slides were digitally scanned at 20x magnification using the Aperio AT automated slide scanner. An operator blinded to the specimen identity performed the histological measurements. Using the ruler tool in Aperio ImageScope software (Aperio Technologies, Inc., Vista, CA, USA), 1-mm of the alveolar bone starting from the alveolar crest was identified. This height extended to near the floor of the maxillary sinus in the maxilla and the mandibular canal in the mandible. For the maxilla, the region of interest (ROI) from the buccal cortex to the mid-palatal suture, while from the mandible, the ROI extended from the buccal to the lingual cortices.

Epithelium to alveolar crest distance was measured in the palatal side of the maxilla and in the lingual side of the mandible. To quantify periosteal bone thickness, the ruler tool was used to measure the three greatest areas of the buccal periosteal thickness that were then averaged. All the measurements were performed according to published studies.[30,31,33]

This article is protected by copyright. All rights reserved

Accepted Article

Within the ROI, the total number of empty osteocytic lacunae and the osteonecrotic area(s), defined as a loss of more than five contiguous osteocytes were measured. Lacunae housing necrotic, karyolitic osteocytes, indicated by eosinophilic stained nuclei, were counted as empty osteocytes. Lacunae, both empty and containing osteocytes, were counted manually and the ratio of empty to total lacunae in the ROI was calculated. The Aperio ImageScope software (Aperio, Vista, CA, USA) has an automated tool, the surface area tool, which was used to measure the area of osteonecrosis and the total bone area. The % osteonecrotic area was determined by dividing the surface area of osteonecrosis, as calculated by the software, by the total bone area, as calculated by the software, and multiplying by 100.

For standard histologic assessment in the knees and paws, sagittal sections (4 μm) were stained with H&E to study synovial inflammation, and to determine cartilage and bone destruction. Histopathologic changes were scored as described.[40-42] Briefly, infiltration of cells was scored in a scale of 0-3, depending on the amount of inflammatory cells in the synovial cavity and synovial tissues (0 = no cells, 1 = mild cellularity, 2 = moderate cellularity, and 3 = maximal cellularity). Cartilage destruction was distinctly graded on a scale of 0-3, ranging from the non-appearance of dead chondrocytes (empty lacunae) to a complete loss of chondrocytes in the cartilage. Bone erosion was scored on a scale of 0 to 5 ranging from no damage to complete bone loss.[40] Histopathologic changes in the knee joints were scored in the femur/tibia region. For the ankle joint, we scored the calcaneus and ankle region. Scoring was done in a blinded manner.

To assess osteoclast numbers, sections were stained using the Leukocyte Acid Phosphatase 387-A kit (Sigma-Aldrich, St. Louis, MO, USA). TRAP-positive multinucleated cells containing 2 or more nuclei were counted in the mandible, maxilla, ankle and knee in a total of 6 mice per group.

Histology and digital imaging was done at the UCLA Translational Pathology Core Laboratory.

This article is protected by copyright. All rights reserved

Accepted Article

Statistics

Analyses were performed on GraphPad Prism Software (GraphPad Software, Inc., La Jolla, CA). Group measures were expressed as mean and the standard error of the mean (SEM). Statistical significance was assessed using two-way analysis of variance (ANOVA) followed by the Bonferroni post-hoc test for multiple comparisons among groups. Data between groups (healthy vs. diseased) were compared using the Student's t test. Dental disease, osteonecrosis and bone exposure were also recorded as present or absent. These categorical data (Table 1) were analyzed using the Fisher's exact test.

RESULTS

Radiographic features of ONJ in the maxilla and mandible

μCT of healthy maxillae in all groups showed normal alveolar crest extending just inferior of the CEJ, around the molar roots with absence of bone expansion and bone loss (Figure 1, A-D). On the other hand, diseased vehicle and CIA mice demonstrated substantial bone destruction and loss of crest height increasing the distance between the CEJ to the alveolar bone, extending almost to the root apex of the 1st molar. Substantial palatal and buccal bone expansion of the alveolar ridge were also observed (Figure 1, A1 and C1). Bone loss was also present for the ZA and CIA-ZA mice, however the extent of bone loss was significantly reduced and was associated with extensive areas of new periosteal bone apposition, which resulted in substantial expansion of the palatal and buccal thickness of the maxillary alveolar ridge (Figure 1, B1 and D1). Similar findings were observed for the mandible in non-drilled and drilled sites of all groups (Supplemental Figure 1).

To quantitate bone loss, the CEJ to ABC distance were measured. In the healthy side of all animals a short CEJ to ABC distance was observed (Figure 2, A-D and E). Significantly increased distance was observed for vehicle and CIA mice with dental disease, indicating significant bone loss

This article is protected by copyright. All rights reserved

Accepted Article

(Figure 2, A1, C1 and E; white arrows). As expected, in ZA and CIA-ZA mice this distance was reduced, although CIA-ZA animals showed significantly more bone loss compared to ZA treated mice (Figure 2, B1, D1 and E). Similar findings were seen in the mandibles with periapical disease (Supplemental Figure 2, A-D1 and E).

We then quantified the changes in the lamina dura thickness and PDL space width in sagittal slices, at the furcation area of the 1st molar. In the healthy side of all animals, a uniform lamina dura thickness and PDL space were observed albeit in mice with antiresorptive treatment, increased lamina dura thickness was noted (Figure 2, A-D and F-G). In the diseased site of vehicle and CIA mice, there was significant loss of lamina dura thickness and significant increase of PDL space width (Figure 2, A1, C1, F and G). ZA and CIA-ZA treated mice demonstrated increased lamina dura thickness and PDL space preserved. Statistically significant inhibition of PDL widening was observed for ZA treated mice compared to other groups (Figure 2, B1, D1, F and G). Comparable results were also noted in mandibular teeth (Supplemental Figure 2, A-D1, F and G).

Then, the palatal and buccal bone thickness at the apical third of the molar roots was measured on axial slices. Healthy site of all mice showed normal palatal and buccal bone thickness without bone expansion (Figure 2, H and I-L). As previously reported,[31,32] significant expansion of the alveolar bone with exuberant osteolysis was noted for dental diseased vehicle and CIA treated mice (Figure 2, H and I1, K1). In contrast, ZA and CIA-ZA treated mice exhibited increased bone thickness (Figure 2, H and J1, L1). Importantly, in CIA-ZA treated mice a statistically significant difference in bone thickness was noted compared to all other groups (Figure 2, H, I1-L1; white arrowheads). Similar features were observed at the mandibular alveolar ridge (Supplemental Figure 2, H-K1, L; yellow arrows).

To assess the overall effects in bone structure, BV, TV and BV/TV of the alveolar bone were measured. Dental disease in vehicle and CIA mice decreased BV, and BV/TV, while antiresorptive treatment substantially increased all of these measurements compared to the vehicle and CIA mice

This article is protected by copyright. All rights reserved

Accepted Article

(Supplemental Figure 3, A, A1, D, D1 and E-G; white arrows). Interestingly, CIA-ZA mice showed slightly higher BV compared to the ZA animals probably due to increased periosteal bone deposition in the buccal side (Supplemental Figure 3, D1; arrowheads and Supplemental Figure 4).

Increased severity of ONJ in CIA mice treated with ZA

To evaluate histologic features of ONJ, coronal sections were obtained between the 1st and 2nd molars. All healthy groups showed normal alveolar bone (Figure 3, A, C, E, G; turquoise arrow), marginal epithelium (Figure 3, A, C, E, G; red arrows), PDL and absence of inflammatory infiltrate. In diseased vehicle and CIA mice, abundant inflammatory infiltrate (Figure 3, B-B1, F-F1), periosteal bone deposition and bone resorption were noted (Figure 3, B-B1). The reduction of the alveolar crest height in the diseased site of vehicle and CIA treated mice resulted in an increase of the distance between the marginal epithelium to the ABC (Figure 3, B-B1, F-F1; turquoise and red arrows). No histologic evidence of osteonecrosis was observed in any of the samples.

Infiltrate of inflammatory cells was also noted in the diseased site of ZA and CIA-ZA mice appearing more intense in the CIA-ZA mice (Figure 3, D, D1, H, H1; Supplemental Figure 5). Reduced alveolar bone loss resulted in reduction of the epithelial to the ABC distance (Figure 3, D, H; turquoise and red arrows; Supplemental Figure 5). Empty osteocytic lacunae, areas of osteonecrosis (Figure 3, D-D1, H-H1; yellow arrows; Supplemental Figure 5) and periosteal new bone formation (Figure 3, D-D1, H-H1; Supplemental Figure 5) were observed for both ZA and CIA-ZA treated mice. Interestingly, necrotic bone was not covered by epithelium and was exposed to the oral environment in 7 mice for CIA-ZA treated mice compared with 3 mice for ZA treated mice (Figure 3, D,-D1, H-H1; green arrows, Table 1). Importantly, areas of osteonecrosis were significantly more extensive in CIA-ZA

This article is protected by copyright. All rights reserved

Accepted Article

compared to ZA treated animals (Figure 3, D-D1, H-H1; yellow arrows; Supplemental Figure 5). Similar observations were seen in healthy and drilled sites of the mandible (Supplemental Figure 5).

Quantification of histologic findings demonstrated a statistically significant increase in the distance between the marginal epithelium to the ABC in diseased sites of vehicle and CIA mice. This distance was decreased in ZA and CIA-ZA mice (Figure 3, I). Importantly, the marginal epithelium to the ABC distance was significantly smaller in the CIA-ZA mice compared to all other groups. Number of empty osteocytic lacunae and area of osteonecrosis were measured at the area of the alveolar ridge for healthy and diseased treatment groups. No areas of osteonecrosis were seen in the healthy or diseased sites of the vehicle and CIA treated mice. Presence of empty osteocytic lacunae was not statistically significant between vehicle and CIA treated mice (Figure 3, J and K). Significant increase in empty osteocytic lacunae and areas of osteonecrosis were observed in diseased sites of ZA and CIA-ZA treated mice (Figure 3, J and K). Importantly, statistically significant increase in areas of osteonecrosis and empty osteocytic lacunae were present in CIA-ZA compared to ZA treated animals (Figure 3, J and K; Supplemental Figure 5). Osteonecrotic areas in ZA treated mice without or with CIA extended in significant part of the alveolar ridge and close to the buccal or lingual mandibular cortex in the mandible or the buccal and palatal cortex or the maxillary sinus floor in the maxilla (Supplemental Figure 6).

Few TRAP + cells were noted at the healthy site of all treatment groups. In contrast, diseased sites of all groups showed statistically increase number of TRAP+ cells. TRAP+ cells in controls and CIA animals showed close attachment to the bone with extended bone contact surface. However, in ZA and CIA-ZA mice osteoclasts presented round morphology, with pyknotic nuclei, and occasionally were separated from the bone surface (Figure 4, A-H1 and I). Similar results were found for the healthy and drilled sites of the mandible (Supplemental Figure 7, A-I).

This article is protected by copyright. All rights reserved

Accepted Article

Table 1 summarizes radiographic and histologic features in maxillae and mandibles. Disease incidence such as peri-radicular and periapical disease ranged from 50-62.5% without statistical differences among groups. Areas of osteonecrosis and bone exposure were present only in the ZA and CIA-ZA treated mice. Osteonecrotic areas ranged, in the diseased sites of ZA and CIA-ZA, from 64.3-86.7%, respectively. Interestingly, in CIA-ZA group bone exposure was 2.3-fold higher than ZA treated animals ranging from 21.4-46.7% of the diseased mice.

Changes in clinical course and severity of rheumatoid arthritis

The clinical course of arthritis in DBA-1J mice injected with collagen is shown in Figure 5, A-D3. The rate of clinical CIA progression after onset was not statistically significant altered by ZA treatment. ZA-treated CIA mice showed a slightly reduced severity of clinical arthritis, which was not significant compared to the CIA group (Figure 5, E). Paw thickness and paw swelling were also not significant between veh vs. ZA groups.

To further elucidate bone changes in the hind paws and knee joints, μCT assessment was performed. CIA treated mice demonstrated loss of bone integrity and extensive areas of erosions in the interphalangeal, ankle and calcaneus regions as well as in the knee joints with areas of periosteal new bone formation. Treatment with ZA completely abolished bone erosions but not periosteal formation (data not shown).

Histological analysis of the hind paws and knee joints (Figure 6, A-D1 and E-F) revealed absence of synovitis or inflammatory bone changes in vehicle and ZA treated mice (Figure 6, A-B1 and E). In contrast, CIA and CIA-ZA treated mice showed inflammatory infiltrate in the ankle, calcaneus and knee (Figure 6, C-D1 and E; black arrows). CIA treated mice presented with cartilage and bone resorption (Figure 6, C-C1, F), while ZA treatment protected and maintained cartilage and bone

This article is protected by copyright. All rights reserved

Accepted Article

architecture of the ankle, calcaneus and knee joints (Figure 6, D-D1, F). No osteonecrosis was seen adjacent to the inflammatory areas in CIA or CIA-ZA groups.

Finally, to investigate the overall effects of ZA in osteoclast numbers TRAP staining was performed. As expected, significant increase in TRAP + cells were noted for the CIA treated mice. ZA treated CIA mice showed increased number of positive TRAP cells compared to the vehicle and ZA treated mice, but this difference was not significant (Figure 6, G).

DISCUSSION

Clinical studies suggest an increased incidence of ONJ in patients with RA.[8,20,28,29,43] The potential link between RA and ONJ could be due to common etiologic factors of the two diseases.[43] Indeed, RA is a chronic systemic immunologic disease that features persistent high level of proinflammatory cytokines and inflammatory cells very much like other inflammatory diseases in the mouth such as periodontitis and periapical disease.[41] Periodontal and periapical disease are infectious processes mediated and modulated by the host immune system[44-47] and have been considered ONJ risk factors.[20] Furthermore, an increased inflammatory response that might implicate a role of gamma-delta T-cells, release of pro-inflammatory cytokines, increased oxidative stress, and intensified tissue destruction are common denominators in both RA and ONJ.[15,43] Additionally, increased bacterial infection in RA patients could increase the risk and complicate the course of ONJ.[15,43]

Biologic agents, DMARDs and immunosuppressive agents such as methotrexate, NSAIDs, steroids and bisphosphonates have led to substantial long-term improvements in patients with RA.[48-50] However, biologics agents increase the risk of opportunistic infections,[51] corticosteroids have been shown to impair bone and wound healing,[52] methotrexate may affect bone healing through inhibition of osteoblastic proliferation and bone turnover suppression,[53] steroids reduce bone remodeling,[54]

This article is protected by copyright. All rights reserved

Accepted Article

suppress bone turnover and angiogenesis, result in osteoblast and osteocyte apoptosis,[55] increasing the risk for infection and necrosis.[56] Furthermore, these common medications for RA including steroids and methotrexate have been associated with ONJ.[8,15,27,57,58]

Whether RA itself or medications used for RA management potentially exacerbate ONJ occurrence and severity is not known.[8,43] Given the low incidence of ONJ, particularly in patients treated with low dose BPs, clinical studies can be limited in providing accurate causal association between the two diseases, particularly in the presence of confounding variables.[18,21] Animal studies can complement clinical findings, since they can be designed in a controlled environment, where experimental variables are more predictable and adjustable. Several animal models of ONJ have been reported that provide powerful tools in assessing disease pathophysiology.[30-33,59,60] In the studies presented herein, we employed two mouse ONJ models in animals treated with high levels ZA in the absence of tooth extractions, but in the presence of either experimental periapical disease or naturally occurring periradicular infection.[30-32] We have reported that these animals develop ONJ-like lesions with clinical bone exposure, and radiographic and histologic features, such as periosteal bone formation, bone sclerosis, thickening of lamina dura, empty presence of osteocytic lacunae, and osteonecrosis resembling the human disease.[30-33,59]

We also utilized the well-established CIA mouse model to induce aggressive arthritis with RA features such as paw swelling, synovial inflammation and focal erosions at the joints.[61] Similar to our previous observations,[30-33] dental disease resulted in periradicular inflammation and bone loss reflected by increased CEJ to ABC distance and PDL space width, decreased BV, BV/TV, lamina dura and lingual bone thickness, increased inflammatory infiltrate and marginal epithelium to the ABC distance. No statistical differences in quantitative indices of alveolar bone loss between control and CIA mice were noted, suggesting that CIA did not complicate periapical or periradicular disease.

This article is protected by copyright. All rights reserved

Accepted Article

Radiographic assessment demonstrated that ZA treatment prevented bone changes and increased the overall alveolar bone volume in the diseased sites even in the presence of CIA. Interestingly, CIA-ZA group demonstrated increased bone thickness for both palatal/lingual and buccal sides probably due to increased periosteal bone formation compared to all the other groups. Histologically, successful induction of ONJ-like lesions was observed in both ZA and CIA-ZA treated mice, including presence of empty osteocytic lacunae and areas of osteonecrosis. Importantly, in ZA treated CIA mice significant differences in empty osteocytic lacunae number and osteonecrotic area, as well as in areas of exposed bone were observed, characterizing a more severe incidence and development of ONJ. Notably, in these experiments, mice were not treated with agents utilized for the management of RA, and any increased burden of ONJ in CIA-ZA mice should be attributed to the effects of heightened systemic effects induced by collagen injection in these animals. In our experiments, although the number of animals with osteonecrosis in the CIA-ZA group was higher than that in the ZA group, the results did not reach statistical significance. This was most probably due to the number of animals. Collectively, our findings suggest that RA complicates ONJ severity and possibly incidence in the mouse models employed, and suggest that RA might be a risk factor for ONJ.

Clinical features of RA, including paw swelling, redness, and sometimes ankylosis of the hind paws were observed in both CIA and CIA-ZA treated mice. As expected, [50,61-63] cartilage destruction, bone erosions and periosteal bone formation in animals with CIA was present. Similar to previously published data,[50] inhibition of bone destruction, but presence of periosteal bone formation was seen in CIA-ZA mice. These results parallel observations with the osteoclastogenesis inhibitor osteoprotegerin (OPG), emphasizing the preeminence of osteoclastic activity in mediating bone destruction.[61,63]

Although, extensive osteonecrosis was seen in the maxilla and mandible around areas of periapical or periradicular inflammation, no areas of osteonecrosis were observed in the interphalangeal and knee joints in CIA-ZA mice, despite the robust synovial and periarticular inflammation. This

This article is protected by copyright. All rights reserved

Accepted Article

disparate response of the jaws vs. other bones to inflammation could be due to basic differences in the inflammatory conditions around the jaws vs. long bone joints. Both periapical or periradicular inflammation are caused by bacterial infection[18,64] while the collagen-induced periarticular inflammation develops in sterile conditions. Alternatively, the presence of osteonecrosis in the maxilla and mandible could be due to a unique response of the jaws vs. other bones to the harmful inflammatory environment. Such a heightened sensitivity could explain the near exclusive presentation of ONJ in the jaws compared to the remaining skeleton.[18,64]

As our data are translated in the clinical setting, three considerations should be made. First, the ZA doses administered to the animals parallel those for oncologic patients.[65,66] We utilized these higher doses to increase the incidence of ONJ in mice without or with CIA, such that we could derive statistically significant conclusions. Given the fact that most RA patients receive much lower BP doses for the management of osteoporosis,[1,8,28] the ONJ incidence in these patients is expected to be lower that observed in the CIA-ZA animals. Nevertheless, despite the anticipated lower disease incidence with lower BP doses, our data suggest a relative increase in ONJ burden in patients with RA.

A second consideration is that our models utilized dental disease as the initiating factor for ONJ. Although dental disease is associated with ONJ occurrence[20] and is considered a local risk factor for the disease[18,21], the major local precipitating factor associated with ONJ is dentoalveolar surgery and particularly tooth extraction.[67-69] We elected not to utilize tooth extraction in our models, as we intended to explore the impact of RA in the early phases of ONJ development prior to surgical intervention.

A final consideration is that our studies did not address the potential effect of RA treatment modalities as risk factors for ONJ. It would be expected that such pharmacologic agents would have a detrimental effect in the response of the alveolar bone to osteonecrosis development. However, these treatments would reduce the systemic inflammatory response of CIA and would attenuate its negative

This article is protected by copyright. All rights reserved

Accepted Article

consequences in ONJ development. Clearly, further studies utilizing appropriate animal models are required to assess the association of specific RA treatment regimens and ONJ pathogenesis.

In summary, using two different ONJ mouse models, we report at radiographic and histologic level, that ZA treated CIA mice caused more extensive ONJ changes in the maxilla and mandible. Osteonecrosis in long bones or in the ankle was not observed even in the presence of abundant inflammatory cells infiltration in the synovium. Moreover, ZA treatment completely abolished cartilage and bone destruction but not synovitis. Accordingly, high-dose administration of BPs, combined with dental disease and RA, might increase the risk for ONJ development and severity. Indeed, to the best of our knowledge, this is the first animal study to show that RA might be a risk factor for ONJ.

ACKNOWLEDGEMENTS

This work was supported by NIH/NIDCR R01 DE019465 (ST) and R21 DE023901 (FQP). de Molon RS was supported by the State of Sao Paulo Research Foundation (FAPESP) #2012/09968-5, the Coordination for the Improvement of Higher Level -or Educational- Personnel (CAPES) #11575/31-1 and the Lemann Foundation.

CONFLICT OF INTEREST

All authors state that they do not have any conflicts of interest regarding this manuscript.

This article is protected by copyright. All rights reserved

Accepted Article

AUTHOR CONTRIBUTIONS

Study conception and design. RSM, CH, OB, SMD, FQP, AS, FQC, JAC, TLA, and ST; Acquisition of data. RSM, CH, OB, SMD, FQP, AS, FQC, JAC, TLA, and ST; Analysis and interpretation of data. RSM, SMD, JAC, TLA, and ST; Edition of the manuscript: RSM, CH, OB, SMD, FQP, AS, FQC, JAC, TLA, and ST; Drafted the manuscript: RSM and ST. All authors were involved in revising the paper critically for important intellectual content, and all authors approved the final version to be published. RSM and ST had full access to all of the data in the study and take responsibility for the integrity of the data and the accuracy of the data analysis.

Accepted Article

This article is protected by copyright. All rights reserved

Accepted Article

REFERENCES

1. Scott DL, Wolfe F, Huizinga TW. Rheumatoid arthritis. Lancet. 2010;376:1094-108.
2. Firestein GS. Evolving concepts of rheumatoid arthritis. Nature. 2003;423:356-61.
3. Gravallese EM, Harada Y, Wang JT, Gorn AH, Thornhill TS, Goldring SR. Identification of cell types responsible for bone resorption in rheumatoid arthritis and juvenile rheumatoid arthritis. Am J Pathol. 1998;152:943-51.
4. Gough A, Sambrook P, Devlin J, et al. Osteoclastic activation is the principal mechanism leading to secondary osteoporosis in rheumatoid arthritis. J Rheumatol. 1998;25:1282-9.
5. Tanaka Y. Recent progress and perspective in JAK inhibitors for rheumatoid arthritis: from bench to bedside. J Biochem. 2015.
6. Russell G, Mueller G, Shipman C, Croucher P. Clinical disorders of bone resorption. Novartis Found Symp. 2001;232:251-67; discussion 67-71.
7. Clayton ES, Hochberg MC. Osteoporosis and osteoarthritis, rheumatoid arthritis and spondylarthropathies. Curr Osteoporos Rep. 2013;11:257-62.
8. Lescaille G, Coudert AE, Baaroun V, et al. Osteonecrosis of the jaw and nonmalignant disease: is there an association with rheumatoid arthritis? J Rheumatol. 2013;40:781-6.
9. Lee SG, Park YE, Park SH, et al. Increased frequency of osteoporosis and BMD below the expected range for age among South Korean women with rheumatoid arthritis. Int J Rheum Dis. 2012;15:289-96.
10. Bock O, Felsenberg D. Bisphosphonates in the management of postmenopausal osteoporosis--optimizing efficacy in clinical practice. Clin Interv Aging. 2008;3:279-97.
11. Berenson JR, Lipton A. Bisphosphonates in the treatment of malignant bone disease. Annu Rev Med. 1999;50:237-48.
12. Black DM, Delmas PD, Eastell R, et al. Once-yearly zoledronic acid for treatment of postmenopausal osteoporosis. N Engl J Med. 2007;356:1809-22.
13. Boonen S, Laan RF, Barton IP, Watts NB. Effect of osteoporosis treatments on risk of non-vertebral fractures: review and meta-analysis of intention-to-treat studies. Osteoporos Int. 2005;16:1291-8.
14. Cranney A, Wells G, Willan A, et al. Meta-analyses of therapies for postmenopausal osteoporosis. II. Meta-analysis of alendronate for the treatment of postmenopausal women. Endocr Rev. 2002;23:508-16.
15. Conte-Neto N, Bastos AS, Marcantonio RA, Junior EM. Epidemiological aspects of rheumatoid arthritis patients affected by oral bisphosphonate-related osteonecrosis of the jaws. Head Face Med. 2012;8:5.
16. Adler RA, Fuleihan GE, Bauer DC, et al. Managing Osteoporosis in Patients on Long-Term Bisphosphonate Treatment: Report of a Task Force of the American Society for Bone and Mineral Research. J Bone Miner Res. 2015.
17. Ruggiero SL, Mehrotra B, Rosenberg TJ, Engroff SL. Osteonecrosis of the jaws associated with the use of bisphosphonates: a review of 63 cases. J Oral Maxillofac Surg. 2004;62:527-34.
18. Khan AA, Morrison A, Hanley DA, et al. Diagnosis and management of osteonecrosis of the jaw: a systematic review and international consensus. J Bone Miner Res. 2015;30:3-23.
19. Khosla S, Burr D, Cauley J, et al. Bisphosphonate-associated osteonecrosis of the jaw: report of a task force of the American Society for Bone and Mineral Research. J Bone Miner Res. 2007;22:1479-91.

This article is protected by copyright. All rights reserved

20. Marx RE, Sawatari Y, Fortin M, Broumand V. Bisphosphonate-induced exposed bone (osteonecrosis/osteopetrosis) of the jaws: risk factors, recognition, prevention, and treatment. J Oral Maxillofac Surg. 2005;63:1567-75.
21. Ruggiero SL, Dodson TB, Fantasia J, et al. American Association of Oral and Maxillofacial Surgeons position paper on medication-related osteonecrosis of the jaw--2014 update. J Oral Maxillofac Surg. 2014;72:1938-56.
22. Aghaloo T, Hazboun R, Tetradis S. Pathophysiology of Osteonecrosis of the Jaws. Oral Maxillofac Surg Clin North Am. 2015;27:489-96.
23. Allen MR, Burr DB. The pathogenesis of bisphosphonate-related osteonecrosis of the jaw: so many hypotheses, so few data. J Oral Maxillofac Surg. 2009;67:61-70.
24. Allen MR, Ruggiero SL. A review of pharmaceutical agents and oral bone health: how osteonecrosis of the jaw has affected the field. Int J Oral Maxillofac Implants. 2014;29:e45-57.
25. Khan A, Morrison A, Cheung A, Hashem W, Compston J. Osteonecrosis of the jaw (ONJ): diagnosis and management in 2015. Osteoporos Int. 2015.
26. Zhang Q, Yu W, Lee S, Xu Q, Naji A, Le AD. Bisphosphonate Induces Osteonecrosis of the Jaw in Diabetic Mice via NLRP3/Caspase-1-Dependent IL-1beta Mechanism. J Bone Miner Res. 2015.
27. Conte-Neto N, Bastos AS, Spolidorio LC, Marcantonio RA, Marcantonio E, Jr. Oral bisphosphonate-related osteonecrosis of the jaws in rheumatoid arthritis patients: a critical discussion and two case reports. Head Face Med. 2011;7:7.
28. Landesberg R, Taxel P. Osteonecrosis of the jaw and rheumatoid arthritis. Is it the disease or the drugs? J Rheumatol. 2013;40:749-51.
29. Park W, Kim NK, Kim MY, Rhee YM, Kim HJ. Osteonecrosis of the jaw induced by oral administration of bisphosphonates in Asian population: five cases. Osteoporos Int. 2010;21:527-33.
30. Aghaloo TL, Cheong S, Bezouglaia O, et al. RANKL inhibitors induce osteonecrosis of the jaw in mice with periapical disease. J Bone Miner Res. 2014;29:843-54.
31. de Molon RS, Cheong S, Bezouglaia O, et al. Spontaneous osteonecrosis of the jaws in the maxilla of mice on antiresorptive treatment: a novel ONJ mouse model. Bone. 2014;68:11-9.
32. de Molon RS, Shimamoto H, Bezouglaia O, et al. OPG-Fc but Not Zoledronic Acid Discontinuation Reverses Osteonecrosis of the Jaws (ONJ) in Mice. J Bone Miner Res. 2015;30:1627-40.
33. Kang B, Cheong S, Chaichanasakul T, et al. Periapical disease and bisphosphonates induce osteonecrosis of the jaws in mice. J Bone Miner Res. 2013;28:1631-40.
34. Kilkenny C, Browne WJ, Cuthill IC, Emerson M, Altman DG. Improving bioscience research reporting: the ARRIVE guidelines for reporting animal research. Osteoarthritis Cartilage. 2012;20:256-60.
35. Clarke MC, Taylor RJ, Hall GA, Jones PW. The occurrence in mice of facial and mandibular abscesses associated with Staphylococcus aureus. Lab Anim. 1978;12:121-3.
36. Grant N, Jackson K, Lee R, Scharf B. Mandibular mass in a young Swiss-Webster mouse. Lab Anim (NY). 2002;31:25-6.
37. Lawson GW. Etiopathogenesis of mandibulofacial and maxillofacial abscesses in mice. Comp Med. 2010;60:200-4.
38. Brand DD, Latham KA, Rosloniec EF. Collagen-induced arthritis. Nat Protoc. 2007;2:1269-75.
39. Komatsu N, Okamoto K, Sawa S, et al. Pathogenic conversion of Foxp3+ T cells into TH17 cells in autoimmune arthritis. Nat Med. 2014;20:62-8.
40. Coppieters K, Dreier T, Silence K, et al. Formatted anti-tumor necrosis factor alpha VHH proteins derived from camelids show superior potency and targeting to inflamed joints in a murine model of collagen-induced arthritis. Arthritis Rheum. 2006;54:1856-66.

This article is protected by copyright. All rights reserved

Accepted Article

41. de Aquino SG, Abdollahi-Roodsaz S, Koenders MI, et al. Periodontal pathogens directly promote autoimmune experimental arthritis by inducing a TLR2- and IL-1-driven Th17 response. J Immunol. 2014;192:4103-11.
42. Marijnissen RJ, Roeleveld DM, Young D, et al. Interleukin-21 receptor deficiency increases the initial toll-like receptor 2 response but protects against joint pathology by reducing Th1 and Th17 cells during streptococcal cell wall arthritis. Arthritis Rheumatol. 2014;66:886-95.
43. Conte Neto N, Bastos AS, Chierici-Marcantonio RA, Marcantonio E, Jr. Is rheumatoid arthritis a risk factor for oral bisphosphonate-induced osteonecrosis of the jaws? Med Hypotheses. 2011;77:905-11.
44. de Molon RS, de Avila ED, Cirelli JA. Host responses induced by different animal models of periodontal disease: a literature review. J Investig Clin Dent. 2013;4:211-8.
45. de Molon RS, de Avila ED, Boas Nogueira AV, et al. Evaluation of the host response in various models of induced periodontal disease in mice. J Periodontol. 2014;85:465-77.
46. de Molon RS, Mascarenhas VI, de Avila ED, et al. Long-term evaluation of oral gavage with periodontopathogens or ligature induction of experimental periodontal disease in mice. Clin Oral Investig. 2015 (epub ahead of print) doi. 10.1007/s00784-015-1607-0.
47. Cavagni J, de Macedo IC, Gaio EJ, et al. Obesity and Hyperlipidemia Modulate Alveolar Bone Loss in Wistar Rats. J Periodontol. 2016;87:e9-e17.
48. Ward MM. Decreases in rates of hospitalizations for manifestations of severe rheumatoid arthritis, 1983-2001. Arthritis Rheum. 2004;50:1122-31.
49. Finckh A, Choi HK, Wolfe F. Progression of radiographic joint damage in different eras: trends towards milder disease in rheumatoid arthritis are attributable to improved treatment. Ann Rheum Dis. 2006;65:1192-7.
50. Sims NA, Green JR, Glatt M, et al. Targeting osteoclasts with zoledronic acid prevents bone destruction in collagen-induced arthritis. Arthritis Rheum. 2004;50:2338-46.
51. Giles JT, Bartlett SJ, Gelber AC, et al. Tumor necrosis factor inhibitor therapy and risk of serious postoperative orthopedic infection in rheumatoid arthritis. Arthritis Rheum. 2006;55:333-7.
52. Howe CR, Gardner GC, Kadel NJ. Perioperative medication management for the patient with rheumatoid arthritis. J Am Acad Orthop Surg. 2006;14:544-51.
53. Gerster JC, Bossy R, Dudler J. Bone non-union after osteotomy in patients treated with methotrexate. J Rheumatol. 1999;26:2695-7.
54. Patschan D, Loddenkemper K, Buttgereit F. Molecular mechanisms of glucocorticoid-induced osteoporosis. Bone. 2001;29:498-505.
55. Greenberger S, Boscolo E, Adini I, Mulliken JB, Bischoff J. Corticosteroid suppression of VEGF-A in infantile hemangioma-derived stem cells. N Engl J Med. 2010;362:1005-13.
56. Zizic TM, Marcoux C, Hungerford DS, Dansereau JV, Stevens MB. Corticosteroid therapy associated with ischemic necrosis of bone in systemic lupus erythematosus. Am J Med. 1985;79:596-604.
57. Sonis ST, Watkins BA, Lyng GD, Lerman MA, Anderson KC. Bony changes in the jaws of rats treated with zoledronic acid and dexamethasone before dental extractions mimic bisphosphonate-related osteonecrosis in cancer patients. Oral Oncol. 2009;45:164-72.
58. Christodoulou C, Pervena A, Klouvas G, et al. Combination of bisphosphonates and antiangiogenic factors induces osteonecrosis of the jaw more frequently than bisphosphonates alone. Oncology. 2009;76:209-11.
59. Aghaloo TL, Kang B, Sung EC, et al. Periodontal disease and bisphosphonates induce osteonecrosis of the jaws in the rat. J Bone Miner Res. 2011;26:1871-82.
60. Cheong S, Sun S, Kang B, et al. Bisphosphonate uptake in areas of tooth extraction or periapical disease. J Oral Maxillofac Surg. 2014;72:2461-8.

This article is protected by copyright. All rights reserved

Accepted Article

61. Romas E, Gillespie MT, Martin TJ. Involvement of receptor activator of NFkappaB ligand and tumor necrosis factor-alpha in bone destruction in rheumatoid arthritis. Bone. 2002;30:340-6.
62. Bogoch ER, Lee TC, Fornasier VL, Berger SA. Articular damage is associated with intraosseous inflammation in the subchondral bone marrow of joints affected by experimental inflammatory arthritis and is modified by zoledronate treatment. J Rheumatol. 2007;34:1229-40.
63. Redlich K, Hayer S, Maier A, et al. Tumor necrosis factor alpha-mediated joint destruction is inhibited by targeting osteoclasts with osteoprotegerin. Arthritis Rheum. 2002;46:785-92.
64. Katsarelis H, Shah NP, Dhariwal DK, Pazianas M. Infection and Medication-related Osteonecrosis of the Jaw. J Dent Res. 2015;94:534-9.
65. Ibrahim A, Scher N, Williams G, et al. Approval summary for zoledronic acid for treatment of multiple myeloma and cancer bone metastases. Clin Cancer Res. 2003;9:2394-9.
66. Maerevoet M, Martin C, Duck L. Osteonecrosis of the jaw and bisphosphonates. N Engl J Med. 2005;353:99-102; discussion 99-.
67. Vahtsevanos K, Kyrgidis A, Verrou E, et al. Longitudinal cohort study of risk factors in cancer patients of bisphosphonate-related osteonecrosis of the jaw. J Clin Oncol. 2009;27:5356-62.
68. Saad F, Brown JE, Van Poznak C, et al. Incidence, risk factors, and outcomes of osteonecrosis of the jaw: integrated analysis from three blinded active-controlled phase III trials in cancer patients with bone metastases. Ann Oncol. 2012;23:1341-7.
69. Fehm T, Beck V, Banys M, et al. Bisphosphonate-induced osteonecrosis of the jaw (ONJ): Incidence and risk factors in patients with breast cancer and gynecological malignancies. Gynecol Oncol. 2009;112:605-9.

Accepted Article

This article is protected by copyright. All rights reserved

Accepted Article

FIGURE LEGENDS

Figure 1. 3D µCT reconstructed images of maxilla. (A-D) 3D reformatted views of healthy site in vehicle, ZA, CIA and CIA-ZA, respectively. (A1-D1) 3D reformatted views of diseased site in all the groups. Blue arrows point to normal alveolar bone crest. Red arrow point to periodontal bone loss and areas of osteolysis in the diseased site of vehicle and RA treated mice. Yellow arrows point to increased bone deposition.

Figure 2. Sagittal and axial µCT sections through the maxillary alveolar ridge and quantification of the µCT findings . (A-D) Sagittal and (I-L) axial sections of healthy maxillae of vehicle, ZA, CIA and CIA-ZA mice, respectively. (A1-D1) Sagittal and (I1-L1) axial sections of diseased maxillae in all groups. White arrows point to areas of bone resorption and/or osteolysis. White arrowheads point to bone deposition and areas of bone expansion. (E-H) Quantification of CEJ to ABC distance, lamina dura thickness, PDL space width and palatal bone thickness in all mice, respectively. (n = 6 mice per group). & Statistically significant different compared to diseased mice, $p < 0.0001$. +Statistically significant different from indicated groups, $p < 0.0001$. **Statistically significant different from indicated groups, $p < 0.001$. *Statistically significant different from indicated groups, $p < 0.05$. Differences among groups were calculated by two-way ANOVA and between groups by Student's t test. Data represent the mean ± SEM.

Figure 3. Representative H&E-stained images from maxilla of all groups and quantification of the histologic findings. (A, C, E and G) Healthy and (B, D, F and H) diseased site of vehicle, ZA, CIA and CIA-ZA mice. Original magnification, x5. (B1, D1, F1 and H1) Histologic appearance of periodontal and alveolar crest area of maxillae in magnified views of the diseased site. Original magnification, x10. Red arrows point to marginal gingival epithelium, turquoise arrows to alveolar crest, yellow arrows to osteonecrotic areas, and green arrows to areas of bone exposure. (I-K)

This article is protected by copyright. All rights reserved

Quantification of the histologic findings: The shortest epithelial-crest distance, percentage of osteocytic lacunae and percentage of areas of osteonecrosis were measure, respectively. + Statistically significant different from indicated groups, $p < 0.0001$. ** Statistically significant different from indicated groups, $p < 0.001$. * Statistically significant different from indicated groups, $p < 0.05$. Differences among groups were calculated by two-way ANOVA and between groups by Student's t test. Data represent the mean ± SEM.

Figure 4. Representative sections of the maxilla stained for TRAP+ cells. (A, C, E and G) Healthy site of vehicle, ZA, CIA and CIA-ZA, respectively. Original magnification, x5. Insets are magnified views of individual TRAP+ cells. Original Magnification, x20. (B, D, F and H) Diseased site at the end of the treatment. (B1, D1, F1 and H1) Magnified views of the diseased site in vehicle, ZA, CIA and CIA-ZA, respectively. Original magnification, x10. (I) Quantification of TRAP + cell number in all mice and groups. (n = 6 mice per group). + Statistically significant different from indicated groups, $p < 0.0001$. ** Statistically significant different from indicated groups, $p < 0.001$. * Statistically significant different from indicated groups, $p < 0.05$. Differences among groups were calculated by two-way ANOVA and between groups by Student's t test. Data represent the mean ± SEM.

Figure 5. Clinical course of RA. Clinical evaluation of the paws were performed and scored for arthritis every other day from day 21 after the first immunization until the time of euthanasia. (A, A1, B, B1) Frontal and lateral views of vehicle and ZA treated mice. (C, C1, C2, C3, D, D1, D2, D3) Frontal and lateral views of CIA and CIA-ZA treated mice. All fingers of forepaws, hind paws, wrists and ankles were totaled for each mouse (maximum possible score of 12 for each mouse). (E) Mean and standard deviation of the clinical assessment until day 35 after second immunization.

Figure 6. Histopathologic effects of ZA treatment in the hind paws and TRAP + cells staining. Total ankle joints were isolated for histopathologic analysis (n = 6 mice per group). (A-D) Sagittal sections of the vehicle, ZA, CIA and CIA-ZA, respectively. Original magnification, x5. (A1-D1)

This article is protected by copyright. All rights reserved

Accepted Article

Magnified views of the area represented by the black squares. Original magnification, x10. Black arrows point to inflammatory infiltration. Yellow arrows point to periosteal bone formation. (E-F) Quantification of the histopathologic findings in the ankle: Synovial inflammation, and bone erosions were measured in all groups at the end of the treatment. (G) Quantification of the TRAP+ cells number in all mice and groups. # Statistically significant different compared to all the other groups, $p < 0.0001$. + Statistically significant different from indicated groups, $p < 0.0001$. Differences among groups were calculated by two-way ANOVA and between groups by Student's t test. Data represent the mean ± SEM.

Accepted Article

This article is protected by copyright. All rights reserved

Table 1 – Summary of radiographic and histologic findings on various groups.

Group	Total hemi-mandible & hemi-maxillae	Healthy (%)	Diseased (%)	Osteonecrosis (%)	Bone Exposure (%)
Vehicle	24	12 (50)*	12 (50)*	$0^{\$}$ (0)* (0)$^{\#}$	$0^{@}$ (0)* (0)$^{\#}$ (0)$^{+}$
ZA	24	10 (41.7)*	14 (58.3)*	9 (37.5)* (64.3)$^{\#}$	3 (12.5)* (21.4)$^{\#}$ (33.3)$^{+}$
CIA	24	9 (37.5)*	15 (62.5)*	$0^{\$}$ (0)* (0)$^{\#}$	$0^{@}$ (0)* (0)$^{\#}$ (0)$^{+}$
CIA-ZA	24	9 (37.5)*	15 (62.5)*	13 (54.2)* (86.7)$^{\#}$	7 (29.2)* (46.7)$^{\#}$ (53.4)$^{+}$

* % of total hemimaxillae and hemimandible;

% of diseased hemimaxillae and hemimandible;

+ % of hemimaxillae and hemimandible with osteonecrosis;

$^{\$}$ Statistically significantly different, $p < 0.001$ compared to ZA and CIA-ZA;

$^{@}$ Statistically significantly different, $p < 0.001$ compared to CIA-ZA;

This article is protected by copyright. All rights reserved

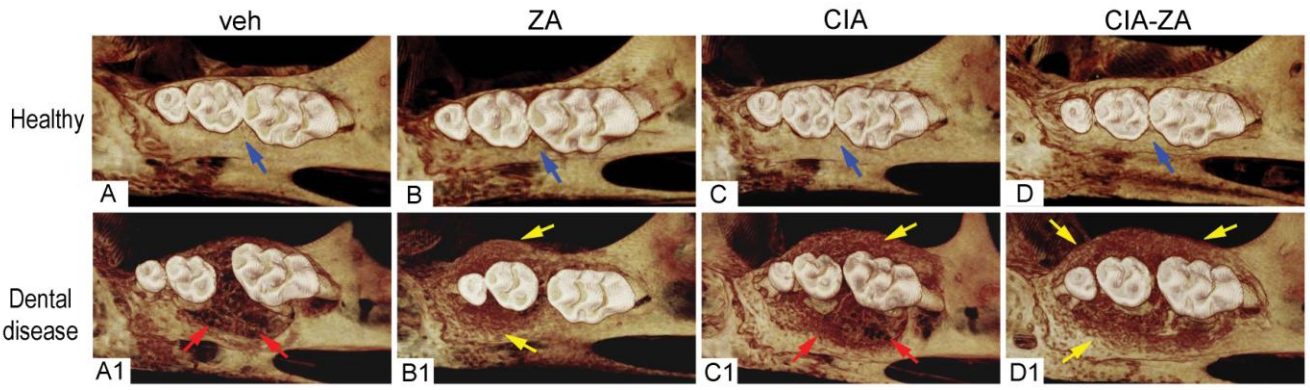

Figure 1

Accepted Article

This article is protected by copyright. All rights reserved

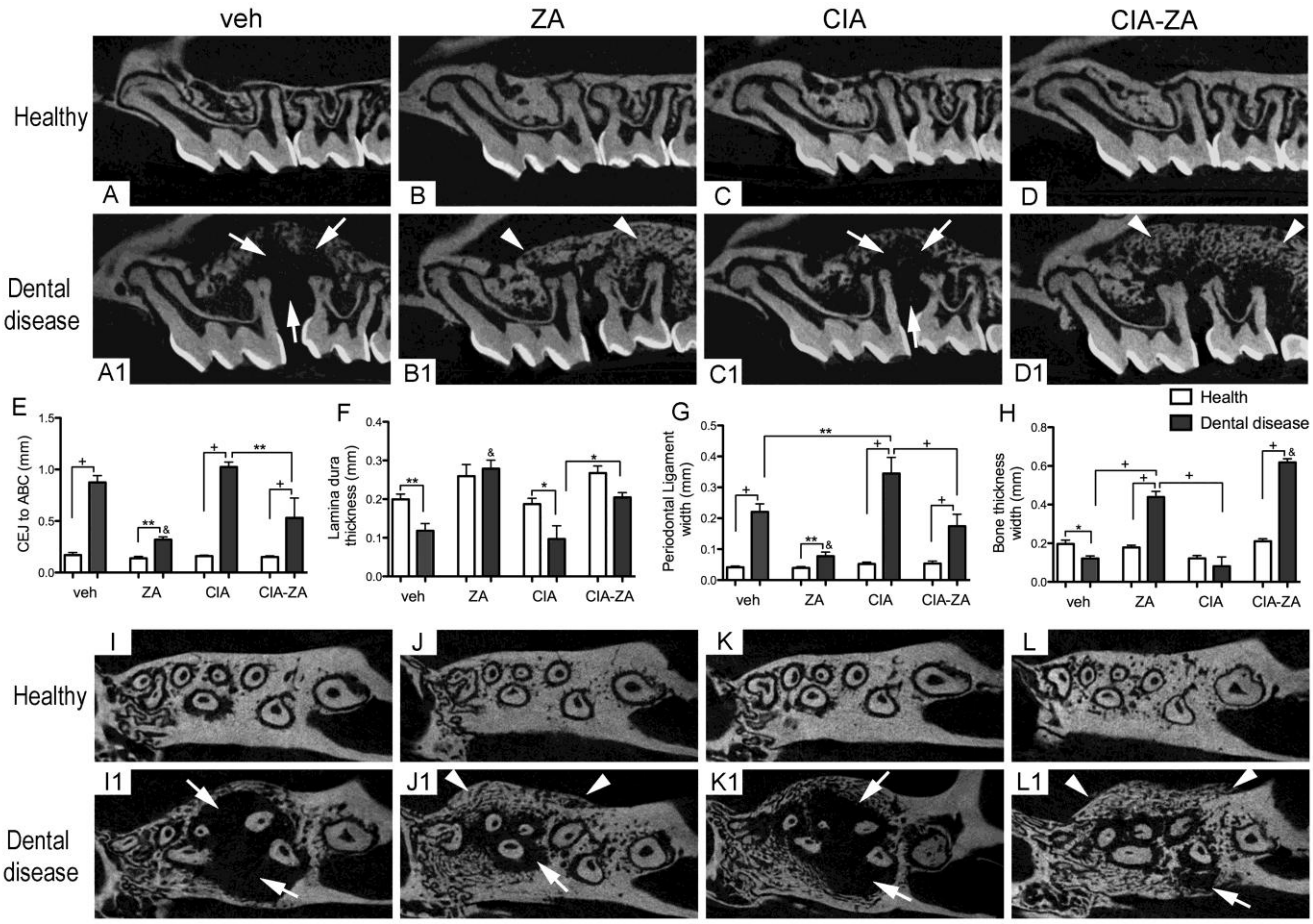

Figure 2

This article is protected by copyright. All rights reserved

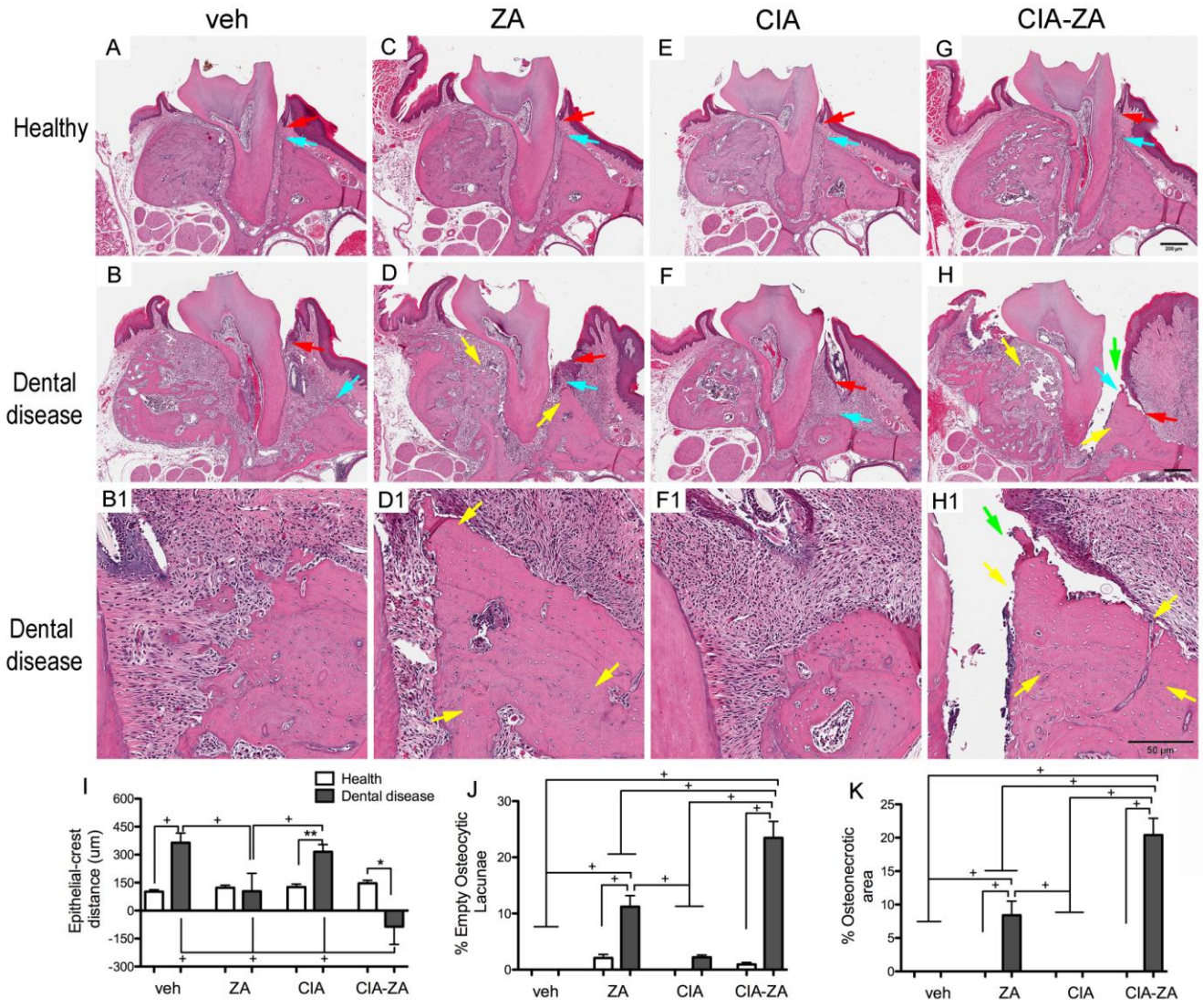

Figure 3

Accepted Article

This article is protected by copyright. All rights reserved

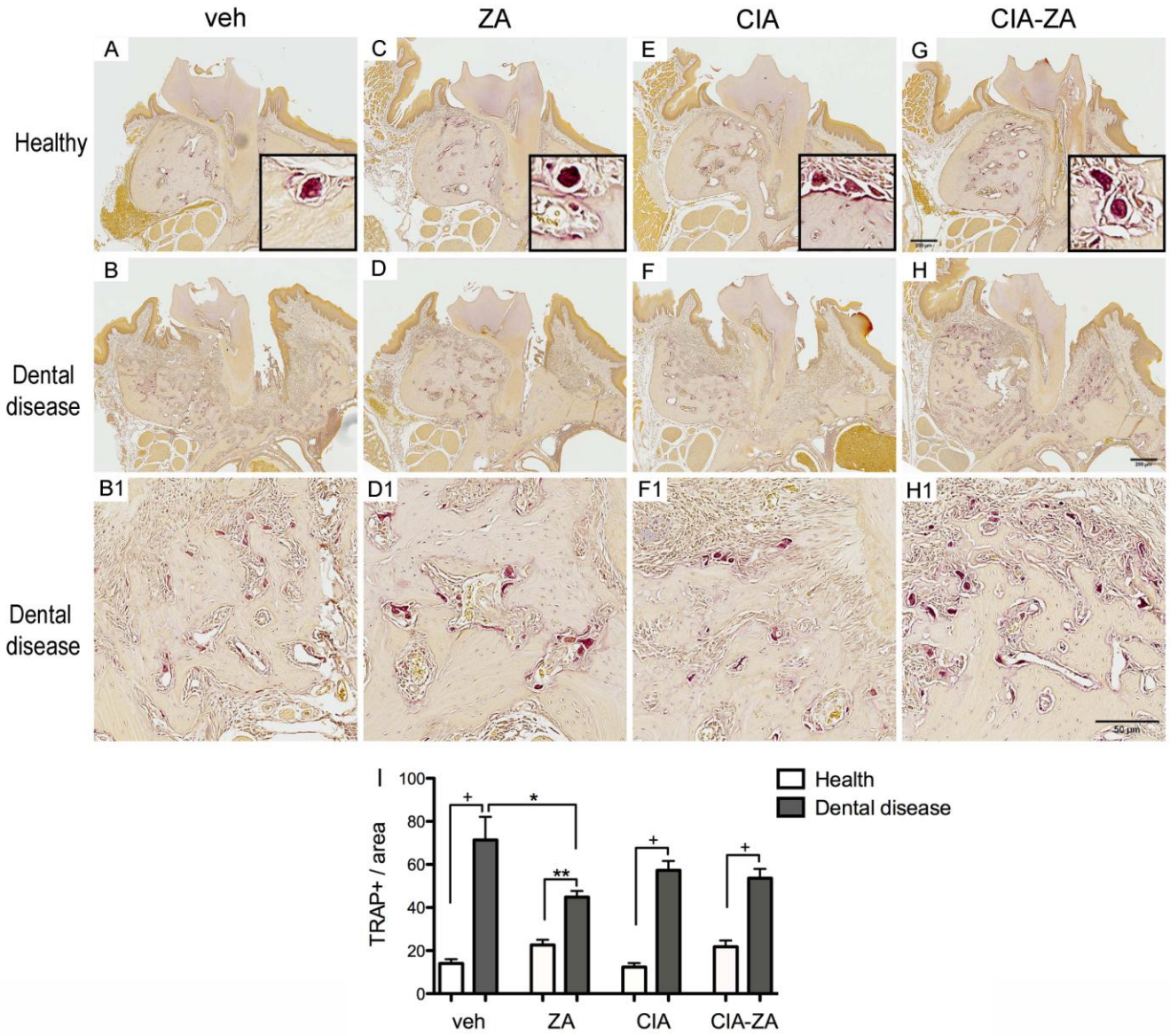

Figure 4

Accepted Article

This article is protected by copyright. All rights reserved

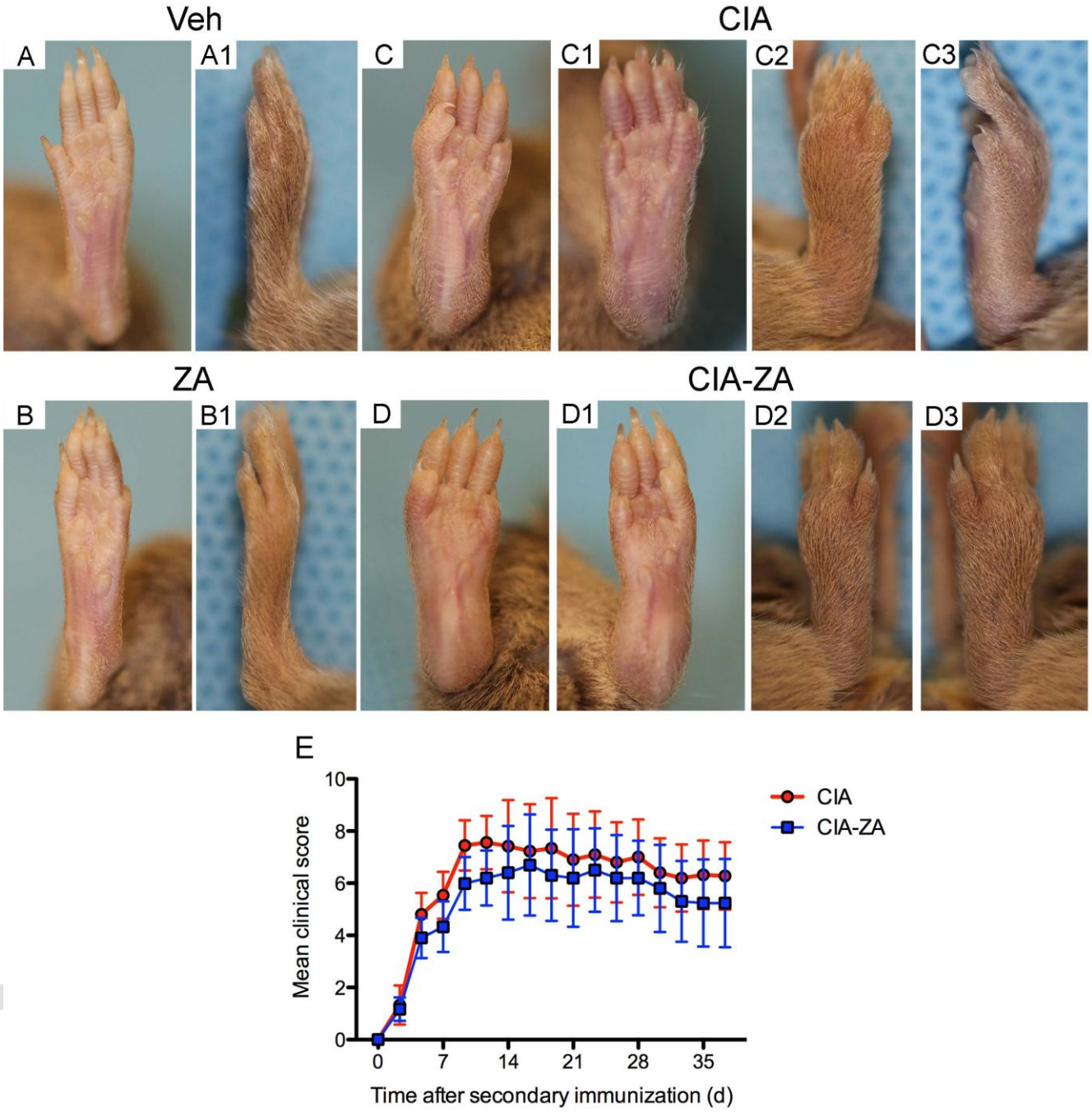

Figure 5

Accepted Article

This article is protected by copyright. All rights reserved

Accepted Article

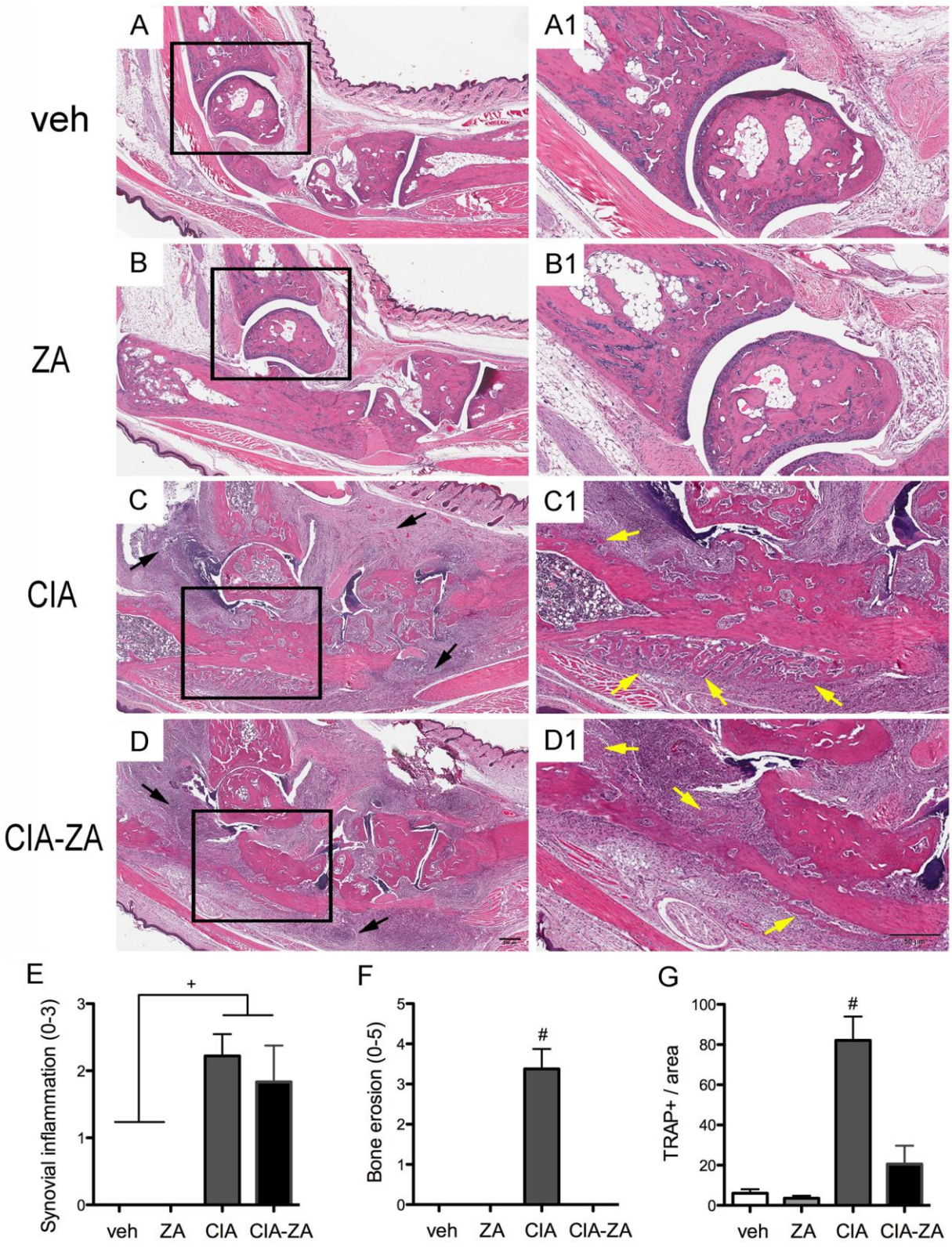

Figure 6

This article is protected by copyright. All rights reserved

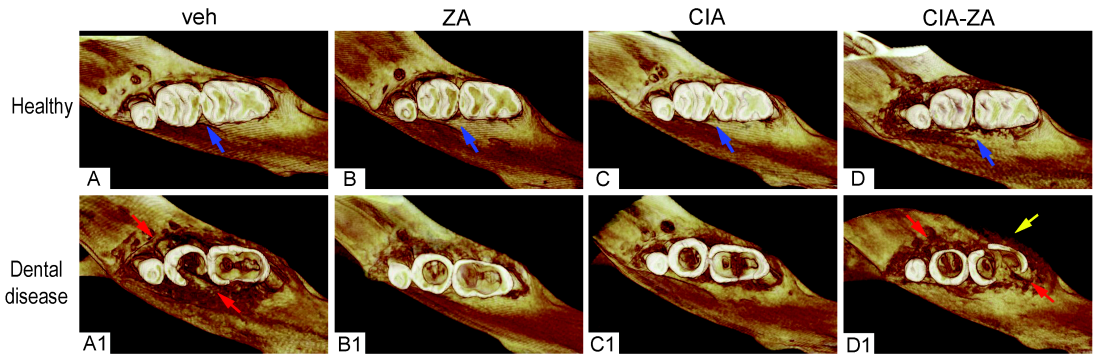

Supplemental Figure 1. 3D µCT reconstructed images of mandibles. (A-D) Axial views in healthy site of vehicle, ZA, CIA and CIA-ZA. (A1-D1) Diseased site of all groups at the end of the treatment. Blue arrows point to normal alveolar bone crest in the interproximal area between the distal root of the first molar and mesial root of the second molar. Red arrow point to periodontal bone loss and areas of osteolysis. Yellow arrows point to increased bone deposition.

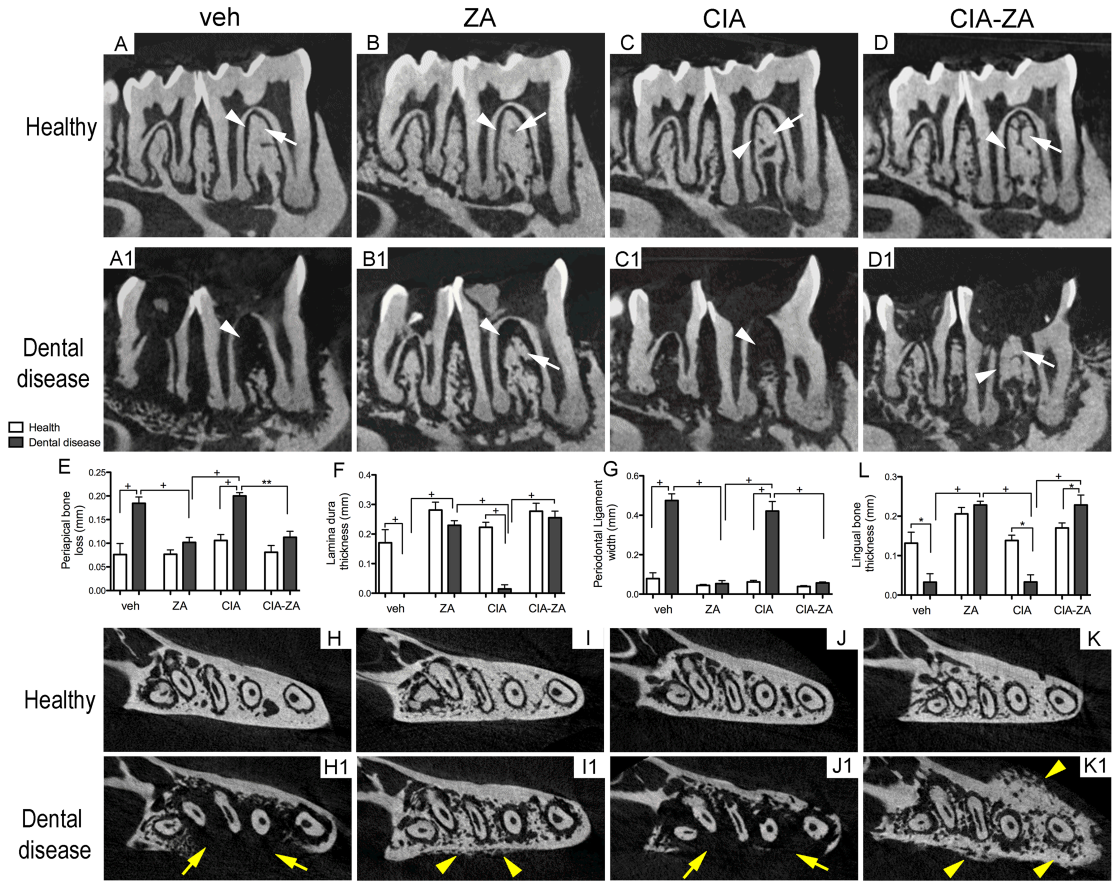

Supplemental Figure 2. Sagittal and axial µCT sections of the mandible and quantification of the findings. (A-D) Sagittal views of non-drilled site of veh, ZA, CIA and CIA-ZA treated animals. (A1-D1) Drilled molars after 9 weeks of treatment. Thin white arrows point to lamina dura and white arrowheads point to PDL space. (n = 6 mice per group). (E-G) Quantification of periapical bone loss at the distal root and mesial root of the first and second molars were analyzed. Quantification of the changes in the furcational periodontium was performed measuring the thickness of lamina dura and width of the PDL space. (H-K) Axial sections of non-drilled site of all groups. (H1-K1) Drilled site in vehicle, ZA, CIA and CIA-ZA treated animals. Yellow arrows point to areas of osteolysis. Yellow arrowheads point to new bone deposition. (L) Quantification of lingual bone thickness. +Statistically significant different from indicated groups, $p < 0.0001$. **Statistically significant different from indicated groups, $p < 0.001$. *Statistically significant different from indicated groups, $p < 0.05$. Statistically significant Differences among groups were calculated by two-way ANOVA and between groups by Student's t test. Data represent the mean ± SEM.

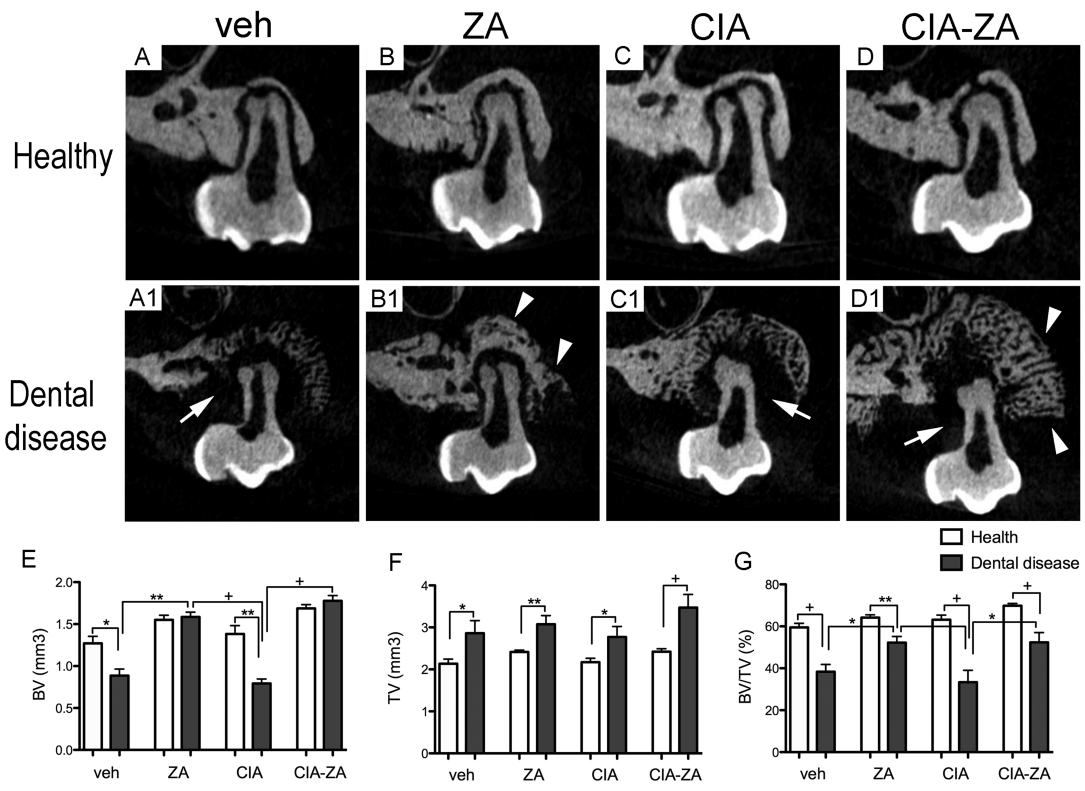

Supplemental Figure 3. Coronal µCT slices of the maxillary alveolar bone at the area of the distal root of the first molars and quantification of BV, TV and BV/TV. (A-D) Healthy site in vehicle, ZA, CIA and CIA-ZA, respectively. (A1-D1) Diseased site of all the groups. White arrows point to bone resorption. White arrowheads point to periosteal new bone formation in the buccal side and in the root apex of ZA and CIA-ZA treated mice. (E-G) Quantification of BV, TV and BV/TV in the maxilla of all mice, respectively. (n = 6 mice per group). + Statistically significant different from indicated groups, $p < 0.0001$. ** Statistically significant different from indicated groups, $p < 0.001$. * Statistically significant different from indicated groups, $p < 0.05$. Differences among groups were calculated by two-way ANOVA and between groups by Student's t test. Data represent the mean ± SEM.

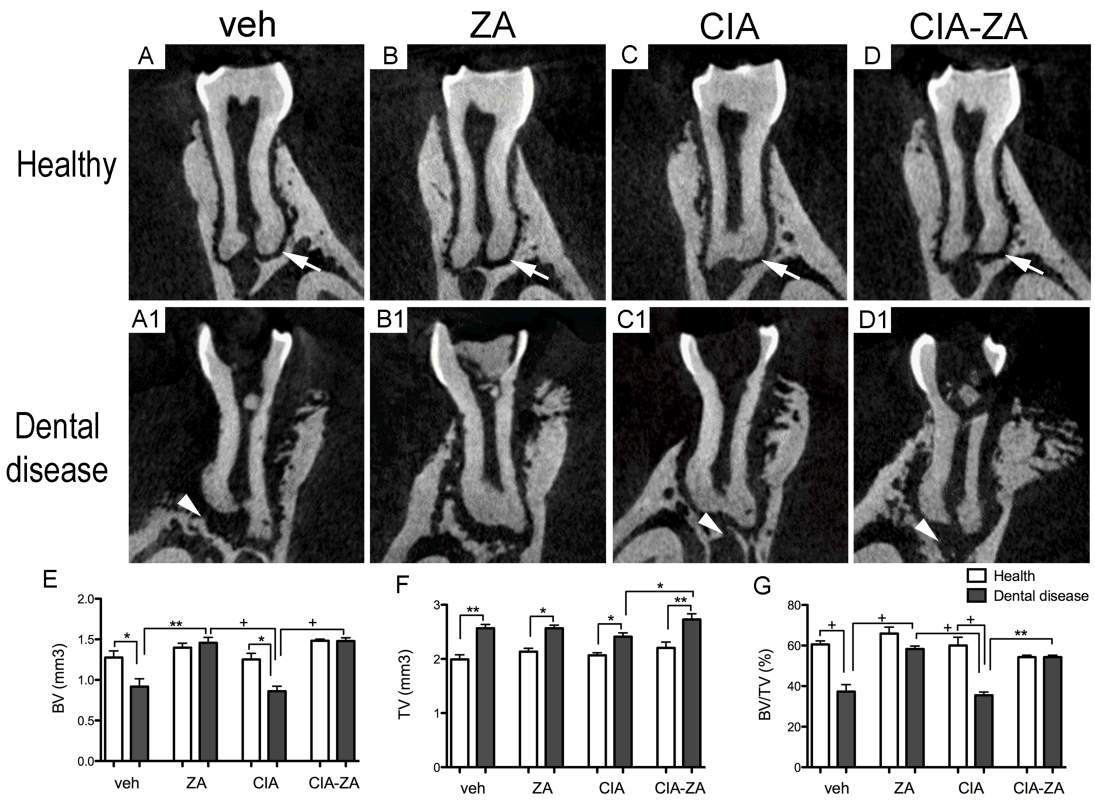

Supplemental Figure 4. µCT cross-sections of the periapical area of first molars and quantification of BV, TV and BV/TV. (A-D) Non-drilled mesial root of first molars in all groups. (A1-D1) Drilled molars after 9 weeks of treatment. Thin arrows point to normal PDL space. Arrowheads point to periapical bone loss. (n = 6 mice per group). Quantification of BV, TV and BV/TV. +Statistically significant different from indicated groups, $p < 0.0001$. **Statistically significant different from indicated groups, $p < 0.001$. *Statistically significant different from indicated groups, $p < 0.05$. Statistically significant Differences among groups were calculated by two-way ANOVA and between groups by Student's t test. Data represent the mean ± SEM.

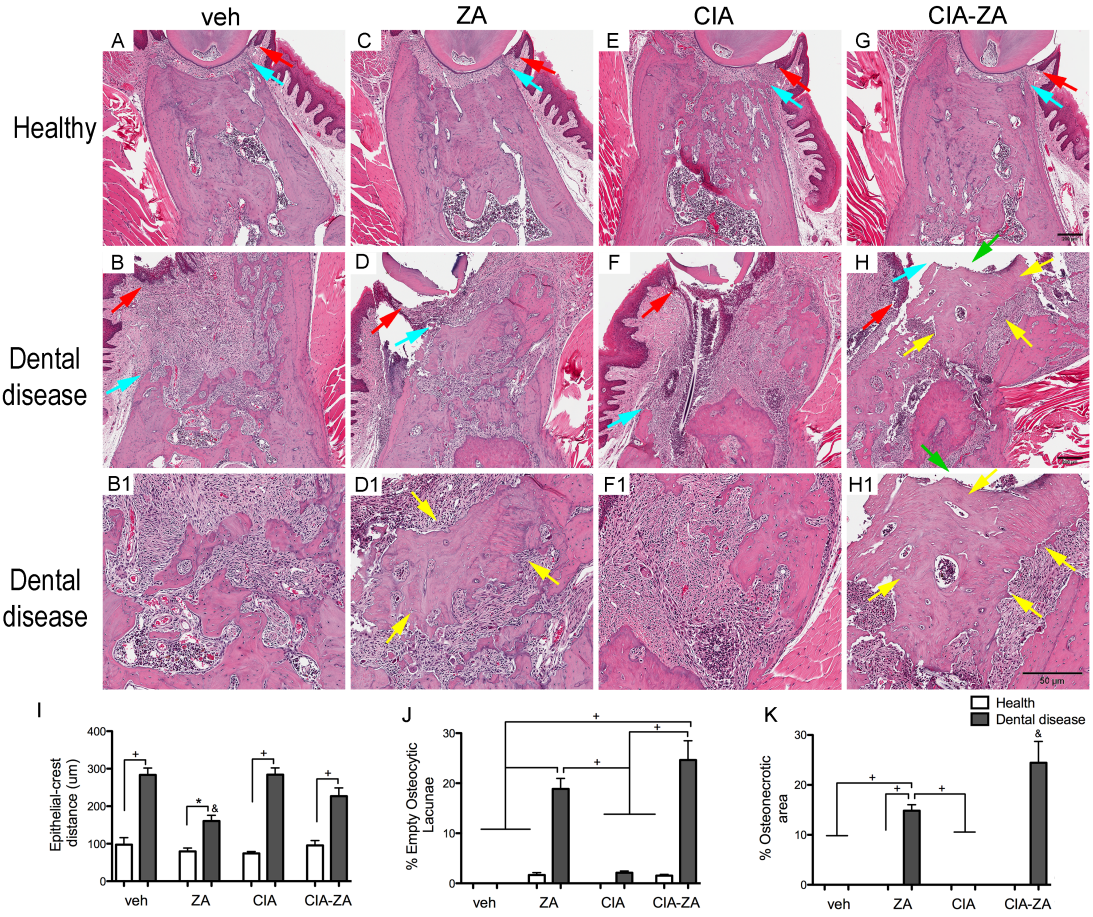

Supplemental Figure 5. Representative H&E-stained images from mandible of all groups. (A, C, E and G) Healthy site of veh, ZA, CIA and CIA-ZA animals. (B, D, F and H) Drilled site at 9 weeks at the end of antiresorptive treatment. Original magnification, x5. (B1, D1, F1 and H1) Magnified views of drilled site in all groups. Original magnification, x10. Red arrows point to marginal gingival epithelium, turquoise arrows to alveolar crest, yellow arrows to osteonecrotic areas, and green arrows to areas of bone exposure. (n = 6 mice per group). (I-L) Quantification of histologic findings in the mandible. The shortest epithelial-crest distance was determined. Osteocytic lacunae were measured and empty lacunae were expressed as percent of total. Area of osteonecrosis was measured and expressed as % of total bone area. +Statistically significant different from indicated groups, $p < 0.0001$. **Statistically significant different from indicated groups, $p < 0.001$. *Statistically significant different from indicated groups, $p < 0.05$. Differences among groups were calculated by two-way ANOVA and between groups by Student's t test. Data represent the mean ± SEM.

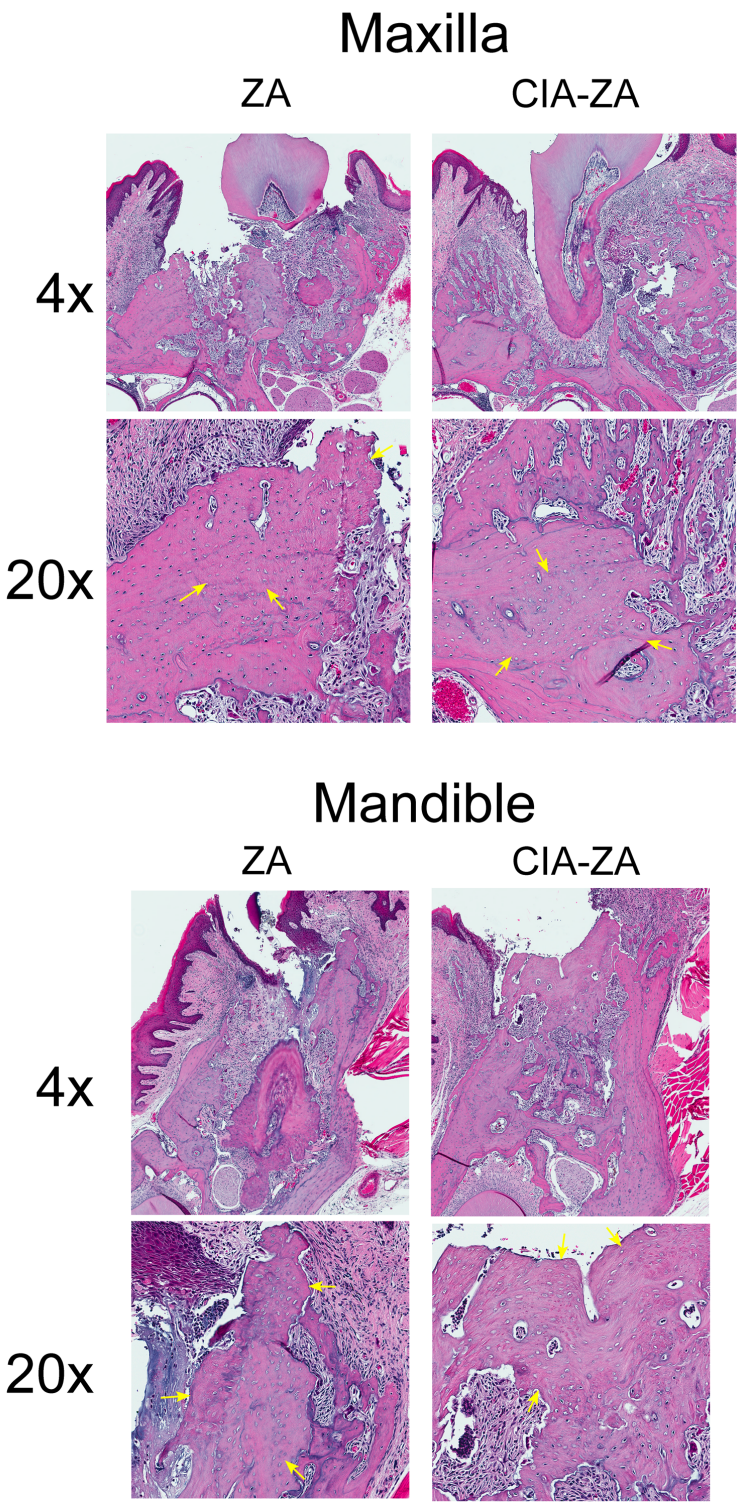

Supplemental Figure 6. Representative H&E-stained images from maxilla and mandible of ZA and CIA-ZA diseased groups. Histologic sections from 4 representative animals (2 ZA and 2 CIA-ZA maxillae, and 2 ZA and 2 CIA-ZA mandibles). Osteonecrotic areas are indicated by yellow arrows. Osteonecrotic areas beyond the areas of periodontal bone to reach the maxillary sinus floor or the mandibular cortex and are noted, especially in the CIA-ZA animals.

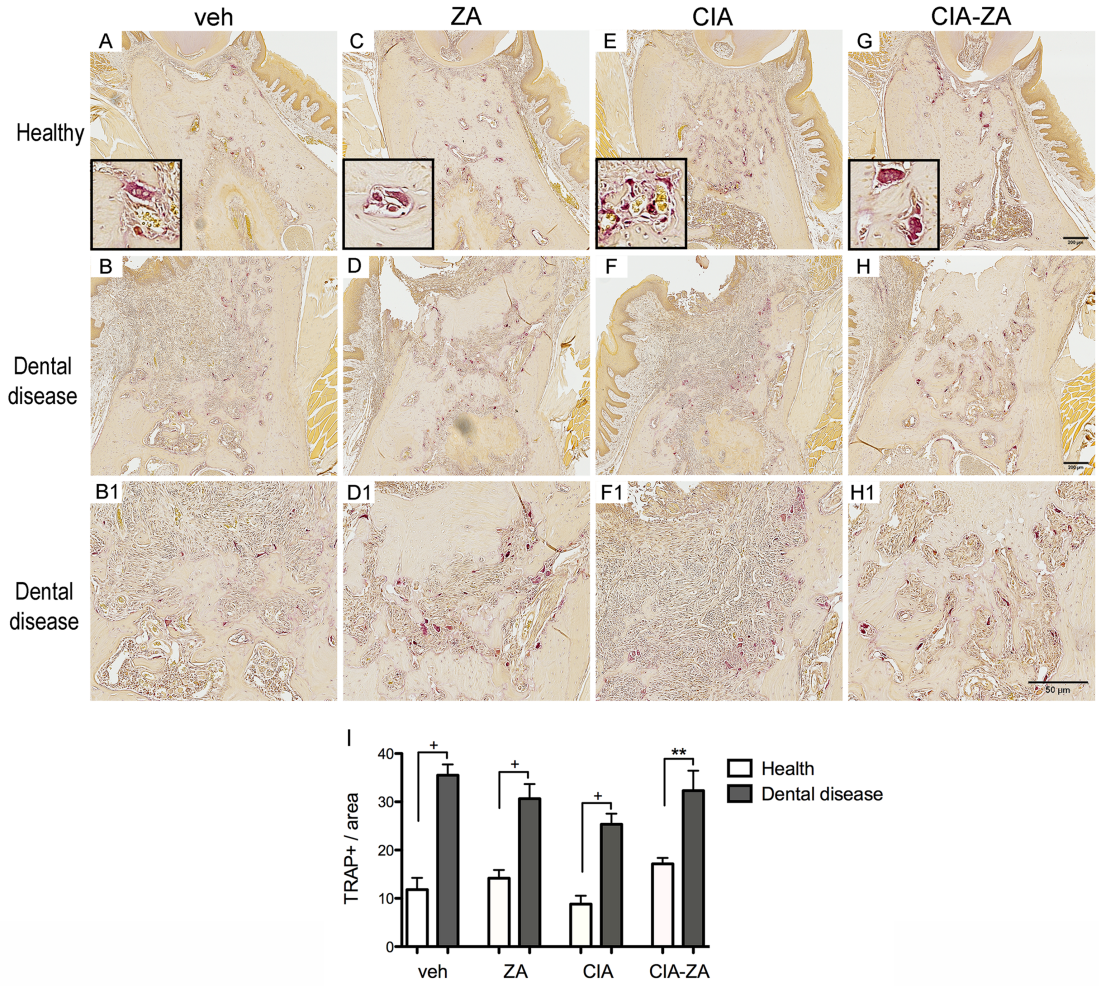

Supplemental Figure 7. Representative sections of mandibles stained for TRAP+ cells. (A, C, E and G) Non-drilled site of veh, ZA, CIA and CIA-ZA animals. Insets are magnified views of individual TRAP+ cells. Original Magnification, x20. (B, D, F and H) Drilled site at 9 weeks, at the end of antiresorptive treatment. Original magnification, x5. (B1, D1, F1 and H1) Magnified views of drilled molars in all groups. Original magnification, x10. (n = 6 mice per group). (I) Quantification of TRAP+ cell number. +Statistically significant different from indicated groups, $p < 0.0001$. **Statistically significant different from indicated groups, $p < 0.001$. Differences among groups were calculated by two-way ANOVA and between groups by Student's t test. Data represent the mean ± SEM.

4 CONSIDERAÇÕES FINAIS

Bisfosfonatos e inibidores de RANK-L são medicamentos anti-reabsortivos que quando administrados por via intravenosa, gerenciam as condições oncológicas, incluindo hipercalcemia maligna, complicações ósseas relacionadas à metástases com tumores sólidos, tais como: câncer de mama, próstata, e pulmão, e controle de lesões líticas de mieloma múltiplo[8,50,87]. BPs e DMAb apresentaram um significativo efeito positivo sobre a qualidade de vida dos pacientes com doenças ósseas avançada envolvendo o esqueleto, promovendo, principalmente, aumento da densidade óssea mineral e inibição da atividade osteoclástica. Contudo, há aproximadamente uma década atrás, uma série crescente de relatos na literatura vem associando estas drogas ao desenvolvimento de necrose óssea nos maxilares[4,7-9,15,50,52,54,86,87].

Os primeiros casos de ONJ foram relatados entre 2003 e 2004 e, embora progressos significativos tenham ocorrido na compreensão da doença, os efeitos colaterais indesejados provocados quando na administração deste medicamento, destacam a necessidade de mais estudos para explicar completamente a respectiva patofisiologia[66,88]. Desde então, muitas hipóteses vem sendo propostas, dentre as quais, muitas com bases empíricas para definir possíveis tratamentos. Como é improvável que uma única hipótese possa explicar a patofisiologia de ONJ, por ser de fato uma doença multifatorial, é também pouco provável que uma única modalidade de tratamento se torne bem sucedida para todos os pacientes. Dentre as hipóteses propostas na literatura, destacam-se: inibição da remodelação óssea, inflamação e infecção, inibição de angiogênese, toxicidade dos tecidos moles e disfunção da imunidade inata e adquirida[2,47,80]. Contudo, para que os pressupostos sejam investigados e a patofisiologia da doença melhor compreendida, é mandatório a existência de modelos de estudo em animais que simulem as condições clinicas, previamente a testes em humanos.

A literatura científica é bastante ampla e ao mesmo tempo divergente no que se refere ao desenvolvimento de um modelo de ONJ. O extenso número de variáveis, tais como: diferentes terapias com BPs, diferentes espécies de animais utilizadas, extrações dentárias, indução de doença periodontal e doença periapical, e uso concomitante de outros medicamentos, dificulta a reprodutibilidade dos testes e o estabelecimento de critérios padronizados para a melhor compreensão da doença[3,5,6,25,61,67,112,115]. Em vista dos argumentos apresentados, no primeiro capítulo,

focamos na redução do número de variáveis para o desenvolvimento do modelo de ONJ. Para isto, áreas de osso exposto e necrótico foram criadas apenas com injeções intraperitoneais de BPs e de inibidores de RANK-L, concomitantemente ao desenvolvimento de doença periodontal espontânea. Após um estudo mais aprofundado sobre as causas da doença periodontal espontânea nos animais de nosso laboratório, constatamos que a ração não esterilizada provocava as lesões evidenciadas neste primeiro estudo. Sendo assim, considerando a ocorrência natural da doença periodontal crônica nesses animais, acreditamos que esta abordagem esteja mais próxima da realidade clínica. Acreditamos também que os modelos que utilizam a extração do dente para induzir ONJ em animais não refletem a realidade clínica. Isto se deve ao fato de todos estes modelos animais, removerem os dentes íntegros após um período de pré-tratamento com BPs ou inibidores de RANK-L. No entanto, a maioria dos dentes extraídos em adultos ocorre devido à presença de doenças associadas, seja periodontal ou endodônticas e/ou pela presença de cáries extensas. Além disso, a extração dentária em pacientes em tratamento com medicamentos anti-reabsortivos é restrita a casos de necessidade indiscutível. Assim, estudos preliminares realizados por nosso grupo de pesquisa foram focados na tentativa de estabelecer modelos animais de ONJ em camundongos e ratos, confrontando a relação da extração de dentes saudáveis versus dentes com doença periodontal. Os resultados são muito encorajadores, indicando que a extração de dentes com doença periodontal grave induz elevada taxa de ONJ (mais do que 70%), em contraste com a extração de dentes íntegros. Estes dados foram, recentemente, enviados para publicação e sugerem que a doença dental admite um papel central no desenvolvimento de ONJ e são suportados por observações clínicas as quais confirmaram que a incidência de ONJ diminui após medidas preventivas dentárias[37,81]. Assim, no primeiro estudo desenvolvemos um novo modelo animal com características radiográficas e histológicas que se assemelham com as condições em humanos, indicando o papel fundamental da inibição da atividade osteoclástica na patofisiologia de ONJ.

Devido ao fato da principal forma de ação de BPs e DMAb ser inibir a função dos osteoclastos por diferentes mecanismos, não é surpresa que a remodelação óssea alterada é a principal hipótese para o desenvolvimento de ONJ[16,53,103]. Vale ressaltar que a prevalência de ONJ em pacientes que receberam DMAb e BPs não é significativamente diferente[38,91,97,109]. Além disso, estudos em animais demonstram uma taxa semelhante de deposição óssea periosteal, necrose histológica, e exposição

óssea quando roedores com doença periodontal ou periapical, ou após passarem por extrações dentárias são tratados com zoledronato ou inibidores de RANKL[2,3,5,8].

Para combater os efeitos da supressão do turnover ósseo, a interrupção temporária dos medicamentos anti-reabsortivos ("drug holiday") antes da extração dentária ou de outros procedimentos cirúrgicos é muitas vezes defendido para, potencialmente, reduzir o risco de ONJ[33,46,113]. Porém, BPs ligam-se à hidroxiapatita exposta e se incorporam à matriz óssea, onde são mantidos com uma meia vida de muitos anos. Já o DMAb, não se integra à matriz óssea, possui meia-vida significativamente mais curta, resultando em rápida reversibilidade dos efeitos[94]. Em concordância, o trabalho apresentado no capitulo 2 evidencia uma normalização mais rápida dos níveis de TRACP-5B após a descontinuação do inibidor de RANKL - OPG-Fc, um substituto para o DMAb (que não reconhece o anticorpo de ratos e camundongos), em comparação com o acido zoledrônico. Além disso, índices radiográficos e histológicos de necrose retornaram ao nível dos animais controle após a retirada de OPG-Fc, enquanto que os camundongos tratados com ZA ainda demonstraram características histológicas e radiográficas de necrose. Se validados em estudos clínicos controlados, estes achados poderão apoiar a justificativa para a interrupção temporária do DMAb no tratamento de pacientes com ONJ e demonstrar os benefícios deste medicamento frente à terapia com bisfosfonatos previamente a intervenções cirúrgicas. Desta forma, o estudo 2 revelou que a descontinuação do tratamento com inibidores de RANK-L (OPG-Fc) mas não com bisfosfonatos, reverteu as características clinicas e radiográficas de ONJ em camundongos.

Em paralelo aos estudos farmacológicos e terapêuticos de ONJ, pesquisas que avaliem a associação de outras doenças sistêmicas com a prevalência e severidade de ONJ permitem um melhor entendimento da etiopatogenia e mecanismos de progressão. Contudo, estudos epidemiológicos, fisiopatológicos, e clínicos sobre ONJ em doenças não malignas ainda permanecem escassos na literatura, especialmente pela baixa prevalência de ONJ nesses pacientes, que varia de 1/20.000 até 1/110.000 casos por ano[82]. ONJ tem sido relacionada ao tratamento com anti-reabsortivos orais e mais de 200 casos de ONJ associados à osteoporose têm sido relatados até o presente momento[42,44,59,64,75,74]. Em uma recente revisão de literatura, os autores encontraram 28 casos de ONJ em pacientes com artrite reumatoide[28]. Embora este número surpreenda, ainda não há uma forte evidência sobre a associação da ONJ e terapias com medicamentos anti-reabsortivos em doenças não malignas. Por outro lado, o

número crescente de indivíduos submetidos ao tratamento crônico com BPs administrados por via oral, instiga novas investigações para identificar com precisão a patogenia, os fatores de risco e as estratégias intervencionais para ONJ em pacientes com doença não oncológica. Outra questão de interesse é a forma como as doenças não malignas afetam o surgimento e a progressão da osteonecrose Em um estudo clínico recente[60], os autores avaliaram a associação de ONJ com doenças benignas (osteoporose e artrite reumatoide) comparando a evolução clínica nos pacientes que faziam uso de BPs por via oral. E apesar de os resultados terem indicado ausência de correlação de ONJ em pacientes com ou sem osteoporose e/ou artrite, as limitações deste estudo podem ter interferido na conclusão final. Especificando cada uma delas, o tamanho amostral reduzido (devido a baixa prevalência de ONJ em pacientes com artrite), a ausência de um grupo controle (pacientes com osteoporose com ou sem artrite e sem tratamento com BPs), e finalmente, o fato de os pacientes em estudos clínicos, geralmente buscarem tratamento da ONJ somente quando já se apresentam com algum sintoma, são critérios decisivos para um confiável delineamento experimental. Outro fator importante se refere aos pacientes portadores de artrite reumatoide e que geralmente estão sobre tratamento associando, muitas vezes, BPs com esteroides e/ou drogas antirreumáticas, os quais alterariam o curso de osteonecrose. Desta forma, em uma tentativa de diminuir as variáveis presentes em estudos clínicos, e consequentemente os questionamentos a respeito da confiabilidade dos dados, o capítulo 3 teve como objetivo avaliar se a presença de AR poderia exacerbar as características clínicas de ONJ. A utilização do modelo animal desenvolvido no estudo 1 permitiu o controle estrito das variáveis encontradas em humanos, ao mesmo tempo em que possibilitou uma abordagem mais controlada, randomizada e prospectiva da investigação com padronização da dosagem e duração do medicamento, e sem o uso concomitante de outras drogas para o tratamento de artrite, o que poderia interferir nos resultados. Desta forma, foi possível demonstrar que o uso de BPs para o tratamento da AR associada a infecções orais aumenta o risco para o desenvolvimento e severidade de ONJ, induzida pela administração de altas doses de bisfosfonatos. Vale ressaltar, que as doses de BPs empregadas neste estudo são doses utilizadas em pacientes oncológicos e não em pacientes portadores de doenças não malignas. A escolha na administração de doses elevadas de BPs se deu para aumentar a incidência de ONJ nos nossos animais. Em face aos dados apresentados e discutidos, estudos futuros adicionais utilizando-se destes modelos

animais são necessários para avaliar a real associação de medicamentos específicos para o tratamento de AR e a etiopatogenia de ONJ. Acreditamos que este estudo abrirá uma nova frente de pesquisa com o intuito de revelar os mecanismos moleculares envolvidos nesta associação e, consequentemente, propor possíveis novas alternativas terapêuticas para ONJ.

5 CONCLUSÃO

Em resumo:

1. Este estudo demonstrou potencialmente importantes conhecimentos sobre a patogenia de ONJ por meio do desenvolvimento de um modelo animal com características radiográficas e histológicas que se assemelham com as condições em humanos, indicando o papel fundamental da inibição da atividade osteoclástica na patofisiologia de ONJ. Além disso, um possível link entre severidade da inflamação e severidade clinica de ONJ foi estabelecido, suportando a importância da infecção/inflamação combinado com a inibição da atividade de osteoclastos na patogênese de ONJ.

2. Este estudo revelou que a descontinuação do tratamento com inibidores de RANK-L (OPG-Fc) mas não bisfosfonatos, reverteu as características clinicas e radiográficas de ONJ em camundongos. Estes achados fornecem um fundamento lógico que auxiliam nas decisões clinicas para descontinuação do tratamento no gerenciamento dos pacientes com ONJ. Assim, os resultados do presente estudo sugerem que em pacientes recebendo altas doses de medicamentos anti-reabsortivos para o gerenciamento de condições malignas, a descontinuação de inibidor de RANK-L ofereceria uma resolução mais rápida e completa de ONJ comparado com bisfosfonatos.

3. Este estudo demonstrou que a administração de altas doses de BPs associada a infecções orais e artrite reumatoide pode aumentar o risco para o desenvolvimento e severidade de ONJ. Assim, evidenciamos que a presença de artrite reumatoide pode ser um fator de risco para um desenvolvimento mais severo de ONJ.

REFERÊNCIAS*

1. Abtahi J, Agholme F, Aspenberg P. Prevention of osteonecrosis of the jaw by mucoperiosteal coverage in a rat model. Int J Oral Maxillofac Surg. 2013; 42(5): 632-6.

2. Aghaloo T, Hazboun R, Tetradis S. Pathophysiology of Osteonecrosis of the Jaws. Oral Maxillofac Surg Clin North Am. 2015; 27(4): 489-96.

3. Aghaloo TL, Cheong S, Bezouglaia O, Kostenuik P, Atti E, Dry SM, et al. RANKL inhibitors induce osteonecrosis of the jaw in mice with periapical disease. J Bone Miner Res. 2014; 29(4): 843-54.

4. Aghaloo TL, Dry SM, Mallya S, Tetradis S. Stage 0 osteonecrosis of the jaw in a patient on denosumab. J Oral Maxillofac Surg. 2014; 72(4): 702-16.

5. Aghaloo TL, Kang B, Sung EC, Shoff M, Ronconi M, Gotcher JE, et al. Periodontal disease and bisphosphonates induce osteonecrosis of the jaws in the rat. J Bone Miner Res. 2011; 26(8): 1871-82.

6. Allen MR. Animal models of osteonecrosis of the jaw. J Musculoskelet Neuronal Interact. 2007; 7(4): 358-60.

7. Allen MR. Bisphosphonates and osteonecrosis of the jaw: moving from the bedside to the bench. Cells Tissues Organs. 2009; 189(1-4): 289-94.

8. Allen MR. Medication-Related Osteonecrosis of the Jaw: Basic and Translational Science Updates. Oral Maxillofac Surg Clin North Am. 2015; 27(4):497-508.

9. Allen MR, Burr DB. The pathogenesis of bisphosphonate-related osteonecrosis of the jaw: so many hypotheses, so few data. J Oral Maxillofac Surg. 2009; 67(5 Suppl): 61-70.

10. Allen MR, Ruggiero SL. Higher bone matrix density exists in only a subset of patients with bisphosphonate-related osteonecrosis of the jaw. J Oral Maxillofac Surg. 2009; 67(7): 1373-7.

11. Allen MR, Ruggiero SL. A review of pharmaceutical agents and oral bone health: how osteonecrosis of the jaw has affected the field. Int J Oral Maxillofac Implants. 2014; 29(1): e45-57.

* De acordo com o Guia de Trabalhos Acadêmicos da FOAr, adaptado das Normas Vancouver. Disponível no site da Biblioteca: http://www.foar.unesp.br/#biblioteca/manual.

12. Amadori D, Aglietta M, Alessi B, Gianni L, Ibrahim T, Farina G, et al. Efficacy and safety of 12-weekly versus 4-weekly zoledronic acid for prolonged treatment of patients with bone metastases from breast cancer (ZOOM): a phase 3, open-label, randomised, non-inferiority trial. Lancet Oncol. 2013; 14(7): 663-70.

13. Anastasilakis AD, Toulis KA, Goulis DG, Polyzos SA, Delaroudis S, Giomisi A, et al. Efficacy and safety of denosumab in postmenopausal women with osteopenia or osteoporosis: a systematic review and a meta-analysis. Horm Metab Res. 2009; 41(10): 721-9.

14. Asagiri M, Takayanagi H. The molecular understanding of osteoclast differentiation. Bone. 2007; 40(2): 251-64.

15. Bamias A, Kastritis E, Bamia C, Moulopoulos LA, Melakopoulos I, Bozas G, et al. Osteonecrosis of the jaw in cancer after treatment with bisphosphonates: incidence and risk factors. J Clin Oncol. 2005; 23(34): 8580-7.

16. Baron R, Ferrari S, Russell RG. Denosumab and bisphosphonates: different mechanisms of action and effects. Bone. 2011; 48(4): 677-92.

17. Barrett-Lee P, Casbard A, Abraham J, Hood K, Coleman R, Simmonds P, et al. Oral ibandronic acid versus intravenous zoledronic acid in treatment of bone metastases from breast cancer: a randomised, open label, non-inferiority phase 3 trial. Lancet Oncol. 2014; 15(1): 114-22.

18. Bekker PJ, Holloway D, Nakanishi A, Arrighi M, Leese PT, Dunstan CR. The effect of a single dose of osteoprotegerin in postmenopausal women. J Bone Miner Res. 2001; 16(2): 348-60.

19. Body JJ, Greipp P, Coleman RE, Facon T, Geurs F, Fermand JP, et al. A phase I study of AMGN-0007, a recombinant osteoprotegerin construct, in patients with multiple myeloma or breast carcinoma related bone metastases. Cancer. 2003; 97(3 Suppl): 887-92.

20. Bonacina R, Mariani U, Villa F, Villa A. Preventive strategies and clinical implications for bisphosphonate-related osteonecrosis of the jaw: a review of 282 patients. J Can Dent Assoc. 2011; 77(1): b147.

21. Bonnet N, Lesclous P, Saffar JL, Ferrari S. Zoledronate effects on systemic and jaw osteopenias in ovariectomized periostin-deficient mice. PLoS One. 2013; 8(3): e58726.

22. Boonyapakorn T, Schirmer I, Reichart PA, Sturm I, Massenkeil G. Bisphosphonate-induced osteonecrosis of the jaws: prospective study of 80 patients with multiple myeloma and other malignancies. Oral Oncol. 2008; 44(9): 857-69.

23. Boyle WJ, Simonet WS, Lacey DL. Osteoclast differentiation and activation. Nature. 2003; 423(6937): 337-42.

24. Bruzzaniti A, Baron R. Molecular regulation of osteoclast activity. Rev Endocr Metab Disord. 2006; 7(1-2): 123-39.

25. Cheong S, Sun S, Kang B, Bezouglaia O, Elashoff D, McKenna CE, et al. Bisphosphonate uptake in areas of tooth extraction or periapical disease. J Oral Maxillofac Surg. 2014; 72(12): 2461-8.

26. Conte Neto N, Bastos AS, Chierici-Marcantonio RA, Marcantonio E, Jr. Is rheumatoid arthritis a risk factor for oral bisphosphonate-induced osteonecrosis of the jaws? Med Hypotheses. 2011; 77(5): 905-11.

27. Conte Neto N, Spolidorio LC, Andrade CR, A SB, Guimaraes M, Marcantonio E, Jr. Experimental development of bisphosphonate-related osteonecrosis of the jaws in rodents. Int J Exp Pathol. 2013; 94(1): 65-73.

28. Conte-Neto N, Bastos AS, Marcantonio RA, Junior EM. Epidemiological aspects of rheumatoid arthritis patients affected by oral bisphosphonate-related osteonecrosis of the jaws. Head Face Med. 2012; 8(1): 5.

29. Conte-Neto N, Bastos AS, Spolidorio LC, Marcantonio RA, Marcantonio E, Jr. Oral bisphosphonate-related osteonecrosis of the jaws in rheumatoid arthritis patients: a critical discussion and two case reports. Head Face Med. 2011; 7(1): 7.

30. Cummings SR, San Martin J, McClung MR, Siris ES, Eastell R, Reid IR, et al. Denosumab for prevention of fractures in postmenopausal women with osteoporosis. N Engl J Med. 2009; 361(8): 756-65.

31. Cundy T, Davidson J, Rutland MD, Stewart C, DePaoli AM. Recombinant osteoprotegerin for juvenile Paget's disease. N Engl J Med. 2005; 353(9): 918-23.

32. Curtis JR, Westfall AO, Cheng H, Lyles K, Saag KG, Delzell E. Benefit of adherence with bisphosphonates depends on age and fracture type: results from an analysis of 101,038 new bisphosphonate users. J Bone Miner Res. 2008; 23(9): 1435-41.

33. Damm DD, Jones DM. Bisphosphonate-related osteonecrosis of the jaws: a potential alternative to drug holidays. Gen Dent. 2013; 61(5): 33-8.

34. de Molon RS, Cheong S, Bezouglaia O, Dry SM, Pirih F, Cirelli JA, et al. Spontaneous osteonecrosis of the jaws in the maxilla of mice on antiresorptive treatment: a novel ONJ mouse model. Bone. 2014; 68: 11-9.

35. de Molon RS, Hsu C, Bezouglaia O, Dry SM, Pirih FQ, Soundia A, et al. Rheumatoid arthritis exacerbates the severity of osteonecrosis of the jaws (ONJ) in mice. A randomized, prospective, controlled animal study. J Bone Miner Res. 2016 Mar 7 [Epub ahead of print]

36. de Molon RS, Shimamoto H, Bezouglaia O, Pirih FQ, Dry SM, Kostenuik P, et al. OPG-Fc but not zoledronic acid discontinuation reverses osteonecrosis of the jaws (ONJ) in mice. J Bone Miner Res. 2015; 30(9): 1627-40.

37. Dimopoulos MA, Kastritis E, Bamia C, Melakopoulos I, Gika D, Roussou M, et al. Reduction of osteonecrosis of the jaw (ONJ) after implementation of preventive measures in patients with multiple myeloma treated with zoledronic acid. Ann Oncol. 2009; 20(1): 117-20.

38. Dranitsaris G, Hatzimichael E. Interpreting results from oncology clinical trials: a comparison of denosumab to zoledronic acid for the prevention of skeletal-related events in cancer patients. Support Care Cancer. 2012; 20(7): 1353-60.

39. Eghbali-Fatourechi G, Khosla S, Sanyal A, Boyle WJ, Lacey DL, Riggs BL. Role of RANK ligand in mediating increased bone resorption in early postmenopausal women. J Clin Invest. 2003; 111(8): 1221-30.

40. Elford PR, Felix R, Cecchini M, Trechsel U, Fleisch H. Murine osteoblastlike cells and the osteogenic cell MC3T3-E1 release a macrophage colony-stimulating activity in culture. Calcif Tissue Int. 1987; 41(3): 151-6.

41. Emery JG, McDonnell P, Burke MB, Deen KC, Lyn S, Silverman C, et al. Osteoprotegerin is a receptor for the cytotoxic ligand TRAIL. J Biol Chem. 1998; 273(23): 14363-7.

42. Favia G, Pilolli GP, Maiorano E. Osteonecrosis of the jaw correlated to bisphosphonate therapy in non-oncologic patients: clinicopathological features of 24 patients. J Rheumatol. 2009; 36(12): 2780-7.

43. Fizazi K, Lipton A, Mariette X, Body JJ, Rahim Y, Gralow JR, et al. Randomized phase II trial of denosumab in patients with bone metastases from prostate cancer, breast cancer, or other neoplasms after intravenous bisphosphonates. J Clin Oncol. 2009; 27(10): 1564-71.

44. Ghirardi A, Scotti L, Zambon A, Della Vedova G, Cavalieri D'oro L, Lapi F, et al. Risk of severe upper gastrointestinal complications among oral bisphosphonate users. PLoS One. 2013; 8(12): e73159.

45. Guerrini MM, Sobacchi C, Cassani B, Abinun M, Kilic SS, Pangrazio A, et al. Human osteoclast-poor osteopetrosis with hypogammaglobulinemia due to TNFRSF11A (RANK) mutations. Am J Hum Genet. 2008; 83(1): 64-76.

46. Hellstein JW, Adler RA, Edwards B, Jacobsen PL, Kalmar JR, Koka S, et al. Managing the care of patients receiving antiresorptive therapy for prevention and treatment of osteoporosis: executive summary of recommendations from the American Dental Association Council on Scientific Affairs. J Am Dent Assoc. 2011; 142(11): 1243-51.

47. Kabilova TO, Kovtonyuk LV, Zonov EV, Ryabchikova EI, Popova NA, Nikolin VP, et al. Immunotherapy of hepatocellular carcinoma with small double-stranded RNA. BMC Cancer. 2014; 14(1): 338.

48. Kang B, Cheong S, Chaichanasakul T, Bezouglaia O, Atti E, Dry SM, et al. Periapical disease and bisphosphonates induce osteonecrosis of the jaws in mice. J Bone Miner Res. 2013; 28(7): 1631-40.

49. Katsarelis H, Shah NP, Dhariwal DK, Pazianas M. Infection and medication-related osteonecrosis of the jaw. J Dent Res. 2015; 94(4): 534-9.

50. Khan AA, Morrison A, Hanley DA, Felsenberg D, McCauley LK, O'Ryan F, et al. Diagnosis and management of osteonecrosis of the jaw: a systematic review and international consensus. J Bone Miner Res. 2015; 30(1): 3-23.

51. Khan AA, Rios LP, Sandor GK, Khan N, Peters E, Rahman MO, et al. Bisphosphonate-associated osteonecrosis of the jaw in Ontario: a survey of oral and maxillofacial surgeons. J Rheumatol. 2011; 38(7): 1396-402.

52. Khosla S, Burr D, Cauley J, Dempster DW, Ebeling PR, Felsenberg D, et al. Bisphosphonate-associated osteonecrosis of the jaw: report of a task force of the American Society for Bone and Mineral Research. J Bone Miner Res. 2007; 22(10): 1479-91.

53. Kimmel DB. Mechanism of action, pharmacokinetic and pharmacodynamic profile, and clinical applications of nitrogen-containing bisphosphonates. J Dent Res. 2007; 86(11): 1022-33.

54. King AE, Umland EM. Osteonecrosis of the jaw in patients receiving intravenous or oral bisphosphonates. Pharmacotherapy. 2008; 28(5): 667-77.

55. Kong YY, Yoshida H, Sarosi I, Tan HL, Timms E, Capparelli C, et al. OPGL is a key regulator of osteoclastogenesis, lymphocyte development and lymph-node organogenesis. Nature. 1999; 397(6717): 315-23.

56. Kostenuik PJ, Nguyen HQ, McCabe J, Warmington KS, Kurahara C, Sun N, et al. Denosumab, a fully human monoclonal antibody to RANKL, inhibits bone resorption and increases BMD in knock-in mice that express chimeric (murine/human) RANKL. J Bone Miner Res. 2009; 24(2): 182-95.

57. Lacey DL, Boyle WJ, Simonet WS, Kostenuik PJ, Dougall WC, Sullivan JK, et al. Bench to bedside: elucidation of the OPG-RANK-RANKL pathway and the development of denosumab. Nat Rev Drug Discov. 2012; 11(5): 401-19.

58. Lacey DL, Timms E, Tan HL, Kelley MJ, Dunstan CR, Burgess T, et al. Osteoprotegerin ligand is a cytokine that regulates osteoclast differentiation and activation. Cell. 1998; 93(2): 165-76.

59. Lapi F, Cipriani F, Caputi AP, Corrao G, Vaccheri A, Sturkenboom MC, et al. Assessing the risk of osteonecrosis of the jaw due to bisphosphonate therapy in the secondary prevention of osteoporotic fractures. Osteoporos Int. 2013; 24(2): 697-705.

60. Lescaille G, Coudert AE, Baaroun V, Javelot MJ, Cohen-Solal M, Berdal A, et al. Osteonecrosis of the jaw and nonmalignant disease: is there an association with rheumatoid arthritis? J Rheumatol. 2013; 40(6): 781-6.

61. Li CL, Lu WW, Seneviratne CJ, Leung WK, Zwahlen RA, Zheng LW. Role of periodontal disease in bisphosphonate-related osteonecrosis of the jaws in ovariectomized rats. Clin Oral Implants Res. 2016; 27(1): 1-6.

62. Lipton A, Steger GG, Figueroa J, Alvarado C, Solal-Celigny P, Body JJ, et al. Extended efficacy and safety of denosumab in breast cancer patients with bone metastases not receiving prior bisphosphonate therapy. Clin Cancer Res. 2008; 14(20): 6690-6.

63. Lopez-Jornet P, Camacho-Alonso F, Martinez-Canovas A, Molina-Minano F, Gomez-Garcia F, Vicente-Ortega V. Perioperative antibiotic regimen in rats treated with pamidronate plus dexamethasone and subjected to dental extraction: a study of the changes in the jaws. J Oral Maxillofac Surg. 2011; 69(10): 2488-93.

64. Manfredi M, Merigo E, Guidotti R, Meleti M, Vescovi P. Bisphosphonate-related osteonecrosis of the jaws: a case series of 25 patients affected by osteoporosis. Int J Oral Maxillofac Surg. 2011; 40(3): 277-84.

65. Martin T, Gooi JH, Sims NA. Molecular mechanisms in coupling of bone formation to resorption. Crit Rev Eukaryot Gene Expr. 2009; 19(1): 73-88.

66. Marx RE. Pamidronate (Aredia) and zoledronate (Zometa) induced avascular necrosis of the jaws: a growing epidemic. J Oral Maxillofac Surg. 2003; 61(9): 1115-7.

67. Marx RE, Sawatari Y, Fortin M, Broumand V. Bisphosphonate-induced exposed bone (osteonecrosis/osteopetrosis) of the jaws: risk factors, recognition, prevention, and treatment. J Oral Maxillofac Surg. 2005; 63(11): 1567-75.

68. McClung MR, Lewiecki EM, Cohen SB, Bolognese MA, Woodson GC, Moffett AH, et al. Denosumab in postmenopausal women with low bone mineral density. N Engl J Med. 2006; 354(8): 821-31.

69. Morgans AK, Smith MR. Bone-targeted agents: preventing skeletal complications in prostate cancer. Urol Clin North Am. 2012; 39(4): 533-46.

70. Mori Y, Tsuji S, Inui M, Sakamoto Y, Endo S, Ito Y, et al. Inhibitory immunoglobulin-like receptors LILRB and PIR-B negatively regulate osteoclast development. J Immunol. 2008; 181(7): 4742-51.

71. Nicolatou-Galitis O, Papadopoulou E, Sarri T, Boziari P, Karayianni A, Kyrtsonis MC, et al. Osteonecrosis of the jaw in oncology patients treated with bisphosphonates: prospective experience of a dental oncology referral center. Oral Surg Oral Med Oral Pathol Oral Radiol Endod. 2011; 112(2): 195-202.

72. Ominsky MS, Kostenuik PJ, Cranmer P, Smith SY, Atkinson JE. The RANKL inhibitor OPG-Fc increases cortical and trabecular bone mass in young gonad-intact cynomolgus monkeys. Osteoporos Int. 2007; 18(8): 1073-82.

73. Orwoll E, Teglbjaerg CS, Langdahl BL, Chapurlat R, Czerwinski E, Kendler DL, et al. A randomized, placebo-controlled study of the effects of denosumab for the treatment of men with low bone mineral density. J Clin Endocrinol Metab. 2012; 97(9): 3161-9.

74. Otto S, Abu-Id MH, Fedele S, Warnke PH, Becker ST, Kolk A, et al. Osteoporosis and bisphosphonates-related osteonecrosis of the jaw: not just a sporadic coincidence--a multi-centre study. J Craniomaxillofac Surg. 2011; 39(4): 272-7.

75. Palaska PK, Cartsos V, Zavras AI. Bisphosphonates and time to osteonecrosis development. Oncologist. 2009; 14(11): 1154-66.

76. Papapoulos S, Chapurlat R, Libanati C, Brandi ML, Brown JP, Czerwinski E, et al. Five years of denosumab exposure in women with postmenopausal osteoporosis: results from the first two years of the FREEDOM extension. J Bone Miner Res. 2012; 27(3): 694-701.

77. Park S, Kanayama K, Kaur K, Tseng HC, Banankhah S, Quje DT, et al. Osteonecrosis of the Jaw Developed in Mice: Disease variants regulated by gammadelta t cells in oral mucosal barrier immunity. J Biol Chem. 2015; 290(28): 17349-66.

78. Peer A, Khamaisi M. Diabetes as a risk factor for medication-related osteonecrosis of the jaw. J Dent Res. 2015; 94(2): 252-60.

79. Pierroz DD, Bonnet N, Baldock PA, Ominsky MS, Stolina M, Kostenuik PJ, et al. Are osteoclasts needed for the bone anabolic response to parathyroid hormone? A study of intermittent parathyroid hormone with denosumab or alendronate in knock-in mice expressing humanized RANKL. J Biol Chem. 2010; 285(36): 28164-73.

80. Reid IR, Bolland MJ, Grey AB. Is bisphosphonate-associated osteonecrosis of the jaw caused by soft tissue toxicity? Bone. 2007; 41(3): 318-20.

81. Ripamonti CI, Maniezzo M, Campa T, Fagnoni E, Brunelli C, Saibene G, et al. Decreased occurrence of osteonecrosis of the jaw after implementation of dental preventive measures in solid tumour patients with bone metastases treated with bisphosphonates. The experience of the National Cancer Institute of Milan. Ann Oncol. 2009; 20(1): 137-45.

82. Rizzoli R, Burlet N, Cahall D, Delmas PD, Eriksen EF, Felsenberg D, et al. Osteonecrosis of the jaw and bisphosphonate treatment for osteoporosis. Bone. 2008; 42(5): 841-7.

83. Roelofs AJ, Thompson K, Gordon S, Rogers MJ. Molecular mechanisms of action of bisphosphonates: current status. Clin Cancer Res. 2006; 12(20 Pt 2): 6222s-30s.

84. Ruggiero SL. Bisphosphonate-related osteonecrosis of the jaw: an overview. Ann N Y Acad Sci. 2011; 1218(1): 38-46.

85. Ruggiero SL. Guidelines for the diagnosis of bisphosphonate-related osteonecrosis of the jaw (BRONJ). Clin Cases Miner Bone Metab. 2007; 4(1): 37-42.

86. Ruggiero SL, Dodson TB, Assael LA, Landesberg R, Marx RE, Mehrotra B, et al. American Association of Oral and Maxillofacial Surgeons position paper on bisphosphonate-related osteonecrosis of the jaws--2009 update. J Oral Maxillofac Surg. 2009; 67(5 Suppl): 2-12.

87. Ruggiero SL, Dodson TB, Fantasia J, Goodday R, Aghaloo T, Mehrotra B, et al. American Association of Oral and Maxillofacial Surgeons position paper on medication-related osteonecrosis of the jaw--2014 update. J Oral Maxillofac Surg. 2014; 72(10): 1938-56.

88. Ruggiero SL, Mehrotra B, Rosenberg TJ, Engroff SL. Osteonecrosis of the jaws associated with the use of bisphosphonates: a review of 63 cases. J Oral Maxillofac Surg. 2004; 62(5): 527-34.

89. Russell G, Mueller G, Shipman C, Croucher P. Clinical disorders of bone resorption. Novartis Found Symp. 2001; 232(1): 251-67; discussion 67-71.

90. Russell RG, Watts NB, Ebetino FH, Rogers MJ. Mechanisms of action of bisphosphonates: similarities and differences and their potential influence on clinical efficacy. Osteoporos Int. 2008; 19(6): 733-59.

91. Saad F, Brown JE, Van Poznak C, Ibrahim T, Stemmer SM, Stopeck AT, et al. Incidence, risk factors, and outcomes of osteonecrosis of the jaw: integrated analysis from three blinded active-controlled phase III trials in cancer patients with bone metastases. Ann Oncol. 2012; 23(5): 1341-7.

92. Schaffler MB. Role of bone turnover in microdamage. Osteoporos Int. 2003; 14(Suppl 5): S73-7; discussion S7-80.

93. Schwarz EM, Ritchlin CT. Clinical development of anti-RANKL therapy. Arthritis Res Ther. 2007; 9(Suppl 1): S7.

94. Silva I, Branco JC. Denosumab: recent update in postmenopausal osteoporosis. Acta Reumatol Port. 2012; 37(4): 302-13.

95. Simonet WS, Lacey DL, Dunstan CR, Kelley M, Chang MS, Luthy R, et al. Osteoprotegerin: a novel secreted protein involved in the regulation of bone density. Cell. 1997; 89(2): 309-19.

96. Smith MR, Egerdie B, Hernandez Toriz N, Feldman R, Tammela TL, Saad F, et al. Denosumab in men receiving androgen-deprivation therapy for prostate cancer. N Engl J Med. 2009; 361(8): 745-55.

97. Smith MR, Saad F, Coleman R, Shore N, Fizazi K, Tombal B, et al. Denosumab and bone-metastasis-free survival in men with castration-resistant prostate cancer: results of a phase 3, randomised, placebo-controlled trial. Lancet. 2012; 379(9810): 39-46.

98. Smith MR, Saad F, Egerdie B, Szwedowski M, Tammela TL, Ke C, et al. Effects of denosumab on bone mineral density in men receiving androgen deprivation therapy for prostate cancer. J Urol. 2009; 182(6): 2670-5.

99. Sobacchi C, Frattini A, Guerrini MM, Abinun M, Pangrazio A, Susani L, et al. Osteoclast-poor human osteopetrosis due to mutations in the gene encoding RANKL. Nat Genet. 2007; 39(8): 960-2.

100. Sordillo EM, Pearse RN. RANK-Fc: a therapeutic antagonist for RANK-L in myeloma. Cancer. 2003; 97(3 Suppl): 802-12.

101. Stolina M, Schett G, Dwyer D, Vonderfecht S, Middleton S, Duryea D, et al. RANKL inhibition by osteoprotegerin prevents bone loss without affecting local or systemic inflammation parameters in two rat arthritis models: comparison with anti-TNFalpha or anti-IL-1 therapies. Arthritis Res Ther. 2009; 11(6): R187.

102. Stopeck AT, Fizazi K, Body JJ, Brown JE, Carducci M, Diel I, et al. Safety of long-term denosumab therapy: results from the open label extension phase of two phase 3 studies in patients with metastatic breast and prostate cancer. Support Care Cancer. 2016; 24(1): 447-55.

103. Suzuki K, Takeyama S, Sakai Y, Yamada S, Shinoda H. Current topics in pharmacological research on bone metabolism: inhibitory effects of bisphosphonates on the differentiation and activity of osteoclasts. J Pharmacol Sci. 2006; 100(3): 189-94.

104. Tella SH, Gallagher JC. Prevention and treatment of postmenopausal osteoporosis. J Steroid Biochem Mol Biol. 2014; 142(1): 155-70.

105. Theill LE, Boyle WJ, Penninger JM. RANK-L and RANK: T cells, bone loss, and mammalian evolution. Annu Rev Immunol. 2002; 20(1): 795-823.

106. Tolia M, Zygogianni A, Kouvaris JR, Meristoudis C, Margari N, Karakitsos P, et al. The key role of bisphosphonates in the supportive care of cancer patients. Anticancer Res. 2014; 34(1): 23-37.

107. Voss PJ, Stoddart MJ, Bernstein A, Schmelzeisen R, Nelson K, Stadelmann V, et al. Zoledronate induces bisphosphonate-related osteonecrosis of the jaw in osteopenic sheep. Clin Oral Investig. 2016; 20(1): 31-8.

108. Wada S, Fukawa T, Kamiya S. [New bone density conservation agents for osteoporosis under research and development: Anti-RANKL antibody]. Nihon Rinsho. 2007; 65(Suppl 9): 459-62.

109. Walsh PC. Re: Denosumab and bone-metastasis-free survival in men with castration-resistant prostate cancer: results of a phase 3, randomised, placebo-controlled trial. J Urol. 2012; 187(6): 2098.

110. Weinstein RS, Roberson PK, Manolagas SC. Giant osteoclast formation and long-term oral bisphosphonate therapy. N Engl J Med. 2009; 360(1): 53-62.

111. Whyte MP, Mumm S. Heritable disorders of the RANKL/OPG/RANK signaling pathway. J Musculoskelet Neuronal Interact. 2004; 4(3): 254-67.

112. Williams DW, Lee C, Kim T, Yagita H, Wu H, Park S, et al. Impaired bone resorption and woven bone formation are associated with development of osteonecrosis of the jaw-like lesions by bisphosphonate and anti-receptor activator of NF-kappaB ligand antibody in mice. Am J Pathol. 2014; 184(11): 3084-93.

113. Woo SB, Hellstein JW, Kalmar JR. Narrative [corrected] review: bisphosphonates and osteonecrosis of the jaws. Ann Intern Med. 2006; 144(10): 753-61.

114. Yoshida H, Hayashi S, Kunisada T, Ogawa M, Nishikawa S, Okamura H, et al. The murine mutation osteopetrosis is in the coding region of the macrophage colony stimulating factor gene. Nature. 1990; 345(6274): 442-4.

115. Zhang Q, Yu W, Lee S, Xu Q, Naji A, Le AD. Bisphosphonate Induces Osteonecrosis of the Jaw in Diabetic Mice via NLRP3/Caspase-1-Dependent IL-1beta Mechanism. J Bone Miner Res. 2015; 30(12): 2300-12.

ANEXO A

MATERIAL E MÉTODO

MÉTODOS: CAPITULO 1

Animais

Os animais foram mantidos e tratados de acordo com diretrizes do comitê de ética em pesquisa da UCLA. Ao longo do período experimental, os camundongos foram alojados em gaiolas de plástico, alimentados com uma dieta de laboratório, e água ad libitum. 76 camundongos machos C57BL/6J, de 2 meses de idade (Jackson Laboratories, Bar Harbor, ME, EUA) receberam injeções intraperitoneais (*ip*) de soro (endotoxin free saline) ou 200 ug/kg ácido zoledrônico (ZA, Z-5744 LKT Laboratories, St. Paul, MN) três vezes por semana ou de 10 mg/kg de RANK-Fc (composto do domínio extracelular de RANK ligado à porção Fc de IgG. Amgen, Inc., Thousand Oaks, CA), três vezes por semana, ou 10 mg/kg de OPG-Fc (composto pelos domínios de ligação de RANKL de osteoprotegerina ligado à porção Fc de IgG. Amgen, Inc., Thousand Oaks, CA), uma vez por semana em um total de12 semanas (Figura 1A). O tempo e dose destes medicamentos foram baseados em estudos prévios que mostraram induzir lesões ONJ.

Figura 1A - *Desenho experimental do estudo 1*

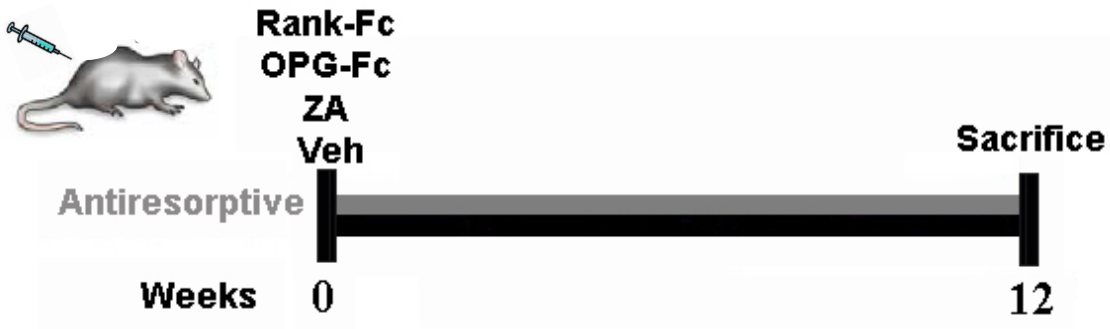

Autor: de Molon et al.[34]

Fonte: *Bone.* 2014; 68: 11-9.

MÉTODOS: CAPITULO 2

Animais

Os animais e os procedimentos cirúrgicos foram tratados de acordo com orientações do Comitê de Ética em Experimentação Animal da Universidade da Califórnia, em Los Angeles. Seguimos um estudo prospectivo, controlado, e randomizado de modelo animal seguindo todas as recomendações do ARRIVE (*Animal Research: Reporting In Vivo Experiments*) para a execução e apresentação de estudos em animais. Os camundongos foram mantidos nas instalações para animais com temperatura controlada (23° C ± 2° C), humidade, e com um com ciclo de claro/escuro de 12-horas. Durante todo o período experimental, os animais foram alojados em gaiolas de plástico e mantidos com uma dieta padrão de laboratório e água ad libitum. Um total de 144 camundongos machos C57BL/6J,de 2 meses de idade (Jackson Laboratories, BarHarbor, ME, EUA), com peso médio de 25 g foram aleatoriamente divididos em três grupos experimentais de 48 animais que receberam injeção intraperitoneal (*ip*) de solução salina (endotoxin free saline) duas vezes por semana (veh grupo), 10 mg/kg de OPG-Fc (composto pelos domínios de ligação de RANKL e osteoprotegerina ligado à porção Fc de IgG. Amgen, Inc., Thousand Oaks, CA, EUA), duas vezes por semana (grupo OPG-Fc), ou 200 mg/kg de ácido zoledrônico (Z-5744, LKT Laboratories, St. Paul, MN, EUA) duas vezes por semana (grupo ZA) (Figura 2A). Estas doses foram utilizadas para aumentar a incidência de lesões ONJ conforme descrito anteriormente.

Figura 2A - *Desenho experimental do estudo 2.*

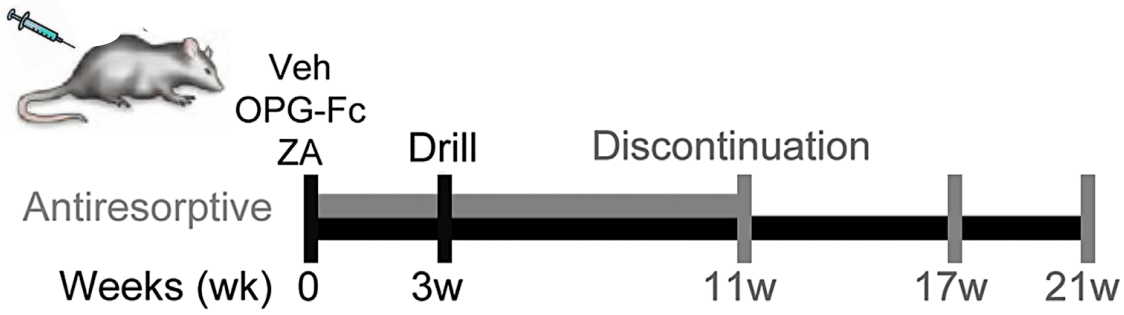

Autor: de Molon et al.[36]

Fonte: *J Bone Miner Res.* 2015; 30(9): 1627-40.

MÉTODOS: CAPITULO 3

Animais

24 camundongos machos, DBA1/J (Jackson Laboratories, Bar Harbor, ME, USA) foram randomicamente divididos em 4 grupos experimentais (n = 6). G1 - grupo veiculo (controle) nos quais os animais foram submetidos a indução de doença nos maxilares seguida da administração de soro fisiológico; G2 - grupo acido zoledronico (ZA) nos quais os animais foram submetidos a indução de doença nos maxilares seguida da administração de bifosfonato; G3 - grupo artrite reumatoide (CIA) nos quais os animais foram submetidos a indução de doença nos maxilares seguida de indução de artrite reumatoide por meio de injeção de colágeno na base da cauda associado a administração de soro fisiológico. G4 - grupo CIA+ZA nos quais os animais foram submetidos a indução de doença nos maxilares seguida de indução de artrite reumatoide por meio de injeção de colágeno na base da cauda associado a administração de bisfosfonato. Animais foram tratados com injeções intraperitoneais de solução fisiológica nos grupos controle e CIA ou com injeções de acido zoledronico (200 μg/kg - ZA, Z-5744 LKT laboratories, St. Paul, MN) nos grupos ZA e CIA-ZA duas vezes por semana, por uma semana antes da indução da doenca periapical (Figura 3A).

Figura 3A - *Desenho experimental do estudo 3.*

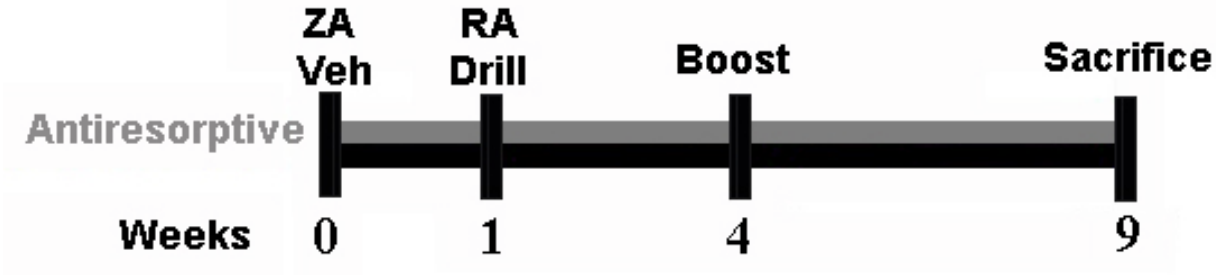

Autor: de Molon et al.[35]

Fonte: *J Bone Miner Res.* 2016.

METODOS - CAPITULOS 1, 2 e 3

Indução de doença periapical

Camundongos foram anestesiados com isofluorano e posicionados em uma mesa operatória. Exposição pulpar foi realizada no primeiro e segundo molares mandibulares direito, utilizando-se uma broca esférica com 0,25 mm de diâmetro evitando-se perfuração na câmara pulpar. Os canais radiculares foram mantidos abertos na cavidade oral para indução da lesão. As coroas dos molares do lado esquerdo foram mantidas intactas.

Doença periodontal espontânea

Doença periodontal espontânea tem sido descrito na literatura. As alterações espontâneas que ocorreram nos animais foram identificados como osteolises e formação de osso periosteal, identificados através de analises micro-tomográficas. Sítios doentes foram comparados com estruturas dento-alveolares sadias.

Indução de artrite reumatoide (CIA)

O modelo de colágeno foi estabelecido usando-se colágeno tipo II bovino (Chondrex 20021; BD Biosciences, San Jose, CA, USA) o qual foi dissolvido a uma concentração de 4 mg/mL em 0.1 M de acido acético por meio de agitação continua a 4°C para prevenção da denaturação do colágeno. Adjuvante completo de Freund's (CFA) foi composto pelo adjuvante incompleto de Freund's (IFA) (Sigma Aldrich – F5506) associado com *Mycobacterium tuberculosis* H37Ra (BD Biosciences, San Jose, CA, USA). Emulsão 1:1 (v/v) consistindo do colágeno (100 μg) e CFA (100 μg of *M. tuberculosis*) foi preparada e os camundongos foram imunizados com uma injeção intradérmica com 50 μL da emulsão na base da cauda. 3 semanas após a imunização primária, uma nova injeção intensificadora com 100 μg de colágeno tipo II bovino em IFA foi administrada na base da cauda.

Avaliação clínica da artrite

Camundongos foram avaliados quanto a presença de artrite a cada dois dias, a partir do dia 21 apos a primeira imunização, ate o dia do sacrifício. Os critérios para avaliação foram: 0 = nenhum inchaço nas patas. 1 = inchaço da articulação de um dedo. 2 = inchaço médio do pulso ou do tornozelo. 3 = inchaço severo do tornozelo. Os escores de todos os dedos das patas dianteiras e traseiras, pulso ou tornozelos foram totalizados para cada camundongo (com um escore máximo de 12 por animal).

Sacrifício dos animais e coleta das amostras

Após o tratamento, os animais de cada grupo experimental foram sacrificados por overdose de anestésico. Mandíbulas, maxilas, fêmur, tíbia e patas traseiras foram cuidadosamente removidas e coletados, fixados em solução de paraformaldeído, e armazenados em álcool 70% em temperatura ambiente até serem escaneados usando-se um sistema de microtomografia computadorizada.

Microtomografia computadorizada (μCT)

Amostras ósseas da mandíbula, maxila, fêmur, tíbia e patas traseiras foram coletadas de cada animal e escaneadas utilizando-se um sistema de microtomografia computadorizada (μCT Skyscan 1172; Skyscan, Kontich, Belgium). Para analises lineares, dados volumétricos foram convertidos em formato DICOM (Digital Imaging and Communications in Medicine) e foram importados no software Dolphin Imaging software (Chatsworth, CA) para geração de imagens reconstruídas 3D e multiplanares.

Na mandíbula, a quantidade de perda óssea periapical foi mensurada a partir da raiz distal no primeiro molar e na raiz mesial do segundo molar (distancia do ápice da raiz ate o osso alveolar) em um corte sagital. A espessura da lamina dura e a largura do espaço do ligamento periodontal foram quantificados a partir da região de furca do primeiro molar ao longo do eixo mesio-distal do dente, em um corte sagital.

Espessura do osso vestibular e lingual foi mensurado em um corte axial no nível do terço apical da raiz do primeiro e segundo molares. Na maxila, a distância da junção cemento-esmalte até a crista óssea alveolar foi mensurada na superfície distal do primeiro molar. As demais análises foram feitas da mesma forma que na mandíbula.

Volume ósseo (BV), tecido ósseo (TV) e fração de volume ósseo (BV/TV) foram analisados utilizando-se o software CTAn (CT Analyzer 1.12.0.0 - Skyscan, Kontich, Belgium) em cortes axiais (1024 x 1024). Todos as imagens foram salvas no Dataviewer (Dataviewer 1.4.3 – Skyscan, Kontich, Belgium). Para isso, uma região de interesse (ROI) foi delineada a partir dos ápices das raízes ate a crista alveolar, e a partir da raiz mesial do primeiro molar ate a raiz distal do terceiro molar. As raízes dentárias e o ligamento periodontal foram excluídos das analises. Os contornos do ROI foram desenhados a cada 10 planos, movendo-se aproximadamente 1.8 mm (60 cortes) no sentido coronal, para mandíbula e maxila.

Os ajustes para o escaneamento dos fêmurs, tíbias, e patas traseiras foram os mesmos para a maxila e mandíbula, exceto pela resolução no qual foi de 12 μm (0.012 mm) em um escaneamento de grandes dimensões (oversized scans). Análises dos fêmurs e tíbias foram realizados usando-se o CTAn em cortes axiais a partir do osso da epífise proximal. ROIs foram identificados da seguinte maneira: metáfise distal do fêmur e metáfise proximal da tíbia incluindo todo osso trabecular e excluindo a cortical óssea de cada amostra, onde osso trabecular ainda estava presente. Os contornos do ROI foram desenhados manualmente, em intervalos regulares a cada 10 cortes, movendo-se aproximadamente 2.4 mm (200 cortes) no sentido do longo eixo. BV, TV, BV/TV, espessura trabecular (Tb.Th), número de trabéculas (Tb.N) e separação de trabéculas (Tb.Sp) foram determinadas utilizando-se o CTAn.

Analise histológica

Mandíbula, maxila, fêmur, tíbia e patas traseiras foram descalcificados em 14,5% EDTA, durante 4 semanas. Amostras foram embebidas em parafina, cortes seriados com 4 μm de espessura foram obtidos e corados com hematoxilina e eosina (H&E).

Todas as lâminas coradas com H&E foram digitalmente escaneadas usando um scaner automatizado (Aperio AT automated slide scanner). Usando a ferramenta régua no software ImageScope Aperio (Aperio Technologies, Inc., Vista, CA,EUA), uma distancia de 1 mm entre a crista óssea e o osso alveolar foi marcada e todas as medições foram realizadas nesta área.

A distância da margem do epitélio até a crista alveolar foi medida no lado palatino da maxila e, no lado lingual da mandíbula. Número total de lacunas osteocíticas vazias e as áreas de osteonecrose, definida como a perda de mais do que cinco osteócitos contíguos foram medidos. Para quantificar a espessura do osso periosteal, a ferramenta régua foi usada para medir as três maiores áreas de espessura do periósteo vestibular que foram, em seguida, calculados para obtenção da média. Todas as medições foram realizadas de acordo com estudos anteriormente publicados.

Para a avaliação histológica nos joelhos e patas, cortes sagitais (4 μm) foram corados com H&E para estudar a inflamação sinovial, e para determinar a destruição da cartilagem e osso. Alterações histopatológicas foram classificadas como descrito: Resumidamente, infiltração de células foi marcada em uma escalade 0-3, dependendo da quantidade de células inflamatórias na cavidade sinovial e tecido sinovial (0 =ausência de células, 1 = celularidade leve, 2 = celularidade moderada, e 3 = celularidade máxima). Destruição da cartilagem foi distintamente classificado em uma escala de 0-3, que variou desde o não aparecimento de condrócitos mortos (lacunas vazias) a uma perda completa de condrócitos na cartilagem. A erosão óssea foi pontuada numa escala de 0 a 5 variando de nenhum dano ate a perda óssea avançada. Alterações histopatológicas nas articulações do joelho foram marcados na região do fêmur/tíbia. A articulação do tornozelo, região do tornozelo e do calcanhar foram avaliadas. As mensurações foram realizadas por um examinador cego e calibrado.

Coloração TRAP

Para examinar a atividade de reabsorção óssea osteoclástica, as laminas foram coradas utilizando um kit de coloração de TRAP (Leukocyte Acid Phosphatase 387-A kit

(Sigma ‐ Aldrich, St. Louis, MO, USA). As lâminas foram desparafinizadas e reidratadas, fixados em solução fixadora durante 30 segundos, e, em seguida, incubadas a 37 ° C em solução de coloração de TRAP (contendo diazotized fast garnet, napthol AS-BI phosphate, acetate, and tartrate solution) durante 60 minutos. Depois de contra-coloração com hematoxilina, secções foram desidratadas e lamínulas foram coladas. O número total de células TRAP-positivas multinucleadas que continha 2 ou mais núcleos foram contados na mandíbula, maxila, joelho e patas.

Autorizo a reprodução deste trabalho.

(Direitos de publicação reservado ao autor)

Araraquara, 24 de Março de 2016.

RAFAEL SCAF DE MOLON